From the:

Walther Straub Institute of Pharmacology and Toxicology

Ludwig-Maximilians-Universität München

Chairman: Univ.-Prof. Dr. med. Thomas Gudermann

Bundeswehr Institute of Pharmacology and Toxicology

Director: Prof. Dr. med. Horst Thiermann

Dissertation

zum Erwerb des Doctor of Philosophy (Ph.D.) an der

Medizinischen Fakultät der

Ludwig-Maximilians-Universität München

Improvement of cold storage of Precision Cut Lung Slices (PCLS) and the use of PCLS as model in organophosphate research

vorgelegt von

Jonas Tigges

aus

Büren, Germany

2022

Mit Genehmigung der Medizinischen Fakultät der

Ludwig-Maximilians-Universität München

First supervisor: Prof. Dr. med. Franz Worek

Second supervisor: PD Dr. med. Timo Wille

Third supervisor: Prof. Dr. med. Dirk Steinritz

Dean: **Prof. Dr. med. Thomas Gudermann**

Datum der Verteidigung:

08.07.2022

Affidavit

Affidavit

Tigges, Jonas
_____
Surname, first name

_____
Street

_____
Zip code, town, country

I hereby declare, that the submitted thesis entitled:

Improvement of cold storage of Precision Cut Lung Slices (PCLS) and the use of PCLS as model in organophosphate research

is my own work. I have only used the sources indicated and have not made unauthorized use of services of a third party. Where the work of others has been quoted or reproduced, the source is always given.

I further declare that the submitted thesis or parts thereof have not been presented as part of an examination degree to any other university.

Cologne, 07.08.2022

Jonas Tigges
_____
(Jonas Tigges)

Confirmation of congruency

Confirmation of congruency between printed and electronic version of the doctoral thesis

Tigges, Jonas

Surname, first name

Street

Zip code, town, country

I hereby declare, that the submitted thesis entitled:

Improvement of cold storage of Precision Cut Lung Slices (PCLS) and the use of PCLS as model in organophosphate research

is congruent with the printed version both in content and format.

Cologne, 07.08.2022

(Jonas Tigges)

Table of content

List of abbreviations

ACh	Acetylcholine
AChE	Acetylcholinesterase
COPD	Chronic obstructive pulmonary disease
CYP	Cytochrome P450
DMEM/F-12	Dulbecco's Modified Eagle Medium/Nutrient Mixture F-12
ELISA	Enzyme-linked immunosorbent assay
FACS	Fluorescence activated cell sorting
GM-CSF	Granulocyte-macrophage colony-stimulating factor
GSH	Glutathione
GSSG	Glutathione disulfide
GST	Glutathione-S-transferase
HO-1	Hemeoxigenase-1
IL-6	Interleukin-6
LDH	Lactate-dehydrogenase
LPS	Lipopolysaccharide
MIP-1α	Macrophage inflammatory protein
NFκB	Nuclear factor 'kappa-light-chain-enhancer' of activated B-cells
OP	Organophosphorus compounds
PCLS	Precision cut lung slices
SOD	Superoxide dismutase
TMRM	Tetramethyl rhodamine methyl ester
VEGF	Vascular endothelial growth factor
WHO	World health organization

List of figures

List of publications and presentations

Publications of the cumulative dissertation

Publication I: **Tigges J**, Eggerbauer F, Worek F, Thiermann H, Rauen U, Wille T (2021). Optimization of long-term cold storage of rat precision cut lung slices (PCLS) with a tissue preservation solution*. American Journal of Physiology - Lung Cellular and Molecular Physiology*, 321:6, L1023-L1035; DOI: 10.1152/ajplung.00076.2021

Publication II: **Tigges J**, Worek F, Thiermann H, Wille T (2022). Organophosphorus pesticides exhibit compound specific effects in rat precision cut lung slices (PCLS): mechanisms involved in airway response, cytotoxicity, inflammatory activation and antioxidative defense. *Archives of Toxicology;* 96, 321–334;
DOI: https://doi.org/10.1007/s00204-021-03186-x

Additional Publication

Kolling J, **Tigges J**, Hellack B, Albrecht C, Schins RPF (2020). Evaluation of the NLRP3 Inflammasome Activating Effects of a Large Panel of TiO2 Nanomaterials in Macrophages. *Nanomaterials (Basel)*; 10(9):1876. DOI:10.3390/nano10091876

Conference contributions:

Poster presentation: 5th German Pharm-Tox Summit - 86th Annual Meeting of the German Society for Experimental and Clinical Pharmacology and Toxicology (DGPT), Leipzig, March 2-5 (2020): **Tigges J**, Thiermann H, Worek F, Wille T. Evaluation of lung injury induced by organophosphorus compounds using precision cut lung slices

Oral presentation: Annual meeting of the Society of Toxicology, Virtual Event, March (2021): **Tigges J**, Wille T. Cold Storage of Rat Precision-Cut Lung Slices: A Model Upgrade to Expand Applicability

1. Authors contribution to the publications

1.1 Contribution to publication I

Tigges J, Eggerbauer F, Worek F, Thiermann H, Rauen U, Wille T (2021). Optimization of long-term cold storage of rat precision cut lung slices (PCLS) with a tissue preservation solution*. American Journal of Physiology - Lung Cellular and Molecular Physiology*, 321:6, L1023-L1035; DOI:10.1152/ajplung.00076.2021.

Journal listing in „Web of Science“ of the Thomson Reuter Institute for Scientific Information (2020): *American Journal of Physiology-Lung Cellular and Molecular Physiology:* **Category Rank** 11 of 81 in the category **“Physiology”**

I investigated the effects of long-term (3-28 days) cold storage of PCLS in optimized tissue preservation solutions to improve the applicability of PCLS in lung toxicology research, to extend the cold storage duration of PCLS and to enable the transport of these slices between different cooperating laboratories. The results from this investigation were published in the *American Journal of Physiology - Lung Cellular and Molecular Physiology*. During these investigations, a broad spectrum of biochemical and functional assays was applied to investigate the effects of cold storage on multiple relevant endpoints studied in PCLS. Hereinafter, I list my contributions to the publication in the *American Journal of Physiology - Lung Cellular and Molecular Physiology*:

- Literature research
- PCLS preparation
- Cold storage experiments (base solutions with or without (experimental) iron chelators etc.)
- Performance of all biochemical assays after PCLS cold storage (Alamar Blue assay and live/dead staining for evaluation of cytotoxic effects, tetramethyl rhodamine methyl ester (TMRM) staining for detection of mitochondrial membrane potential, lipopolysaccharide (LPS) stimulation and enzyme-linked immunosorbent assay (ELISA) to evaluate the inflammatory response, preparation of single cell suspensions and fluorescence activated cell sorting (FACS) analysis to study specific cell-populations and analysis of bronchoconstriction to determine the functional response)
- Data analysis (data visualization and statistical analysis using the software GraphPad Prism)
- Preparation of the manuscript draft

- Planning of additional experiments including the selection of suitable endpoints and methods to address the reviewers' comments
- Preparation of the revised manuscript and response to reviewers' comments

The following contributions to the publication Tigges *et al.* in *American Journal of Physiology - Lung Cellular and Molecular Physiology* (2021) were made by the co-authors:

Author Eggerbauer F:

- Pre-evaluation of cold storage durations and rewarming periods
- Pre-evaluations for bronchoconstriction experiments

Authors Worek F and Thiermann H:

- Scientific advice

Author Rauen U:

- Preparation of cold storage solutions and provision of iron chelators
- Scientific advice

Author Wille, T:

- Project supervision and scientific advice
- Data discussion and preparation of the manuscript

1.2 Contribution to publication II

Tigges J, Worek F, Thiermann H, Wille T (2022). Organophosphorus pesticides exhibit compound specific effects in rat precision cut lung slices (PCLS): mechanisms involved in airway response, cytotoxicity, inflammatory activation and antioxidative defense. *Archives of Toxicology;* 96, 321–334; DOI: https://doi.org/10.1007/s00204-021-03186-x

Journal listing in „Web of Science“ of the Thomson Reuter Institute for Scientific Information (2020): *Archives of Toxicology:* **Category Rank** 16 of 93 in the category **“Toxicology”**

In the present study, PCLS were used to evaluate multiple effects of organophosphate exposure in a complex ex-vivo lung tissue model. Therefore, rat PCLS were exposed to different organophosphorus pesticides and their biotransformation products (oxon-form) and effects on viability as well as functional response were investigated. The results of these investigations are published in *Archives of Toxicology*. Hereinafter, I list my contributions to the publication in *Archives of Toxicology*:

- Literature research
- Study design of the organophosphorus compound (OP) pesticides exposure experiments including the selection of suitable endpoints and methods for evaluation
- PCLS preparation
- Performance of all biochemical assays after OP exposure (Alamar Blue assay and lactate-dehydrogenase (LDH) activity for evaluation of cytotoxic effects, multiplex immunoassay and ELISA to evaluate the inflammatory response, glutathione (GSH) and glutathione disulfide (GSSG) detection, glutathione-S-transferase activity (GST), superoxide dismutase (SOD) activity assays and hemeoxigenase-1 (HO-1) ELISA to evaluate antioxidative response, multiplex immunoassay for evaluation of signaling pathway activation and analysis of bronchoconstriction to determine the functional response)
- Data analysis (data visualization and statistical analysis using the software GraphPad Prism)
- Preparation of the manuscript draft
- Preparation of the revised manuscript and response to reviewers’ comments

The following contributions to the publication Tigges *et al.* in *Archives of Toxicology* (2022) were made by the co-authors:

Author Worek F

- Project supervision and scientific advice

Author Thiermann H:

- Scientific advice

Author Wille, T:

- Project supervision and scientific advice
- Data discussion and preparation of the manuscript

2. Introductory summary

2.1 Organophosphorus compounds

Within the group of plant protection products, insecticides are of fundamental importance for pest control in agricultural farming. Besides carbamates and neonicotinoids, organophosphorus compounds (OP) such as chlorpyrifos or malathion are used. These so-called “organophosphates” are characterized by a central phosphate molecule with alkyl or aromatic substituents. In addition to their application as insecticides, highly toxic OP are also used as nerve agents, e.g. sarin since 2013 in Syria (John et al. 2018). Since an extensive pesticide development program by Gerhard Schrader in the 1930s, a wide range of structurally diverse pesticides and highly toxic nerve agents has been developed (Costa 2006). Although the use of some highly toxic OP in pesticides has been strictly regulated, and self-poisoning is comparably rare in Europe (Hrabetz et al. 2013), OP intoxication is a very common poisoning worldwide, with accidental, but also deliberate poisonings occurring especially in rural South East Asia. Widespread use due to low-costs and easy access to large quantities of OP pesticides, lead to a conservatively estimated ~ 100.000 cases of self-poisoning with fatal outcome each year, posing a major burden for the local health systems (Jeyaratnam 1990; van der Hoek et al. 1998; Mew et al. 2017; Gunnell and Eddleston 2003). Hospitals in rural regions of developing countries, where these substances are increasingly used, are often poorly equipped, which makes efficient treatment of patients difficult, resulting in a case fatality rate of 15-30% (Eddleston et al. 2008).

2.1.1 Toxicokinetic and toxicodynamic of OP

Following absorption via inhalation, ingestion or via the skin, the fate of an OP is dependent on distribution, metabolism and excretion. As especially the parent phosphorothioates like parathion or malathion are lipophilic, accumulation occurs mainly in fat tissue, as well as in kidney, lung and brain (Timchalk 2010). The toxicity of OP after absorption is on the one hand dependent on spontaneous hydrolysis and biotransforming enzymes leading to detoxification (Buratti et al. 2007) and on the other hand on cytochrome P450 (CYP) mediated bioactivation, resulting in the formation of the significantly more potent oxon forms (Timchalk 2010) (Figure 1).

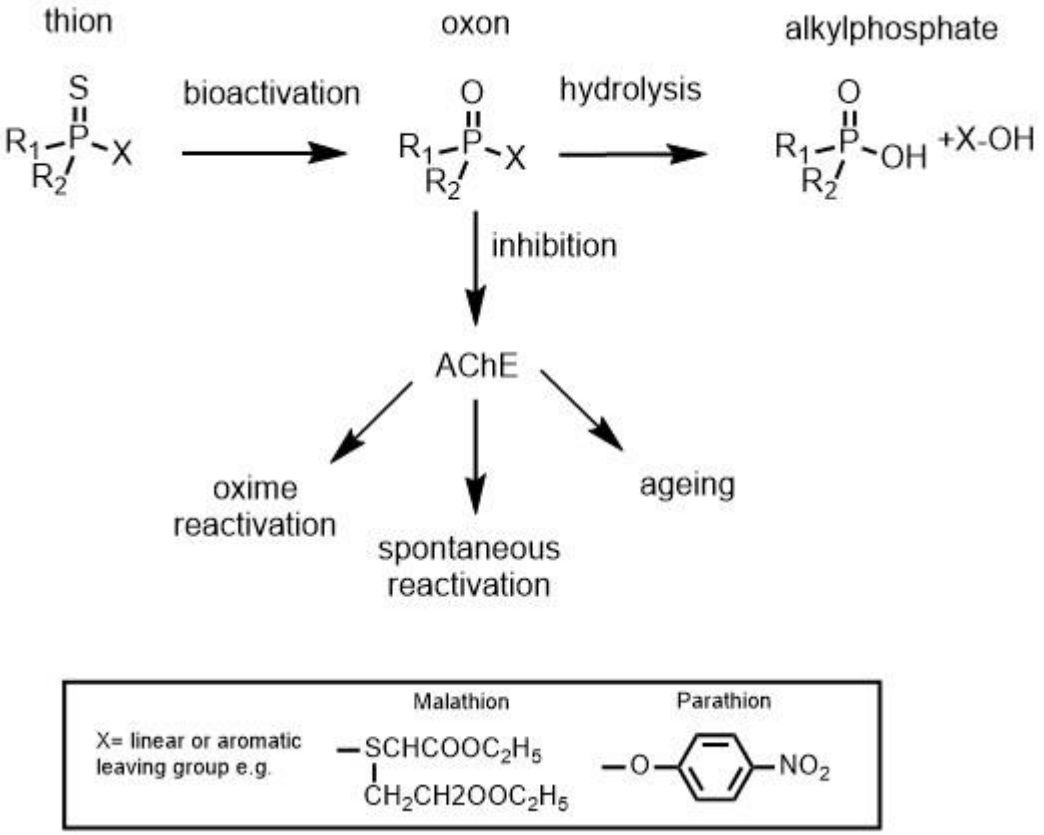

Figure 1: Human enzymatic biotransformation of phosphorothioate pesticides (modified from Wille et al. (2020))

After bioactivation, OP covalently bind to the active serine hydroxyl residue 203 of acetylcholinesterase (AChE), forming an enzyme intermediate and subsequently inhibiting the degradation of the neurotransmitter acetylcholine (ACh) in the synaptic clefts (Worek et al. 2020; Chambers and Oppenheimer 2004). The excess of ACh in the synaptic clefts and the neuromuscular junction leads to permanent excitation and overstimulation at nicotinic and muscarinic ACh receptors, inducing a cholinergic crisis that may ultimately result in respiratory arrest and death if left untreated. Although a stable, covalent bond between OP and AChE is formed, secondary side reactions such as spontaneous reactivation may restore the enzyme activity in mild OP poisoning. On the other hand, dealkylation of R_1 or R_2 (so called “aging”) with enhanced binding stability may occur, which impairs AChE reactivation by oximes (Worek et al. 2004) (Figure 1). Symptoms of cholinergic crisis include hypersecretion of glands, smooth muscle contraction, urination, diarrhea, abdominal cramps and emesis with respiratory arrest being the most common cause of death (Wille et al. 2020; Okumura et al. 1996). The development and progression of symptoms is highly dependent on the type of OP, route of exposure and decontamination efficiency (Eyer et al. 2003).

Standard therapy for OP poisoning consists of repeated administration of atropine as a muscarinic receptor antagonist and an oxime to reactivate the inhibited AChE. However, the efficacy of oxime therapy is controversially discussed and depends on the specific type of OP, body load and start of oxime administration after OP intake (Worek et al. 2020). Recently introduced experimental therapeutic approaches also focus on the development of bio-scavengers, that degrade circulating OP before they reach their physiological target, as well as on scavenging cyclodextrins and receptor-active substances (Wille et al. 2016; Letort et al. 2016; Amend et al. 2020; Stigler et al. 2021).

2.1.2 Respiratory complications after OP exposure

In deliberate poisoning, the primary route of exposure is oral ingestion of OP, with subsequent absorption primarily in the gastrointestinal tract. However, aspiration of stomach content may occur, leading to direct lung cell contact with high OP concentrations (Hulse et al. 2014). In many cases of OP exposure, respiratory complications are observed, whose underlying mechanisms are not well understood. In an autopsy case series of 85 patients with OP poisoning, pulmonary interstitial edema was found in 75% of the patients who died within 24 h after OP exposure (Kamat et al. 1989). In addition, disruption of the endothelial-epithelial barrier after exposure to the nerve agent VX has been observed in animal studies and aspirated dimethoate has been shown to damage the alveoli (Hulse et al. 2014). Epidemiological data from workers involved in organophosphate production also suggest an immunomodulatory effect as they showed increased incidence for upper respiratory infections and reduced neutrophil function (Hermanowicz and Kossman 1984). After inhalational exposure to the OP nerve agent VX, acute lung injury with increased bronchioalveolar lavage protein, neutrophil infiltration and alveolar inflammation was observed in guinea pigs (Wright et al. 2006) and baboons exposed to the OP nerve agent sarin showed pulmonary neutrophilia (Anzueto 1990). Observations from *in vitro* cell culture studies furthermore suggest cytotoxic and immunomodulatory effects of OP in bronchial epithelial cells (Oostingh et al. 2009) and differentiated macrophages (Proskocil et al. 2019).

2.1.3 Non-AChE inhibition related toxicity of OP

While the acute effects and underlying mechanisms of AChE inhibition are well studied, the secondary effects that occur in the further course of treatment after OP exposure are not well understood and there is increasing evidence, that mechanisms other than AChE inhibition are involved in the chronic adverse health effects of OP (Costa 2006). For example, 55 different proteins were identified as binding targets of OP in the mouse brain, which can impair protein function. The investigated OP bound to different

proteins, which could be an explanation for the variable adverse health effects of OP (Lockridge et al. 2005). Furthermore, an impairment of various metabolizing enzymes has been demonstrated, which can likewise lead to adverse health effects (Richards et al. 2000).

These studies provide evidence that OP can react directly with cells and induce damage and inflammatory activation independent from the primary mechanism of AChE inhibition. However, many studies have been carried out either *in vivo* or in cell culture experiments, whereby either the high complexity of the system allows only limited conclusions about direct substance effects and their mechanisms, or the use of single selected cell types is limited in reflecting the cellular interaction and composition of the real lung.

2.1.4 Modell systems to study lung toxicology

The respiratory system is a complex organ system, and constantly exposed to environmental compounds. Recently, more than 50 different cell types have been identified in the human lung, each with their own task and biochemical function, which underlines the complexity of this pivotal organ (Travaglini et al. 2020). The exactly balanced interplay between different cell types involved in breathing mechanics, oxygen supply and immune response enables reliable organ function under challenging conditions, especially the continuous exposure towards environmental pollutants. However, ongoing exposure towards polluted air or other chemical substances can disrupt this balance, leading to impaired lung function and development of numerous lung diseases. To study effects of compounds on the lung, different experimental models are used.

In vivo models are still the gold standard for the detection of adverse effects in drug discovery. As of today, performing studies in living organisms remains the only way to comprehensively assess pharmacodynamics, pharmacokinetics, and safety of a drug candidate or chemical substance before initiating clinical trials in humans. However, they are very complex, which makes the analysis of underlying mechanisms difficult. In addition, they are expensive, time-consuming, labor-intensive and are hardly in agreement with modern animal ethics standards. *In vitro* experiments use lung cell lines or primary cells and represent the characteristics of specific lung cell types like epithelial cells or alveolar macrophages. Cell cultures are well suited to investigate the underlying mechanisms of toxic effects on certain lung cell types but have their limitations when cell-cell interactions or physiological functions need to be analyzed. However, the natural lung tissue with all its different cell types and important cellular sub-units (e.g., blood vessels or airways) cannot be reproduced *in vitro* in its full complexity (Sakagami

2006). As an intermediate approach, complex tissue cultures are used *ex vivo* to fill the gap between *in vivo* animal experiments and *in vitro* cell culture investigations.

2.2 Precision cut lung slices (PCLS) and their use in lung toxicology research

In general, tissue cultures can be generated from many different organs of either human or animal origin, such as liver, kidney, intestine, brain, or lung (Majorova et al. 2021). The PCLS technique combines primary cells in their natural composition and structure with the easy-to-handle procedures and standardized exposure possibilities of cell culture experiments, providing unique insights into toxic effects and their mechanisms in complex tissue. The lung tissue samples can be gained either from laboratory animals, or from human donors with pre-existing diseases allowing the evaluation of therapeutic approaches for specific conditions. As > 150 PCLS can be generated from one rat lung, the *ex vivo* use of this tissues samples can therefore contribute to the reduction and refinement of animal experiments according to the 3Rs principle (reduce, refine and replace animal experiments) (Russell and Burch 1959).

Although precision cut lung slices have already been used for several decades in lung research (Fisher et al. 1994), the use of PCLS has been steeply rising in the last years due to continuous improvements in slicing technique and culture conditions with the rational to reduce animal experiments.

As the lung has no solid consistence, instillation with liquid agarose and solidification after cooling is necessary to prepare the lung tissue slices. After PCLS preparation, the obtained living lung tissue can be exposed to a wide variety of substances and can be evaluated using a broad spectrum of biochemical assays. Cytotoxic effects of chemicals can be determined using metabolic activity assays, where the enzymatic activity is representative for the cellular viability. In addition, viability can be investigated using live/dead staining and confocal microscopy or the release of LDH into the supernatant of PCLS as an indirect indicator of induced cell damage. Recently, these assays have been used to study the cell-damaging effects of nanoparticles or low-molecular-weight chemicals for pre-validation in toxicological risk assessments (Neuhaus et al. 2018; Hirn et al. 2014; Sauer et al. 2014). Although cytotoxic effects can be tested easily by analysis of the overall viability in PCLS, evaluation of the underlying mechanisms is limited, since a large quantity of the cells must be considered as damaged *per se* due to the slicing procedure. In contrast to immortalized tumor cell lines, all cells in lung tissue undergo cell degradation and finally death over time and are only capable of limited proliferation.

Complex three-dimensional lung tissue allows analysis of airway responsiveness and beating frequency of cilia. By adding neurotransmitters such as ACh, bronchoconstriction of airways can be induced. The neurotransmitter is afterwards degraded by tissue resident AChE, leading to smooth muscle relaxation and subsequent reopening of the airway. Using this technique for analysis of airway response, PCLS can be used as a model to test new therapy options for respiratory diseases such as chronic obstructive pulmonary disease (COPD) or asthma as well as for OP poisoning (Wohlsen et al. 2003; Herbert et al. 2017, 2019).

The inflammatory response, which is predominantly dependent on tissue-resident alveolar macrophages, is another important functional marker to study the effects of an exposure towards chemicals in PCLS. Tissue resident immunologically active cells are characterized by the presence of CD45 surface markers and are equally distributed in high numbers throughout the slices (Misharin et al. 2013) (Figure 2).

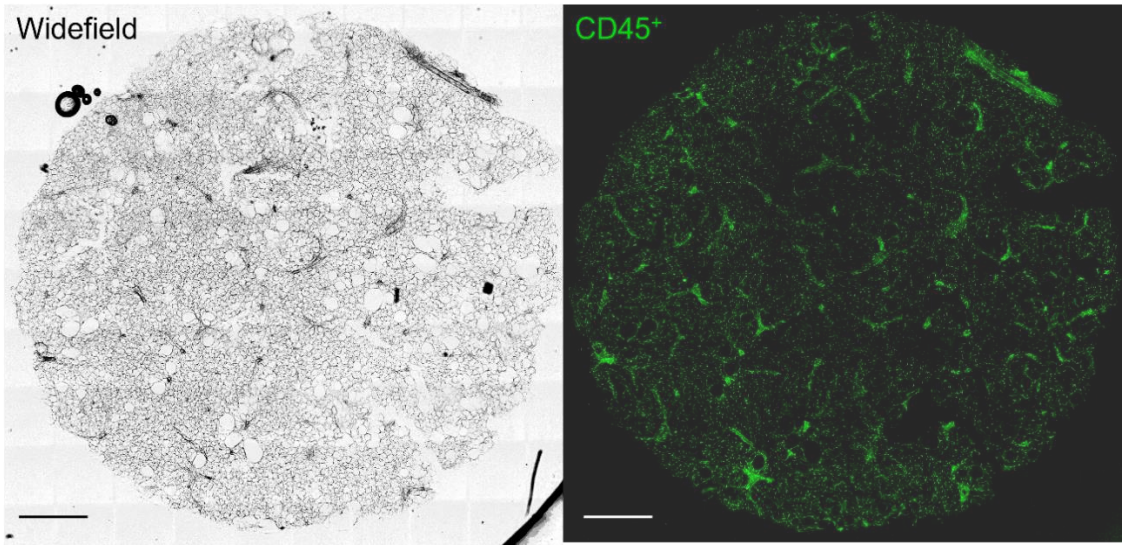

Figure 2: Widefield microscopical image of PCLS (left) and CD45 immunostaining (right). PCLS were stained with mouse anti rat CD45 (FITC) antibody, fixed in 4% paraformaldehyde and mounted on a glass slide. Images were taken by confocal microscopy (Leica DMi-8; Leica Microsystems, Wetzlar, Germany) using a 10x objective and are afterwards digitally combined to obtain a complete PCLS image. Scale bar = 1 mm

To study inflammatory activation in PCLS, the expression of proinflammatory cytokines such as tumor necrosis factor-α (TNF-α) or interleukin-6 (IL-6), that are either concentrated intracellularly or released into the PCLS supernatant, can be detected following exposure to test compounds (Temann et al. 2017). It is important to note that a recruitment of lung external immune cells such as neutrophils is not possible and only the inflammatory response of resident cells is assessed. In recent years, this system has been widely used to test the effects of asthma therapeutics, allergens and irritants or

antiviral drugs on inflammatory cells in the lung, with is a useful approach to reduce *in vivo* experiments (Banerjee et al. 2012; Lauenstein et al. 2014; Danov et al. 2019). However, regional differences in lung tissue might result in a different cell composition in the PCLS, which may complicate interpretation of the results.

Cell damage and inflammatory activation after chemical exposure result in an imbalance of the cellular redox system, which leads to an increased formation of reactive oxygen species. These effects can be detected in PCLS by analyzing key players in the antioxidant defense such as glutathione or the activity of antioxidant enzymes (Sauer et al. 2014).

Cultivation time of PCLS in a standard laboratory incubator is limited. Even with regular medium changes, a decrease of metabolic activity as well as a loss of cells is observed with ongoing incubation time and inflammatory response is highly decreased already after one week (Preuß et al. 2021; Temann et al. 2017). Furthermore, the number of PCLS that can be prepared from a tissue sample, particularly from humans, often exceeds the number of slices that can be used immediately for experimental investigations, making storage of PCLS for a longer period desirable.

2.3 Conservation and storage of PCLS (Publication I)

An extended storage duration enables the transport of PCLS between cooperating institutions, which could significantly increase the usability especially of human tissues. Therefore, various attempts have been made in recent years to extend the cultivation time of PCLS. There are several approaches to extend the lifespan of PCLS by warm storage at 37°C, 5% CO_2 in the incubator. For example, embedding the tissue in a hydrogel biomaterial has shown to be effective in extending viability to at least 21 days (Bailey et al. 2020). Addition of insulin can also significantly prolong airway smooth muscle contraction, although no protective effect on overall viability is observed (Li et al. 2020). However, both approaches require regular medium exchange, which can be very labor-intensive for a large quantity of PCLS. The cryopreservation method, where PCLS are stored at -80°C, does not require much time and effort and allows the establishment of tissue-banks with samples derived from patients suffering from various lung diseases. To prevent damage of cell membranes resulting from intracellular ice crystal formation, a comparatively high amount of dimethyl sulfoxide (10%) is used, which can have adverse effects in the lung tissue. Although this process does not seem to lead to alterations in airway responsiveness, it does reduce the metabolic activity of the cells (Rosner et al. 2014; Watson et al. 2016). A more gentle way of preservation can be storage at 4°C, as this has already been used for liver and kidney slices with good out-

comes (Fisher et al. 1996). By reducing the ambient temperature, the metabolic activity of the cells can be substantially decreased, which also reduces the energy required for maintenance of cellular functions and therefore can be expected to preserve viability over a longer period of time (Guibert et al. 2011). Storage at 4°C also simplifies PCLS transport, as incubators for transport at 37°C and 5% CO_2 are expensive and not easy to handle. In Publication I, I therefore investigated how storage at 4°C for up to 28 days in standard culture medium (DMEM/F-12) as well as in two optimized tissue preservation solutions affects various endpoints in PCLS compared to freshly prepared slices. Both storage solutions contain several protective ingredients that act on different mechanisms to maintain the viability and functionality of the tissue during cold storage. These include for example stabilization of cell membranes (tryptophan), optimized energy supply (α-ketoglutarate, aspartate) and prevention of osmotic swelling (sucrose). While chloride was added to solution 1 for maintenance of ion balance, it was largely replaced by the organic anion lactobionate in solution 2. I was able to show that especially solution 1, with a high chloride concentration, has significant protective effects on viability, inflammatory activation, mitochondrial membrane potential and bronchoconstriction compared to cell culture medium in rat PCLS up to 28 days. In addition, I was able to show that the cell composition of PCLS is preserved, with only the proportion of CD45+ immune cells decreasing faster than EpCAM+ epithelial cells, CD35+ endothelial cells or CD90+ mesenchymal cells. These data are in good correlation with the inflammatory activity and are in line with data from storage of PCLS at 37°C (Neuhaus et al. 2017). Substitution of chloride by lactobionate did not prove to have an additional protective effect. For all endpoints investigated, solution 1, containing chloride, showed a greater protective effect after up to 28 days of cold storage than solution 2, containing lactobionate. However, both solutions showed better tissue preservation than DMEM/F-12. The use of optimized tissue preservation solutions for long-term cold storage of PCLS is therefore a promising approach to prolong the viability and functionality of PCLS and to allow transport at 4°C between cooperating laboratories, thus ensuring an optimal use of these valuable samples and reducing the number of required laboratory animals.

2.4 Use of PCLS in OP research (Publication II)

Although PCLS have been used in lung research for several decades, only few research groups evaluated potential therapeutic improvements in OP poisoning using lung slices in recent years. In particular, the primary toxic effect of AChE inhibition has been therapeutically addressed by investigating effects on airway constriction and subsequent relaxation. The focus of these studies was set on the nerve agents VX and

cyclosarin, while the effects of the widely used pesticides such as malathion were only marginally investigated. Therapeutic approaches were limited to established substances such as atropine and scopolamine (Herbert et al. 2017; Wigenstam et al. 2021) or substances for symptomatic therapy such as formoterol, salbutamol or ipratropium, which are predominantly used for the treatment of COPD or asthma (Herbert et al. 2019). So far, however, only the immediate, acute effects of OP poisoning, resulting in airway constriction, have been investigated in PCLS, while the delayed cell-damaging or inflammatory effects have only been studied in *in vitro* cell culture or *in vivo* experiments.

In Paper II I therefore used PCLS as a realistic model system of the lung to investigate the effects of OP on different endpoints that may play a role in the toxicity of these substances and to gain a better understanding of the underlying mechanisms. The well-studied OP pesticides parathion and malathion as well as their more potent biotransformation products paraoxon and malaoxon were used as test compounds to analyze the effect of different inhibitory potency (world health organization (WHO) class I pesticide parathion vs. class III pesticide malathion) and bioactivation (thion vs. oxon). The acute effects on AChE inhibition were assessed by measuring airway relaxation after OP exposure and ACh stimulation. It was found that only the bio-transformed compounds paraoxon and malaoxon exhibited inhibitory potency, which was stronger for paraoxon than for malaoxon. These results are in line with the inhibitory potency in isolated AChE of rat erythrocyte membranes and illustrate the necessity of bioactivation for substantial AChE inhibition (Worek et al. 2020). A direct cytotoxic effect (detected by metabolic activity and LDH release) could be demonstrated at significantly higher concentrations, with both thion and oxon forms causing cellular damage. The effect of malaoxon was stronger than that of paraoxon, which is contrary to the inhibitory potency. This indicates that i) bioactivation is not essential for the induction of cytotoxic tissue damage and that ii) the underlying mechanism is probably not dependent on AChE inhibition. A similar conclusion can be drawn from the analysis of inflammatory cytokine expression (IL-6, granulocyte-macrophage colony-stimulating factor (GM-CSF), vascular endothelial growth factor (VEGF), macrophage inflammatory protein (MIP-1a)), which was strongest after thion exposure and was not affected by malaoxon. Further investigations using parathion as OP with the highest inflammatory potential revealed, that inflammatory activation is dependent on the nuclear factor 'kappa-light-chain-enhancer' of activated B-cells (NFκB) signaling pathway. Malaoxon showed the strongest effects on the antioxidative system, reducing intracellular glutathione, and, in contrast to the other substances, also increasing glutathione disulfide. In combination with an increased expression of HO-1, that is expressed in response to oxidative

stress, it can therefore be concluded that malaoxon has stronger effects on the antioxidative system than the other investigated compounds. These findings are also supported by the effects of preincubation with the glutathione precursor *N*-acetylcysteine, which significantly reduced malaoxon-induced, but not paraoxon-induced cytotoxicity. Overall, the findings of this study reflect the diverse picture of effects induced by different OP and provide further evidence that mechanisms other than AChE inhibition play a crucial role in lung injury by OP poisoning. The lung model system PCLS provides promising opportunities to test the efficacy of new therapeutics against direct lung injury to improve clinical treatment after OP exposure.

2.5 Concluding remarks

The improved cold storage in the optimized tissue preservation solution 1 compared to the standard medium DMEM/F-12 leads to a superior usability of PCLS and allows the transport of tissue slices between cooperating working groups. The present work provides the basis for further investigation of therapeutic approaches to improve the therapy after OP poisoning, especially for the poorly studied effects of lung damage. Therapeutic approaches arise in particular around the inflammatory activation and antioxidative defense. There is potential for assessment of substances that have already been evaluated *in vivo* for OP therapy, such as cyclooxygenase-2 (COX II) inhibitors (Chapman et al. 2019). Additional approaches may arise by addressing the NFκB signaling pathway using anti-inflammatory drugs. For example, flurbiprofen derivatives can inhibit the NFκB signaling pathway and may have the potential to reduce OP induced inflammatory activation (Tegeder et al. 2001). In addition, antioxidant compounds such as vitamin C have the potential to prevent malaoxon induced alterations in the antioxidative defense (Guaiquil et al. 2001). Taken together, this work shows up promising ways to improve the usability and transport of PCLS in terms of the 3R approach and illustrates that the PCLS model system is suitable for testing potential therapeutics against different mechanisms induced by OP exposure.

3. Publication I

AMERICAN JOURNAL OF PHYSIOLOGY
LUNG CELLULAR AND MOLECULAR PHYSIOLOGY

Am J Physiol Lung Cell Mol Physiol 321: L1023–L1035, 2021.
First published October 13, 2021; doi:10.1152/ajplung.00076.2021

RESEARCH ARTICLE

Translational Physiology

Optimization of long-term cold storage of rat precision-cut lung slices with a tissue preservation solution

Jonas Tigges,[1] Florian Eggerbauer,[2] Franz Worek,[1] Horst Thiermann,[1] Ursula Rauen,[3] and Timo Wille[1]

[1]*Bundeswehr Institute of Pharmacology and Toxicology, Munich, Germany;* [2]*Walther Straub Institute of Pharmacology and Toxicology, Munich, Germany; and* [3]*Institute of Physiological Chemistry, University Hospital, Essen, Germany*

Abstract

Precision-cut lung slices (PCLS) are used as ex vivo model of the lung to fill the gap between in vitro and in vivo experiments. To allow optimal utilization of PCLS, possibilities to prolong slice viability via cold storage using optimized storage solutions were evaluated. Rat PCLS were cold stored in DMEM/F-12 or two different preservation solutions for up to 28 days at 4°C. After rewarming in DMEM/F-12, metabolic activity, live/dead staining, and mitochondrial membrane potential was assessed to analyze overall tissue viability. Single-cell suspensions were prepared and proportions of $CD45^+$, $EpCAM^+$, $CD31^+$, and $CD90^+$ cells were analyzed. As functional parameters, TNF-α expression was analyzed to detect inflammatory activity and bronchoconstriction was evaluated after acetylcholine stimulus. After 14 days of cold storage, viability and mitochondrial membrane potential were significantly better preserved after storage in *solution 1* (potassium chloride rich) and *solution 2* (potassium- and lactobionate-rich analog) compared with DMEM/F-12. Analysis of cell populations revealed efficient preservation of $EpCAM^+$, $CD31^+$, and $CD90^+$ cells. Proportion of $CD45^+$ cells decreased during cold storage but was better preserved by both modified solutions than by DMEM/F-12. PCLS stored in *solution 1* responded substantially longer to inflammatory stimulation than those stored in DMEM/F-12 or *solution 2*. Analysis of bronchoconstriction revealed total loss of function after 14 days of storage in DMEM/F-12 but, in contrast, a good response in PCLS stored in the optimized solutions. An improved base solution with a high potassium chloride concentration optimizes cold storage of PCLS and allows shipment between laboratories and stockpiling of tissue samples.

cold storage; PCLS; 3R; tissue preservation

INTRODUCTION

Precision-cut lung slices (PCLS) are a widely used tool in medical research to study lung biology in an ex vivo tissue system (1). Compared with cell cultures, PCLS exhibit several advantages. Cell cultures usually involve a limited number of different cell types, whereas PCLS consist of all resident lung cells in their natural spatial relationship representing the original complexity of the organ. Cells are embedded in their natural structural arrangement, thus yielding an optimal prediction system to study the effects on lung architecture and physiological organ function including cell-cell interactions and matrix effects (2). PCLS offer the opportunity to study structural and physiological alterations upon treatment in specific airway sections or distal lung, which is of increasing interest for the use in preclinical validation. Thereby, biochemical analysis methods such as viability assays, detection of inflammatory markers, RNA, and protein analysis, as well as microscopical investigations can be applied (3–5). In addition, PCLS are a promising tool not only for the development of novel treatment strategies for airway diseases like asthma, chronic obstructive pulmonary disease (COPD), or inflammation-mediated pulmonary damage but also for the development of medical countermeasures against the cholinergic crisis after exposure to organophosphorus pesticides or nerve agents (1, 6, 7). PCLS contain responsive airways, enabling the quantification of airway constriction after a pharmacological stimulus (6, 8). Addition of the neurotransmitter acetylcholine (ACh) to PCLS medium results in constriction of airway smooth muscle cells and decrease of the airway cross-section area. This bronchoconstriction is spontaneously reversible due to lung-resident active acetylcholinesterase (6, 9). Due to the development of specialized tissue-slicers, it is possible to provide a large number of highly standardized tissue samples with low tissue damage within a short time (10). Numerous PCLS (100–150) can be prepared from one rat lung, thus reducing the number of animals needed for in vivo experiments which is in line with the 3 "R" approach (11). As human lung tissue specimens are rare and samples of diseased patients are even more precious, an optimized storage protocol to process high numbers of PCLS is highly desirable. Storage of

Correspondence: T. Wille (TimoWille@bundeswehr.org).
Submitted 17 February 2021 / Revised 29 September 2021 / Accepted 11 October 2021

PCLS is standardized for cell culture conditions (37°C, 5% CO_2 submersed in a standard cell culture medium) as the required infrastructure is available in most laboratories. PCLS can be maintained at 37°C without significant loss of viability for up to 14 days if the medium is frequently changed (12). Further improvements have been made by modification of the culture medium with supplements like insulin (13). However, the transport on a research campus or shipment to other laboratories is difficult under cell culture conditions. To overcome this issue and to provide tissue samples for cooperation partners at other locations, shipment of PCLS with an easy to standardize storage protocol is highly desirable. In addition, optimized storage of PCLS allows stockpiling of tissue samples for on-demand experiments, minimizes the required number of animals, and maximizes the yield of PCLS from human lung samples.

Cryopreservation of PCLS allows a virtually unlimited storage duration and rewarming on demand (14–16). Yet, freezing of biological samples requires special equipment to control the freezing process, and air shipment using dry ice for temperature control is challenging due to strict regulations of the International Air Transport Association (IATA). Freezing may result in loss of intracellular water, ice crystal formation, and destruction of the cellular architecture, which calls for the use of cryoprotectants that can cause cellular lesions themselves (17–19). Although PCLS seem to withstand freeze-thaw procedures in terms of viability and airway constriction (14), a significant decrease in metabolic activity has been detected after cryopreservation (16, 20). A more "gentle" way to preserve tissue slices is long-term hypothermic (cold) storage at 4°C, which does not necessitate special devices and was already optimized for use in precision cut liver and kidney slices (21–23), but to the best of our knowledge has not been investigated yet for PCLS storage. Recently developed cold storage solutions have been successfully used for the preservation of human lung epithelial cells (A549), hepatocytes, and tissues such as blood vessels and striated muscles (24–26).

Thus, we here set out to analyze the effects of long-term cold storage in standard culture medium and two optimized preservation solutions (either with high potassium chloride concentrations or a chloride-poor, lactobionate-rich analog) on cellular viability, mitochondrial membrane potential, cell composition, inflammatory activation, and bronchoconstriction in rat PCLS.

METHODS

Chemicals

For Tyrode-buffer preparation, 2.68 mmol/L KCl (Carl Roth, Karlsruhe, Germany), 1.05 mmol/L $MgCl_2 \cdot 6H_2O$ (Sigma-Aldrich, St. Louis, MO), 0.42 mmol/L $NaH_2PO_4 \cdot 2H_2O$ (Merck KGaA, Darmstadt, Germany), 137 mmol/L NaCl (Carl Roth, Germany), 1.8 mmol/L $CaCl_2 \cdot 2H_2O$ (Carl Roth, Germany), 22 mmol/L $NaHCO_3$ (Carl Roth, Germany), and 5.5 mmol/L glucose monohydrate (Merck KGaA, Germany) were dissolved in double distilled water and cooled on ice until use for PCLS preparation. Afterward, pH was adjusted to 7.4 by carbogen gassing. Assays were performed in Dulbecco's modified Eagle's medium/nutrient mixture F-12 (1:1) without phenol red and L-glutamine (DMEM/F-12; Sigma-Aldrich, St. Louis, MO) supplemented with 1% penicillin-streptomycin (Sigma-Aldrich) and 0.1% gentamycin (Thermo Fisher, Waltham, MA). The low melting point agarose was purchased from Sigma-Aldrich. The cold storage solutions 1 and 2 were prepared in the Institute of Physiological Chemistry, Essen, Germany (Table 1). The supplement LK 614 (*N*-hydroxy-3,4-dimethoxy-*N*-methylbenzamide) was kindly provided by Dr. Franz Köhler Chemie, Bensheim, Germany, and deferoxamine mesylate was purchased from Novartis Pharma (Basel, Switzerland). For bronchoconstriction experiments, a stock solution (0.1 mol/L in DMEM/F-12) of ACh (Sigma-Aldrich) was prepared and stored at −80°C. The working solution (50 μmol/L in DMEM/F-12, final concentration 0.5 μmol/L) was freshly prepared at the day of the experiment.

Animals

For preparation of PCLS, male Wistar rats were purchased from Charles River Laboratories (Sulzfeld, Germany) and were kept in a standard animal housing unit providing an automated 12-h light/dark cycle and air conditioning. Animals were fed with a standard diet and drinking water ad libitum. Upon arrival in the animal housing, rats were kept for at least seven days before using them for PCLS preparation to allow a proper acclimatization (final weight 400–500 g). All experiments were in accordance with the German Animal Welfare Act of 18th May 2006 (BGB1, I S. 1206, 1313) and the European Parliament and Council Directive of 22nd September 2010 (2010/63/EU).

PCLS Preparation

For preparation of PCLS, a procedure as described by Herbert et al. (6) with some modifications was applied. Briefly, rats were anesthetized by intraperitoneal injection of a mixture of 75 mg/kg ketamine (Ketavet 100 mg/mL, zoetis Deutschland GmbH, Berlin, Germany) and 10 mg/kg

Table 1. *Composition of the applied preservation solutions and DMEM/F-12 culture medium*

	DMEM/F-12	*Solution 1*	*Solution 2*
Cl^-	126	103.1	8.1
Lactobionate			95
Na^+	133	16	16
K^+	0.4	93	93
$H_2PO_4^-$		1	1
SO_4^{2-}	0.4		
Mg^{2+}	1	8	8
Ca^{2+}	2.22	0.05	0.05
Glycine	0.25	10	10
Alanine	0.05	5	5
α-Ketoglutarate		2	2
Aspartate	0.05	5	5
N-acetylhistidine	0.15	30	30
Tryptophan	0.05	2	2
Sucrose		20	20
Glucose	17.5	10	10
HEPES buffer	15		
pH	7.0–7.6	7.0	7.0
Deferoxamine	(0.1)	(0.1)	(0.1)
LK 614	(0.02)	(0.02)	(0.02)

The concentrations of all compounds are given in mmol/L. Brackets mark concentrations of optionally added compounds.

xylazine (Xylasel 20 mg/mL; Selectavet Dr. Otto Fischer GmbH, Weyarn-Holzolling, Germany). The abdominal cavity was opened and the animals were euthanized by exsanguination. Afterward, the thorax was opened and the trachea was cannulated. Low melting point agarose (1.5% in DMEM/F-12) was gently heated until boiling and kept at 37°C. About 20 mL of liquid agarose were filled into the lung in situ, using a 20-mL syringe until the lung lobules were entirely filled. Afterward, the lung was removed from the thoracic cavity and cooled on ice for 10 min, followed by additional storage for 20 min in 4°C precooled DMEM/F-12 to allow complete solidification of the agarose solution. Subsequently, the lung lobes were separated and tissue cylinders with a diameter of 8 mm were generated using a biopsy punch. The cylinders were sliced into 250–300 μm thick PCLS using a Krumdieck Tissue Slicer (Alabama Research and Development, Munford, AL). Freshly prepared, ice-cold Tyrode-buffer (pH 7.4) was used as slicing medium. Slicing medium was changed after 5 cores and PCLS were collected in precooled DMEM/F-12. Afterward, PCLS were placed in an incubator (HeraCell 240i; Thermo Fisher Scientific, Waltham, MA) at 37°C and 5% CO_2 on a shaker (60 rpm) to partly wash out the agarose and to remove cellular debris. Medium was exchanged every 30 min for 1.5 h and afterward every 60 min for another 2 h.

Storage of PCLS and Preparation before Experimental Use

For the evaluation of viability after storage at 37°C, each PCLS was transferred into one well of a 24-well plate filled with 500 μL prewarmed DMEM/F-12. PCLS were incubated for up to 14 days without medium exchange to enable comparison with cold-stored slices. For cold storage, a 24-well plate was filled with DMEM/F-12, *solution 1*, or *solution 2*, each either with or without chelator additives (Table 1). Afterward, slices were transferred into the plates (one slice per well) and stored for 3–28 days at 4°C in the different storage solutions. As control, the following assays were also performed with unstored PCLS, held at 37°C for no longer than 24 h until the start of the experiment. At the end of the cold storage period, PCLS were transferred into 500 μL cold DMEM/F-12 and rewarmed to 37°C in the incubator on a shaker for 3 h (60 rpm) similar to the wash process directly after preparation.

Metabolic Activity in PCLS

To detect the effects of cold storage on overall slice metabolic activity, an Alamar Blue assay (Invitrogen, Carlsbad, CA) was performed. The Alamar Blue assay has been successfully used in PCLS (27) and is based on the reduction of resazurin to the fluorescent dye resorufin by metabolically active cells, and therefore serves as marker for cellular viability. One PCLS per solution was transferred into DMEM/F-12 and the Alamar Blue reagent was added in a relation of 1:10 according to the manual. After 2 h of incubation at 37°C, PCLS supernatant was transferred into a 96-well plate in duplicates. Fluorescence intensity was detected using a plate-reading photometer (Tecan Infinite 220 PRO, Tecan Group Ltd., Mennedorf, Switzerland) at excitation wavelength of 560 nm and an emission wavelength of 590 nm. Background fluorescence was subtracted and the signal intensity of cold-stored and rewarmed PCLS was compared with freshly prepared slices. For evaluation of the metabolic activity during cold storage, the same procedure was also applied to PCLS in the modified storage solutions at 4°C.

Calcein AM/Ethidium Homodimer-1 Staining

For qualitative evaluation of cold storage-induced cell death, a calcein acetoxymethyl/ethidium homodimer-1 (calcein AM/EthD-1) staining kit (Invitrogen, Karlsruhe, Germany) and subsequent evaluation by confocal microscopy was applied. Directly after preparation (*day 0*) as well as after cold storage in the modified solutions or DMEM/F-12 (*day 14*) and subsequent rewarming for 3 h, PCLS were stained with 4 μmol/L calcein AM (enzymatic conversion to the green, fluorescent dye calcein by living cells) and 4 μmol/L EthD-1 (cell impermeable dye that generates a red fluorescent signal at the cell nuclei) in DMEM/F-12 for 45 min. Afterward, lung slices were washed in phosphate buffered saline (PBS) and weighted with steel wires to prevent floating during investigation with a confocal microscope (Leica DMi-8; Leica Microsystems, Wetzlar, Germany) using a ×10 objective [excitation/emission maxima: 494/517 nm (calcein AM) and 528/617 nm (EthD-1)]. Z-stacks were generated for qualitative evaluation of PCLS viability and three-dimensional (3-D) images of PCLS were prepared by channel overlay with surface rendering applying equal settings to all images.

Analysis of Mitochondrial Membrane Potential

To analyze the effects of cold storage on mitochondria in PCLS, a tetramethylrhodamine methyl ester (TMRM) Assay Kit (Abcam, Cambridge, UK) in combination with confocal microscopy analysis was applied. TMRM is a cell permeable dye that accumulates in active mitochondria of viable cells and is used to detect mitochondrial membrane potential without the need for tissue fixation. Directly after preparation or after storage at 4°C, PCLS were transferred into DMEM/F-12 and rewarmed to 37°C for 3 h. TMRM staining was performed as indicated in the manufacturer's instructions. Staining solutions were prepared using serum-free DMEM/F-12 medium. PCLS were examined with an inverted confocal fluorescence microscope (Zeiss LSM 710, Carl Zeiss AG, Oberkochen, Germany), EC Plan-Neofluar ×10/0.30 M27 objective, 90-μm pinhole, in ×100 magnification using an excitation/emission wavelength of 548/573 nm. Two representative regions per slice were examined and Z-Stack images were generated. Mean fluorescence intensity of each image was calculated using ImageJ software (version 1.52a, National Institutes of Health, Bethesda, MD). Mean fluorescence intensity after storage is expressed in relation to that of unstored PCLS.

Preparation of Single-Cell Suspensions and Cell Type Identification

After storage for the indicated time periods and subsequent rewarming, 20 PCLS per solution were combined and incubated for 30 min in a digestion solution, containing 50 U/mL Dispase II (Corning, New York) in DMEM/F-12 medium. Single cells were prepared by passing the suspension through a cut 1-mL tip and afterward through a 100-μm cell

strainer. The strainer was washed with DMEM/F-12 containing 0.04 mg/mL DNAse I (Applichem, Darmstadt, Germany). Then, cells were passed through a 40-μm strainer and counted using a Neubauer counting chamber. Next, 500,000 cells per storage condition were blocked in PBS containing 1% bovine serum albumin (BSA, Sigma-Aldrich, St. Louis, MO) and afterward stained for 1 h with either mouse anti-rat CD45-FITC (Clone OX-1; 1:100) and mouse anti-rat EpCAM/TROP1-AF594 (Clone EGP40/1110; 1:100) or mouse anti-rat CD31/PECAM-1-AF647 (Clone TLD-3A12; 1:100) and mouse anti-rat CD90/Thy1-DL550 (Clone OX-7; 1:100) or respective isotype controls (all from Novus Biologicals, Centennial, CO). Afterward, cells were washed in PBS containing 1% BSA and fixed in 4% paraformaldehyde (PFA) for 15 min. After another washing step, cells were resuspended in PBS with 1% BSA and stored at 4°C until analysis using an Amnis ImageStreamX multispectral imaging flow cytometer (Amnis Corporation, Seattle, WA). Single cells in the focus of the attached microscope were gated and thereof, percentage of positively stained cells was calculated for each marker regarding autofluorescence and isotype controls (Amnis IDEAS version 6.2). Staining was visually confirmed by evaluation of microscopic cell images (×40 objective).

Inflammatory Cytokine Expression

To evaluate the functionality of inflammatory cells after cold storage, PCLS were rewarmed for 3 h and subsequently incubated in the presence or absence of 100 ng/mL lipopolysaccharide (LPS; Sigma-Aldrich, St. Louis, MO) in DMEM/F-12 for 24 h. Afterward, PCLS supernatant was removed, snap-frozen in liquid nitrogen and stored at −80°C. Expression of the inflammatory cytokine tumor necrosis factor-α (TNF-α) was quantified using an enzyme-linked immunosorbent assay kit (ELISA; DuoSet ELISA, R&D, Wiesbaden-Nordenstadt, Germany) according to the manufacturer's instructions.

Bronchoconstriction

PCLS were rewarmed for 3 h in DMEM/F-12 and weighted with a triangular steel wire in a 24-well plate. The prepared plate was transferred to the microplate-holder of an inverted microscope (Axio Observer D1, Carl Zeiss AG). Using the AxioCam HSm camera (Carl Zeiss AG) and the AxioVision software (Version 4.8.2.0, Carl Zeiss AG), airway cross-sections were observed for signs of vitality such as beating cilia on the airway epithelium and spontaneous muscle contractions. Before ACh application, the initial airway area was calculated. If slices showed spontaneous muscle tonus, the picture of the widest opening of the airway was used. Two minutes after ACh application (0.5 μmol/L final concentration), a second picture was taken to evaluate time-dependent airway constriction [Fig. 1; for a detailed discussion on bronchoconstriction and alternatives to ACh stimulation the reader is referred to the study by Herbert et al. (6)]. Afterward, airway area was measured using the AxioVision software. Bronchoconstriction of unstored slices was set as 100% and airway constriction of all cold-stored PCLS was related to that value. During bronchoconstriction experiments, airways were routinely inspected for the presence or absence of ciliary beating by video microscopy, which serves as additional marker for the functional status of PCLS.

Data Analysis

Data are presented as means ± SE. Statistical analyses were performed using GraphPad Prism Version 5.04 (GraphPad Software, San Diego, CA). Statistics were determined by two-way ANOVA with Bonferroni multiple comparison test. Viability of PCLS stored at 37°C was analyzed by one-way ANOVA with Dunnett's multiple comparison test. Detailed *n* numbers used for each experiment can be found in the figure legends. $P < 0.05$ was considered to be statistically significant.

RESULTS

Viability after Storage

To determine storage-dependent effects on PCLS viability, slices were stored for up to 14 days in the incubator at 37°C and 5% CO_2 without DMEM/F-12 medium change. Afterward, an Alamar Blue assay, based on the reduction of resazurin to the fluorescent dye resorufin, was performed, revealing a time-dependent decline in viability, which was significantly different from day ≥7 (68 ± 6%; $P < 0.05$ vs. *day 0*) and further decreased until *day 10* (60 ± 11%) with an almost complete loss on *day 14* (10 ± 7%). During cold storage, metabolic activity was significantly decreased in DMEM/F-12, *solution 1*, and *solution 2* (Table 1) with or without the iron chelators deferoxamine and LK 614 and ranged between 4 ± 1% and 6 ± 1% ($P < 0.001$ vs. incubator stored PCLS).

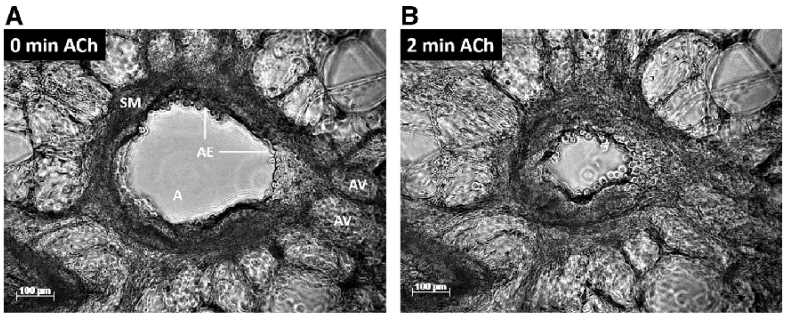

Figure 1. Precision-cut lung slices (PCLS) airway cross sections before (*A*) and 2 min after (*B*) stimulation with acetylcholine (ACh) (×200 magnification). A, airway area; AE, airway epithelium; AV, alveolar spaces; SM, smooth muscle. Scale bar, 100 μm.

To extend storage duration of PCLS without medium change, PCLS were cold-stored in DMEM/F-12 or two specifically designed preservation solutions (Table 1) with and without iron chelators at 4°C for 3–28 days and were subsequently rewarmed in DMEM/F-12 for 3 h. After 3 days of cold storage and rewarming to 37°C, viability decreased to 70%–80% with all tested solutions compared with unstored control PCLS (Fig. 2). After 7 days, viability of PCLS significantly decreased at all tested conditions ($P < 0.05$ vs. unstored). The viability of DMEM/F-12 stored PCLS was 51 ± 5% and 48 ± 6%, with and without addition of iron chelators, respectively. After storage in the chloride-rich *solution 1* and its chloride-poor analog *solution 2*, with and without iron chelators, the viability decreased to a lesser extent and was ~60% even after 14 days with a tendency for higher viability after storage in the chloride-rich *solution 1*. Storage in DMEM/F-12 led to continuously decreased viability with ongoing storage time to 8 ± 3% in the presence, and 4 ± 1% in the absence of iron chelators on *day 14*, which was significantly different to PCLS stored in *solution 1* ($P < 0.05$). After 28 days of cold storage of PCLS in DMEM/F-12 and subsequent rewarming, no resazurin reduction was detectable, indicating a complete loss of viability. Again, PCLS stored in *solution 1* (29 ± 7%) showed a tendency for higher viability compared with PCLS stored in *solution 2* (4 ± 2%). At all examined time points, no significant differences between solutions with and without addition of the chelators LK 614 and deferoxamine were observed (Fig. 2). Iron chelators showed beneficial effects for cold storage of vascular endothelial cells (28) and muscle tissue (25), which are also present in PCLS. In addition, iron chelators showed a tendency for higher viability in the current study and did not exert negative effects. Thus, the cold storage solutions were supplemented with the iron chelators LK 614 and deferoxamine in all subsequent experiments.

In addition to the assessment of the metabolic activity, cellular viability after 14 days of cold storage was evaluated by live/dead staining. After 14 days of cold storage, PCLS stored in DMEM/F-12 showed a strong reduction in viability and an increased number of dead cells (Fig. 3*B*). In contrast, PCLS stored in *solution 1* (Fig. 3*C*) and *solution 2* (Fig. 3*D*) exhibited a tissue viability comparable with unstored slices (Fig. 3*A*).

Mitochondrial Membrane Potential

Mitochondrial membrane potential of PCLS after 3 days of cold storage and rewarming was comparable with unstored PCLS for all preservation solutions (Fig. 4). After 7 days of cold storage in DMEM/F-12, the mitochondrial membrane potential was significantly lower (54 ± 12%; $P < 0.05$) than in nonstored controls (Fig. 5*A*) whereas that was not the case for PCLS stored in *solution 1* (83 ± 12%) or *solution 2* (74 ± 9%). After 14 days, however, there was also a significant difference ($P < 0.05$) of the mitochondrial membrane potential of PCLS stored in DMEM/F-12 (18 ± 5%; Fig. 5*B*) compared with PCLS stored in *solution 1* (95 ± 5%; Fig. 5*C*). Fourteen days of cold storage in *solution 2* resulted in 60 ± 5% mitochondrial membrane potential (Fig. 5*D*). After 28 days, the mitochondrial membrane potential of PCLS stored in *solution 1* was still 56 ± 5% of unstored control which was significantly higher than after cold storage in *solution 2* (9 ± 1%; $P < 0.05$) or DMEM/F-12 (1 ± 1%; Fig. 4).

Preservation of Specific Cell Populations

Single-cell suspension of unstored PCLS contained a total of $3.73 \pm 0.32 \times 10^6$ cells per 20 PCLS. After cold storage, cell numbers significantly decreased in DMEM/F-12 stored samples after 7 (1.46 ± 0.25 mio. cells; $P < 0.001$ vs. unstored) and 14 days (0.51 ± 0.16 mio. cells; $P < 0.001$ vs. unstored). PCLS cold-stored in *solution 2* contained a total of 2.39 ± 0.09 mio. cells after 7 days ($P < 0.01$ vs. unstored), and 1.89 ± 0.16 mio. after 14 days ($P < 0.001$ vs. unstored). In contrast, 2.83 ± 0.11 mio. cells (*day 7*) and 2.75 ± 0.24 mio. cells ($P < 0.05$ vs. unstored; *day 14*) were present after storage in *solution 1*. After 7 and 14 days, cell numbers were significantly higher in PCLS stored in *solution 1* than in DMEM/F-12 ($P < 0.05$). Furthermore, storage in *solution 2* preserved a higher number of cells than DMEM/F-12 after 14 days of cold storage (Fig. 6*A*; $P < 0.05$). Staining for inflammatory (CD45), epithelial (EpCAM), endothelial (CD31), or mesenchymal (CD90) cell types without storage revealed a proportion of 23.7 ± 1.9% $CD45^+$, 14.4 ± 0.9% $EpCAM^+$, 25.3 ± 3.3% $CD31^+$, and 14.7 ± 1.8% $CD90^+$ cells (Fig. 6*B*). Relation of $EpCAM^+$ (Fig. 6*C*) and $CD90^+$ cells (Fig. 6*D*) did not change during cold storage in any of the

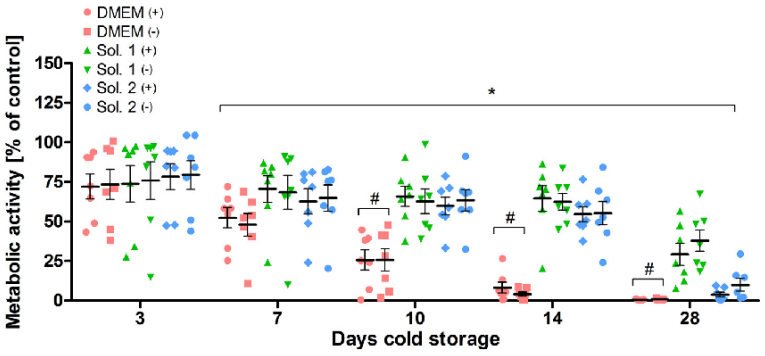

Figure 2. Alamar Blue conversion by precision-cut lung slices (PCLS) stored at 4°C in different cold storage solutions followed by rewarming. After preparation, PCLS were stored at 4°C for 3–28 days in DMEM/F-12, *solution 1* (chloride-rich) or *solution 2* (chloride-poor), either with (+) or without (−) addition of the chelators *N*-hydroxy-3,4-dimethoxy-*N*-methylbenzamide (LK 614, 0.02 mmol/L) and deferoxamine (0.1 mmol/L), followed by 3 h rewarming in DMEM/F-12 medium. Afterward, changes in viability were determined using an Alamar Blue assay and are shown as % of unstored PCLS. Data are presented as means ± SE ($n = 7$ PCLS from 7 different animals). Statistical significance: *$P < 0.05$ vs. control; #$P < 0.05$ vs. slices stored in *solution 1*.

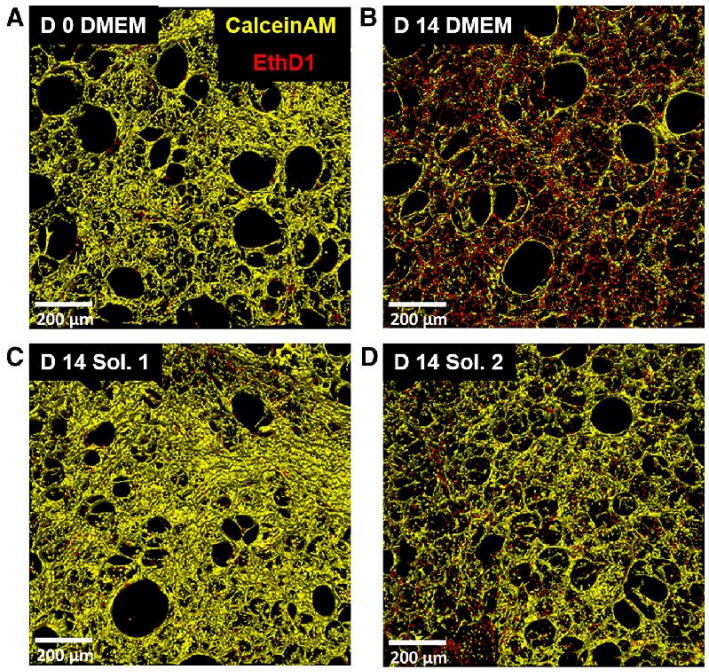

Figure 3. Representative images of live/dead staining in precision-cut lung slices (PCLS) stored at 4°C in different cold storage solutions followed by rewarming. After preparation, PCLS were either analyzed directly (*A*) or stored for 14 days at 4°C in DMEM/F-12 (*B*), *solution 1* (chloride-rich; *C*), or *solution 2* (chloride-poor; *D*), supplemented with the chelators *N*-hydroxy-3,4-dimethoxy-*N*-methylbenzamide (LK 614, 0.02 mmol/L) and deferoxamine (0.1 mmol/L), followed by 3 h rewarming in DMEM/F-12 medium. Afterward, PCLS were stained with calcein acetoxymethyl (calcein AM, yellow, indicating the cytosol of living cells) or ethidium homodimer-1 (EthD1, red, indicating nuclei of dead cells) in DMEM/F-12 and analyzed by confocal microscopy (×100 magnification, scale bar = 200 µm). Images were created by three-dimensional (3-D) surface rendering of Z-stacks and are representative examples of n = 3 PCLS from three different animals.

applied storage solutions. In contrast, proportion of $CD45^+$ cells significantly decreased after 7 days of cold storage in DMEM/F-12 (13.0 ± 1.9%; $P < 0.01$ vs. unstored), whereas storage in *solution 1* or *solution 2* led to a better preservation (18.1 ± 2.0% and 16.0 ± 1.9%, respectively, not significant). After 14 days of cold storage, $CD45^+$ cells further decreased to 11.3 ± 1.3% (*solution 1*) and 12.7 ± 1.1% (*solution 2*), whereas DMEM/F-12 stored PCLS did not contain enough viable cells for analysis (Fig. 6*E*). Proportion of $CD31^+$ cells was only significantly decreased after storage for 14 days in *solution 2* (13.9 ± 1.0%; Fig. 6*F*).

TNF-α Expression

Unstored PCLS expressed only low amounts of TNF-α after 24 h of incubation in DMEM/F-12 at 37°C (9.2 ± 2.1 pg/mL). In contrast, TNF-α expression was significantly ($P < 0.001$) increased after stimulation for 24 h with 100 ng/mL LPS (164.6 ± 27.0 pg/mL; Fig. 7*A*). No change in cytokine expression was observed after storage for up to 28 days in DMEM/F-12, *solution 1*, or *solution 2* without LPS stimulation. Significant TNF-α expression after LPS stimulation was observed in PCLS stored in DMEM/F-12 (65.6 ± 12.3 pg/mL) or

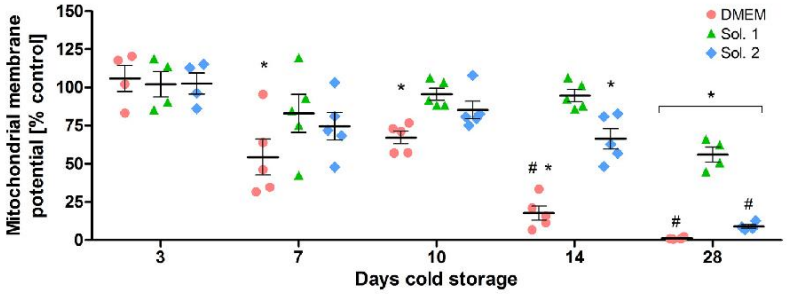

Figure 4. Mitochondrial membrane potential in precision-cut lung slices (PCLS) stored at 4°C in different cold storage solutions followed by rewarming. After preparation, PCLS were stored at 4°C for 3–28 days in DMEM/F-12, *solution 1* (chloride-rich), or *solution 2* (chloride-poor), supplemented with the iron chelators *N*-hydroxy-3,4-dimethoxy-*N*-methylbenzamide (LK 614, 0.02 mmol/L) and deferoxamine (0.1 mmol/L), followed by 3 h rewarming in DMEM/F-12 medium. Afterward, mitochondrial membrane potential was assessed using a tetramethylrhodamine methyl ester (TMRM) staining with subsequent confocal microscopy. Mean fluorescence intensity was calculated using ImageJ software and is shown as % of unstored PCLS. Data are presented as means ± SE ($n_{(D3,\ D28)}$ = 4; $n_{(D7,\ D10,\ D14)}$ = 5 PCLS from 4 or 5 different animals). Statistical significance: *$P < 0.05$ vs. unstored slices; #$P < 0.05$ vs. slices stored in *solution 1*.

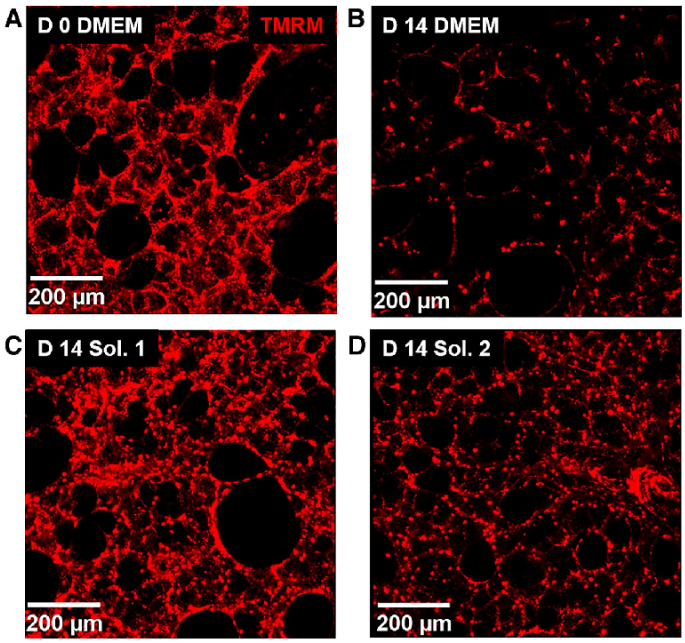

Figure 5. Representative images of tetramethylrhodamine methyl ester (TMRM)-stained precision-cut lung slices (PCLS) after 14 days of cold storage followed by rewarming. After preparation, PCLS were either analyzed directly (*A*) or stored for 14 days at 4°C in DMEM/F-12 (*B*), *solution 1* (*C*), or *solution 2* (*D*) followed by 3 h rewarming in DMEM/F-12 medium. Afterward, mitochondrial membrane potential was assessed by TMRM staining (red, indicating the presence of mitochondrial membrane potential) with subsequent confocal microscopy (×100 magnification, scale bar = 200 µm).

solution 2 (102.7 ± 32.7 pg/mL; Fig. 7*C*) after 3 days but decreased substantially after 7 days of cold storage. In contrast, a significant LPS-dependent TNF-α expression was observable in *solution 1*-stored slices for up to 10 days of storage (45.3 ± 13.6 pg/mL; Fig. 7*B*, $P < 0.05$ vs. unstimulated control).

Bronchoconstriction

As additional, functional parameter for the quality of PCLS after cold storage, the ability of airways in PCLS to constrict upon acetylcholine stimulus was analyzed (Fig. 8). A massive impairment of bronchoconstriction induced by cold storage in DMEM/F-12 was observed between *day 10* and *14*, with an almost complete loss of bronchoconstriction (4.7 ± 2.6%). In addition, bronchoconstriction was significantly impaired after cold storage of PCLS in *solution 2* (59.9 ± 9.4%; $P < 0.05$ vs. unstored) whereas storage in *solution 1* resulted in bronchoconstriction very similar to control values. The constriction after ACh stimulus further decreased after storage in DMEM/F-12 (5.9 ± 2.1%) and in *solution 2* (13.0 ± 3.2%) on *day 28* but was still 74.3 ± 11.7% in *solution 1*-stored PCLS. As a secondary finding during bronchoconstriction experiments, ciliary beating was observed in all slices directly after preparation and after 3 days of cold storage but substantially decreased after 7 days of cold storage in DMEM/F-12 until no beating was observed after 14 days of storage. In contrast, 92% of the airways of PCLS stored in *solution 1* showed ciliary beating after 28 days of cold storage. Ciliary beating in airways of PCLS stored in *solution 2* was also preserved in part of the slices after 28 days of storage (58%).

DISCUSSION

To provide optimal tissue protection during PCLS cold storage, we investigated the protecting properties of standard culture medium DMEM/F-12 as well as of a potassium and chloride-rich tissue preservation solution (*solution 1*, TiProtec) and a chloride-poor, lactobionate-rich version thereof (*solution 2*; detailed composition of the solutions can be found in Table 1). *Solution 1* has been optimized for cold storage of vascular grafts (28), but subsequently also proved to be beneficial for cold storage of muscle tissue (25) and human hepatocytes (29). Its chloride-poor derivative *solution 2* yielded superior protection for rat hepatocytes during prolonged cold storage (24). In addition, use of chloride-rich preservation solutions was found to be beneficial for the preservation of human epithelial cell lines and mice lung tissue samples after cold storage for 3 days (30).

Reducing the preservation temperature is essential to suppress metabolic rate, sustain energy supply, and enhance defense mechanisms, especially when oxygen supply is limited (31). As indicated by the Alamar Blue assay, metabolic activity is highly reduced in all storage solutions during cold storage compared with unstored control PCLS (between 4.0 ± 0.8% and 6.0 ± 1.3%). Under ischemic/hypoxic conditions, oxidative phosphorylation ceases and adenosine triphosphate (ATP) is consumed rapidly during cold storage, resulting in impaired cellular homeostasis and cell function finally causing cellular death (32). Additional cold storage-dependent injury may arise due to the generation of reactive oxygen species (ROS) or increased cytokine production (33, 34). An important underlying mechanism of cold storage-

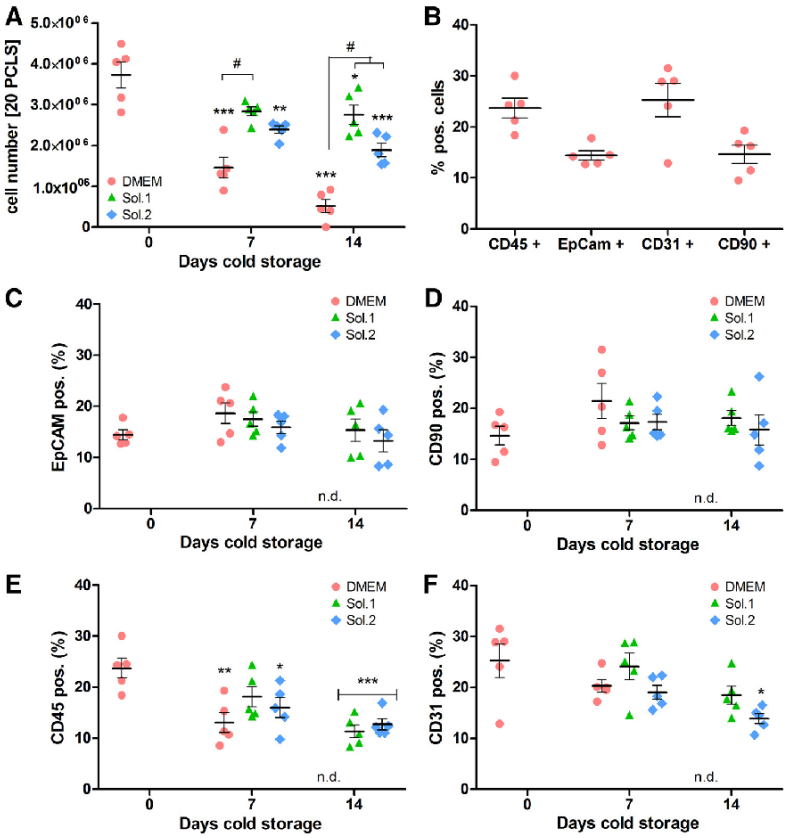

Figure 6. Proportion of cell types present in precision-cut lung slices (PCLS) stored at 4°C in different cold storage solutions followed by rewarming. After preparation, 20 PCLS were either analyzed directly or stored for 14 days at 4°C in DMEM/F-12, *solution 1* (chloride-rich), or *solution 2* (chloride-poor), supplemented with the chelators *N*-hydroxy-3,4-dimethoxy-*N*-methylbenzamide (LK 614, 0.02 mmol/L) and deferoxamine (0.1 mmol/L), followed by 3 h rewarming in DMEM/F-12 medium. Afterward, single-cell suspensions were prepared, cells were counted (*A*) and proportions of $CD45^+$, $EpCam^+$, $CD31^+$, or $CD90^+$ cells, either directly after preparation (*B*) or after 7 and 14 days of cold storage (*C*–*F*), were analyzed. Data are presented as means ± SE (n = 5 samples from 5 different animals). Statistical significance: $*P < 0.05$; $**P < 0.01$; $***P < 0.001$ vs. unstored PCLS, $\#P < 0.05$ vs. DMEM stored PCLS; n.d., not detectable due to low cell number.

dependent ROS formation is an increase in the cellular chelatable iron pool contributing to cold-induced apoptosis (35).

To counteract cold-induced iron-dependent injury, iron chelators were added to the preservation solutions. The small lipophilic iron chelator LK 614 is used to enter cells in the early phase of cold storage and chelate iron before ROS are generated. The large hexadentate chelator deferoxamine has been found to prevent endothelial dysfunction in early stages of cold storage (28). Deferoxamine is a known reducer of iron-dependent ROS formation (36, 37) that acts via complex formation with Fe^{3+} iron. In this study, we were not able to detect significant improvement of viability by the addition of deferoxamine and LK 614 to preservation solutions. However, addition of both chelators led to a nonsignificant improvement of mitochondrial membrane potential of DMEM/F-12 after 10 days (67 ± 4% vs. 50 ± 5%) and *solution 2* after 14 days (66 ± 7% vs. 52 ± 3%; data not shown for chelator-free solutions in Fig. 4) of cold storage. It has already been shown that deferoxamine and LK 614 can prevent mitochondrial alterations during cold storage of rat proximal tubular cells (38), A549 lung epithelial cells (26), and hepatocytes (24, 29). However, previous studies suggested a higher sensitivity of cultured cells toward cold preservation iron-dependent injury compared with more complex tissues or to cells in suspension (24). This might explain why no significant changes occurred during the first 3 days of storage (Fig. 2) and why the effect of iron chelators was small in the present study. Furthermore, A549 cells are adenocarcinomic alveolar cells and elevated ROS production is observed in almost all cancers (39), suggesting also a stronger effect of ROS and thus of antioxidative self-defense strategies.

Warm storage of PCLS at 37°C and 5% CO_2 without medium change resulted in a significant loss of viability from *day 7* to *day 14*, suggesting depletion of energy and loss of buffer capacity (40). The live span of PCLS can be improved for up to 14 days by the introduction of daily medium exchange (12). However, for transport and shipment, maintenance of 37°C and gassing with 5% CO_2 is challenging. Therefore, it was reasonable to evaluate the viability after long-term storage at 4°C in cell culture medium. Cold storage in DMEM/F-12 culture medium and rewarming led to a continuous loss of viability resulting in 30 ± 10% after 10 days, which is substantially lower than in PCLS stored permanently at 37°C (58 ± 14%). The process of cooldown to 4°C, maintenance of this temperature during storage, and the subsequent rewarming in culture medium has been found to induce blebbing of the plasma membrane, cell detachment, and DNA fragmentation finally resulting in apoptosis (41).

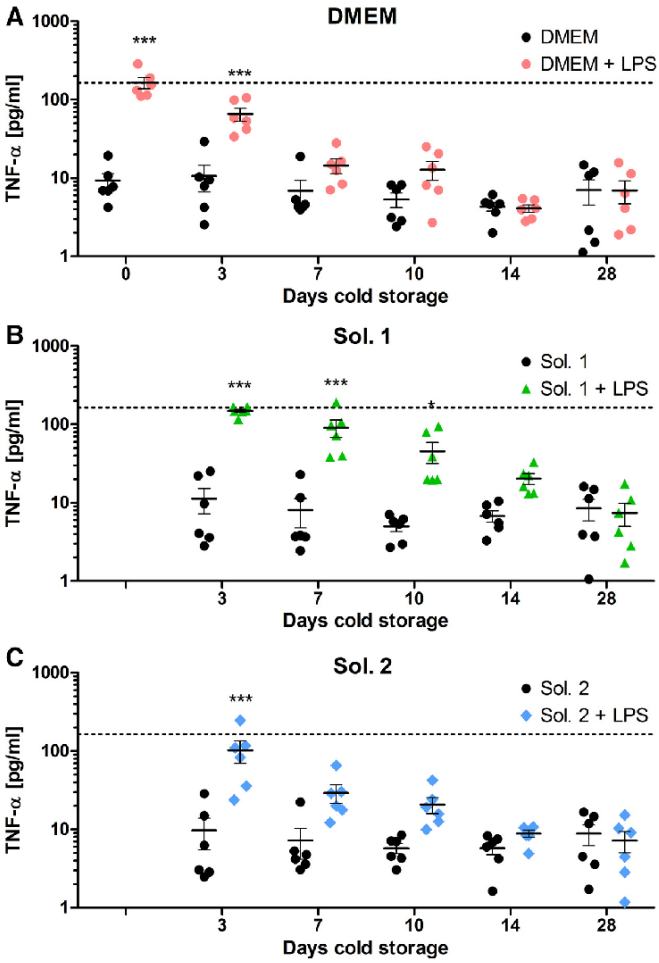

Figure 7. Release of tumor necrosis factor-α (TNF-α) from precision-cut lung slices (PCLS) stored at 4°C in different storage solutions followed by rewarming with or without lipopolysaccharide (LPS) stimulation for 24 h. After preparation, PCLS were either exposed directly to DMEM/F-12 with, or without 100 ng/mL LPS or stored for 14 days at 4°C in DMEM/F-12 (*A*), *solution 1* (chloride-rich; *B*), or *solution 2* (chloride-poor; *C*), supplemented with the iron chelators *N*-hydroxy-3,4-dimethoxy-*N*-methylbenzamide (LK 614, 0.02 mmol/L) and deferoxamine (0.1 mmol/L), followed by 3 h rewarming in DMEM/F-12 medium. Afterward, expression of TNF-α in the supernatant of unstimulated and LPS exposed PCLS was detected by ELISA. Cytokine expression is shown in pg/mL supernatant, dashed line (---) shows the TNF-α expression without cold storage after LPS stimulation. Data are presented as means ± SE, $n = 6$ PCLS from 6 different animals. Statistical significance: $^{*}P < 0.05$, $^{***}P < 0.001$ vs. PCLS incubated with medium without LPS.

During cold storage, function of ion pumps like the Na^+/K^+-ATPase is reduced, which has been suggested to impede maintenance of ion equilibrium leading to cell swelling and necrosis (42). However, in the presence of iron chelators, cold storage in chloride-rich preservation solutions, with chloride concentrations comparable with cell culture medium, proved to be superior to cold storage in chloride-poor organ preservation solutions for cell types such as rat proximal tubules and porcine aortic endothelial cells (28, 43).

To provide an optimal environment for cold storage of tissues, improved preservation solutions were applied containing additional protective compounds. In our experiments, both solutions significantly decreased cell injury compared with DMEM/F-12-stored PCLS after long-term hypothermic storage (Fig. 2). Evaluation of live/dead staining, which is frequently used for analysis of PCLS viability (12, 44), revealed viable tissue after 14 days of cold storage in *solution 1* and *solution 2*, that was comparable with unstored PCLS. In contrast, PCLS cold stored in DMEM/F-12 contained only a few viable cells but a high number of EthD1-stained nuclei, indicating substantial cell death which is in line with the metabolic activity (cf. Figs. 2 and 3).

Mitochondria are thought to play a crucial role in apoptosis and necrosis after cold storage and lose membrane potential during rewarming. Furthermore, swelling of mitochondria and loss of inner mitochondrial membrane was observed after 24 h cold storage of proximal tubular cells (29, 38). Cold storage is known to induce ROS production (45–47) associated with mitochondrial damage (47, 48). Therefore, we analyzed the mitochondrial membrane potential after cold storage and rewarming. After 3 days of storage, no change in membrane potential was observed, thus the process of cooldown and rewarming seems to have no direct negative impact on mitochondria during early phase of cold storage (Fig. 4). *Solutions 1* and *2* both preserved mitochondria significantly better than standard culture medium after 14 days, which underlines the need for the earlier discussed supplements during cold storage of PCLS.

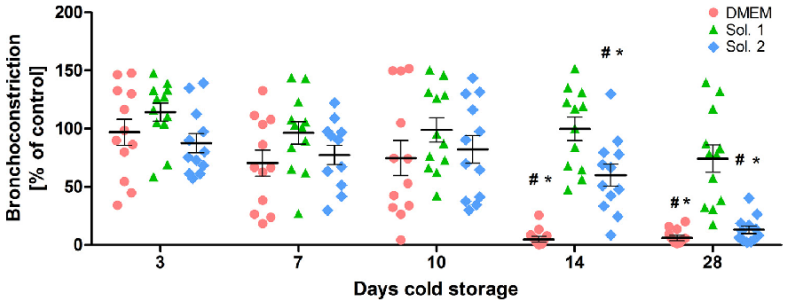

Figure 8. Airway constriction in precision-cut lung slices (PCLS) stored at 4°C in different cold storage solutions followed by rewarming. After preparation, PCLS were stored for up to 28 days at 4°C in DMEM/F-12, *solution 1* (chloride-rich), or *solution 2* (chloride-poor), supplemented with the chelators *N*-hydroxy-3,4-dimethoxy-*N*-methylbenzamide (LK 614, 0.02 mmol/L) and deferoxamine (0.1 mmol/L) followed by 3 h rewarming in DMEM/F-12 medium. Afterward, airway constriction upon acetylcholine (ACh) stimulus (0.5 μmol/L) and 2-min incubation was examined using an inverted microscope. Cross-sectional airway-area was calculated before as well as 2 min after addition of ACh. Thereof, percentage of bronchoconstriction was calculated and expressed as relation to constriction of unstored PCLS. Data are presented as means ± SE ($n = 12$ airways from at least 4 different animals). Statistical significance: $*P < 0.05$ vs. unstored slices. $\#P < 0.05$ vs. *solution 1*-stored PCLS.

As the aforementioned parameters were used to study the overall tissue viability without taking the distribution of specific cell types into account, we analyzed whether cold storage in the modified solutions or DMEM/F-12 has effects on the cell composition of PCLS. Single-cell suspensions of PCLS were prepared and stained for $CD45^+$ immune cells, $EpCAM^+$ epithelial cells, $CD31^+$ endothelial cells, and $CD90^+$ mesenchymal cells to evaluate cell populations that are of interest for PCLS research (49–51). Cell numbers of PCLS stored in DMEM/F-12 were significantly lower than after storage in *solution 1* at *day 7* and after storage in both modified solutions at *day 14*, which is in line with the tissue viability analyzed by Alamar Blue conversion (Fig. 6*A*). This is of special importance because single-cell suspensions from PCLS are used for the investigation of endpoints like immune cell activation or live/dead staining (13, 52).

The observed proportion of cell populations is in line with observations from other groups, where $CD45^+$ cells are represented in high numbers, whereas only a small proportion of cells is EpCAM-positive (53, 54). However, the proportion of cell types observed in single-cell suspensions is highly dependent on the protocol and enzymes used for digestion, which may affect cell dissociation efficiency but also the presence or absence of surface markers (53, 55). Evaluation of immunofluorescence staining data of the single-cell suspensions revealed that the proportions of epithelial ($EpCAM^+$) and mesenchymal ($CD90^+$) cells are not affected by cold storage in the different storage solutions (Fig. 6). In addition, proportion of endothelial cells ($CD31^+$) remained unchanged during storage for 7 days and was only significantly decreased after 14 days of storage in *solution 2*, while no such effect was observed after storage in *solution 1*. Strongest effects of cold storage were seen analyzing the population of $CD45^+$ immune cells (Fig. 6*E*). Thereby, proportion of immunological cells was significantly decreased after cold storage for 7 days in DMEM/F-12, while a less strong decrease was observed after storage in the modified storage solutions. The proportion significantly decreased after storage for 14 days in *solution 1* and *solution 2* and revealed that inflammatory cells like macrophages are more susceptible toward cold storage injury than epithelial, endothelial, or mesenchymal cell populations. The use of modified storage solutions can not only preserve a higher number of cells after cold storage in general but can also protect sensitive immune cells better than standard DMEM/F-12 culture medium. Furthermore, maintenance of the cellular composition enables the use of cold-stored PCLS for metabolomic, proteomic, or transcriptomic approaches (51, 56).

As the population of inflammatory cells decreased after cold storage in all solutions, we analyzed the basal inflammatory activation level and whether PCLS responded to an inflammatory stimulus. Analysis of inflammatory activation is a major advantage of PCLS to study the cellular response toward viral infections or chemical exposures. Thereby, the amount of inflammatory cells in PCLS is comparable with the amount of resident inflammatory cells in vivo which enables a realistic evaluation of inflammatory response (1). Basal TNF-α expression, as marker for inflammatory tissue injury (57), was not increased after cold storage in any of the storage solutions, indicating a minor effect of inflammatory activation (cf. Fig. 7*A*, 0 days vs. other tested conditions). After cold storage for 10 days and subsequent LPS stimulation to induce an inflammatory response (58), PCLS cold-stored in *solution 1* released significantly higher concentrations of TNF-α compared with slices without LPS stimulation. In contrast, PCLS stored in DMEM/F-12 or *solution 2* showed no inflammatory response when stored for longer than 3 days (Fig. 7). Therefore, PCLS cold-stored in *solution 1* respond substantially longer to an inflammatory stimulus than PCLS stored in the other solutions. Compared with overall viability, the inflammatory response after cold storage and rewarming decreased faster in all storage solutions but is well comparable with the proportion of inflammatory cells (compare Fig. 2 vs. Fig. 6 vs. Fig. 7). Inflammatory response of macrophages seems to be more sensitive toward cold storage than overall tissue viability and is in line with data of long-term PCLS warm storage (12). Our data indicate that a chloride-rich environment is essential for long-term cold preservation of inflammatory cells in PCLS and that

chloride substitution by lactobionate is not beneficial to preserve functional inflammatory response.

Besides evaluation of viability and inflammatory activity, PCLS are frequently used for the detection of airway constriction. Concurrently, constriction of airways requires intact tissue architecture and cooperation of different cellular structures which allows a general evaluation of PCLS functionality (6, 12, 59). Our results show well preserved airway response for up to 10 days in all storage solutions (Fig. 8). Keeping in mind that the lung tissue got stressed by agarose filling, slicing, cooldown, cold storage, and rewarming, these results remarkably underline the robustness of the PCLS model. Strong differences were observed after 14 days of cold storage. Although the overall cellular viability, detected via Alamar Blue assay, decreased significantly already after 10 days of storage in DMEM/F-12, bronchoconstriction was fully preserved (cf. Fig. 2 and Fig. 8). This suggests that the airways maintained the ability to constrict, even if overall viability was already decreased. The optimized storage solutions preserved ciliary beating after 28 days of cold storage and rewarming, which is a major improvement toward DMEM/F-12-stored slices that lost ciliary beating completely after 14 days. It is important to note, that only the presence or absence of ciliary beating was visually assessed in the current study but not the speed or frequency of ciliary beating. Future studies should evaluate the beating frequency after cold storage using a high-frame rate camera (8). The aforementioned preservation solutions contain various compounds to address different mechanisms of injury: addition of glycine and alanine to the solutions limits the increase of cytosolic sodium via prevention of nonspecific leak formation, which was found to be protective against hypoxic cell injury that might occur in submersed PCLS (60, 61). However, hypoxic injury is unlikely to occur during PCLS cold storage as the tissue sections are thin (~250 μm) and solubility of oxygen in the storage solutions is increased at lower temperatures. In addition, oxygen consumption during cold storage is decreased and it has been found that low levels of oxygen are beneficial for the preservation of mitochondrial function in cold storage of whole lung (62). Hypoxic injury might play a stronger role for thicker PCLS, that are often prepared from human tissue (>500 μm), and for cold storage of tissue cores before slicing. Tryptophan and α-ketoglutarate are major ingredients of the histidine-tryptophan-ketoglutarate solution used in organ transplantation to stabilize cellular membranes and to serve as substrate for ATP production, which is limited during cold storage (63). In addition, α-ketoglutarate has been found to reduce the generation of hydrogen peroxide, thus it can help to provide protection against reactive oxygen species (64). Aspartate helps to replenish the tricarboxylic acid cycle securing energy supply. Furthermore, to maintain the optimal buffering conditions, the naturally occurring histidine derivate *N*-acetylhistidine was added, which is less cytotoxic than high concentrations of histidine or of phosphate (28, 65). Control of osmotic cell swelling during preservation is essential to maintain cellular viability, which can be achieved by the addition of impermeable osmolytes like sucrose (66), an acidic pH is known to offer protection against hypoxic injury (67), and a low calcium concentration can provide protection against diverse types of injury (68, 69).

Although *solution 1* contains a high physiological extracellular concentration of chloride, the major part of chloride was substituted in *solution 2* by the large organic anion lactobionate (Table 1). *Solution 1* provided significantly better preservation after 14 days of cold storage compared with *solution 2* regarding the functional parameters mitochondrial membrane potential and bronchoconstriction and preserved inflammatory response for longer time. Although 14 days substantially extend shipment durations it is obvious that the PCLS have functional limitations before the cells finally die. Chloride efflux has been found to occur during early stages of cold storage, which can be diminished by high extracellular chloride concentrations used in *solution 1* (70). Lactobionate has been found to prevent tissue edema formation during cold storage (71) but had minor impact on overall tissue viability than using chloride as main anion in our experiments. Therefore, choosing chloride rather than lactobionate as main anion in the improved base solution provides substantial improvement during cold storage of PCLS.

Conclusions

Taken together, the optimized potassium chloride-rich preservation *solution 1* provided superior tissue protection to its chloride-poor analog *solution 2* and standard culture medium DMEM/F-12 for long-term cold storage and shipment of PCLS.

ACKNOWLEDGMENTS

The authors thank Dr. M. Lehmann and Q. Hu for advice in preparation of single-cell suspensions and FACS analysis. Furthermore, the authors thank L. Seck for excellent assistance in PCLS preparation and measurement of bronchoconstriction.

Present address for T. Wille: Bundeswehr Medical Academy, Ingolstädter Straße 240, 80939 Munich, Germany.

GRANTS

This work was supported from the German Research Foundation (GRK 2338, Targets in Toxicology); project P02 (to T.W. and F.W.); J.T. received a PhD stipend in the GRK 2338.

DISCLOSURES

U.R. has been a consultant of Dr. Franz Köhler Chemie and is listed as one of the inventors in the patents the company holds on the preservation solutions Custodiol-N, TiProtec, and Custodiol-MP. U.R. received some funding for scientific projects by the company, but this is unrelated to the current study. None of the other authors has any conflicts of interest, financial or otherwise, to disclose.

AUTHOR CONTRIBUTIONS

J.T., U.R., and T.W. conceived and designed research; J.T. performed experiments; J.T. analyzed data; J.T., U.R., and T.W. interpreted results of experiments; J.T. prepared figures; J.T. drafted manuscript; F.E., F.W., H.T., U.R., and T.W. edited and revised manuscript; J.T., F.E., F.W., H.T., U.R., and T.W. approved final version of manuscript.

REFERENCES

1. **Liu G**, **Betts C**, **Cunoosamy DM**, **Åberg PM**, **Hornberg JJ**, **Sivars KB**, **Cohen TS.** Use of precision cut lung slices as a translational

model for the study of lung biology. *Respir Res* 20: 162, 2019. doi:10.1186/s12931-019-1131-x.

2. **Parrish AR**, **Gandolfi A**, **Brendel K.** Precision-cut tissue slices: applications in pharmacology and toxicology. *Life Sci* 57: 1887–1901, 1995. doi:10.1016/0024-3205(95)02176-J.
3. **Behrsing HP**, **Furniss MJ**, **Davis M**, **Tomaszewski JE**, **Parchment RE.** In vitro exposure of precision-cut lung slices to 2-(4-amino-3-methylphenyl)-5-fluorobenzothiazole lysylamide dihydrochloride (NSC 710305, Phortress) increases inflammatory cytokine content and tissue damage. *Toxicol Sci* 131: 470–479, 2013. doi:10.1093/toxsci/kfs319.
4. **Hirn S**, **Haberl N**, **Loza K**, **Epple M**, **Kreyling WG**, **Rothen-Rutishauser B**, **Rehberg M**, **Krombach F.** Proinflammatory and cytotoxic response to nanoparticles in precision-cut lung slices. *Beilstein J Nanotechnol* 5: 2440–2449, 2014. doi:10.3762/bjnano.5.253.
5. **Henjakovic M**, **Sewald K**, **Switalla S**, **Kaiser D**, **Müller M**, **Veres TZ**, **Martin C**, **Uhlig S**, **Krug N**, **Braun A.** Ex vivo testing of immune responses in precision-cut lung slices. *Toxicol Appl Pharmacol* 231: 68–76, 2008. doi:10.1016/j.taap.2008.04.003.
6. **Herbert J**, **Thiermann H**, **Worek F**, **Wille T.** Precision cut lung slices as test system for candidate therapeutics in organophosphate poisoning. *Toxicology* 389: 94–100, 2017. doi:10.1016/j.tox.2017.07.011.
7. **Herbert J**, **Thiermann H**, **Worek F**, **Wille T.** COPD and asthma therapeutics for supportive treatment in organophosphate poisoning. *Clin Toxicol (Phila)* 57: 644–651, 2019. doi:10.1080/15563650.2018.1540785.
8. **Wohlsen A**, **Martin C**, **Vollmer E**, **Branscheid D**, **Magnussen H**, **Becker WM**, **Lepp U**, **Uhlig S.** The early allergic response in small airways of human precision-cut lung slices. *Eur Respir J* 21: 1024–1032, 2003. doi:10.1183/09031936.03.00027502.
9. **Fryer AD**, **Lein PJ**, **Howard AS**, **Yost BL**, **Beckles RA**, **Jett DA.** Mechanisms of organophosphate insecticide-induced airway hyperreactivity. *Am J Physiol Lung Cell Mol Physiol* 286: L963–L969, 2004. doi:10.1152/ajplung.00343.2003.
10. **Liberati TA**, **Randle MR**, **Toth LA.** In vitro lung slices: a powerful approach for assessment of lung pathophysiology. *Expert Rev Mol Diagn* 10: 501–508, 2010. doi:10.1586/erm.10.21.
11. **Russell WMS**, **Burch RL.** *The Principles of Humane Experimental Technique*. London: Methuen, 1959.
12. **Neuhaus V**, **Schaudien D**, **Golovina T**, **Temann U-A**, **Thompson C**, **Lippmann T**, **Bersch C**, **Pfennig O**, **Jonigk D**, **Braubach P**, **Fieguth H-G**, **Warnecke G**, **Yusibov V**, **Sewald K**, **Braun A.** Assessment of long-term cultivated human precision-cut lung slices as an ex vivo system for evaluation of chronic cytotoxicity and functionality. *J Occup Med Toxicol* 12: 13, 2017. doi:10.1186/s12995-017-0158-5.
13. **Li G**, **Cohen JA**, **Martines C**, **Ram-Mohan S**, **Brain JD**, **Krishnan R**, **Ai X**, **Bai Y.** Preserving airway smooth muscle contraction in precision-cut lung slices. *Sci Rep* 10: 6480, 2020. doi:10.1038/s41598-020-63225-y.
14. **Bai Y**, **Krishnamoorthy N**, **Patel KR**, **Rosas I**, **Sanderson MJ**, **Ai X.** Cryopreserved human precision-cut lung slices as a bioassay for live tissue banking. A viability study of bronchodilation with bitter-taste receptor agonists. *Am J Respir Cell Mol Biol* 54: 656–663, 2016. doi:10.1165/rcmb.2015-0290MA.
15. **Baatz JE**, **Newton DA**, **Riemer EC**, **Denlinger CE**, **Jones EE**, **Drake RR**, **Spyropoulos DD.** Cryopreservation of viable human lung tissue for versatile post-thaw analyses and culture. *In vivo* 28: 411–423, 2014.
16. **Rosner SR**, **Ram-Mohan S**, **Paez-Cortez JR**, **Lavoie TL**, **Dowell ML**, **Yuan L**, **Ai X**, **Fine A**, **Aird WC**, **Solway J**, **Fredberg JJ**, **Krishnan R.** Airway contractility in the precision-cut lung slice after cryopreservation. *Am J Respir Cell Mol Biol* 50: 876–881, 2014. doi:10.1165/rcmb.2013-0166MA.
17. **Bakhach J.** The cryopreservation of composite tissues: principles and recent advancement on cryopreservation of different type of tissues. *Organogenesis* 5: 119–126, 2009. doi:10.4161/org.5.3.9583.
18. **Elliott GD**, **Wang S**, **Fuller BJ.** Cryoprotectants: a review of the actions and applications of cryoprotective solutes that modulate cell recovery from ultra-low temperatures. *Cryobiology* 76: 74–91, 2017. doi:10.1016/j.cryobiol.2017.04.004.
19. **Pegg DE.** Principles of cryopreservation. *Methods Mol Biol* 1257: 3–19, 2015. doi:10.1007/978-1-4939-2193-5_1.
20. **Watson CY**, **Damiani F**, **Ram-Mohan S**, **Rodrigues S**, **de Moura Queiroz P**, **Donaghey TC**, **Rosenblum Lichtenstein JH**, **Brain JD**, **Krishnan R**, **Molina RM.** Screening for chemical toxicity using cryopreserved precision cut lung slices. *Toxicol Sci* 150: 225–233, 2016. doi:10.1093/toxsci/kfv320.
21. **Fisher RL**, **Hasal SJ**, **Sanuik JT**, **Hasal KS**, **Gandolfi AJ**, **Brendel K.** Cold- and cryopreservation of dog liver and kidney slices. *Cryobiology* 33: 163–171, 1996. doi:10.1006/cryo.1996.0016.
22. **Hart N'**, **van der Plaats A**, **Faber A**, **Leuvenink HGD**, **Olinga P**, **Wiersema-Buist J**, **Verkerke GJ**, **Rakhorst G**, **Ploeg RJ.** Oxygenation during hypothermic rat liver preservation: an in vitro slice study to demonstrate beneficial or toxic oxygenation effects. *Liver Transpl* 11: 1403–1411, 2005. doi:10.1002/lt.20510.
23. **Evdokimova E**, **Taper H**, **Buc Calderon P.** Effect of cold hypoxic storage and reoxygenation at 37°C of cultured precision-cut rat liver slices on paracetamol metabolism. *Arch Toxicol* 75: 452–458, 2001. doi:10.1007/s002040100265.
24. **Pless-Petig G**, **Singer BB**, **Rauen U.** Cold storage of rat hepatocyte suspensions for one week in a customized cold storage solution—preservation of cell attachment and metabolism. *PLoS One* 7: e40444, 2012. doi:10.1371/journal.pone.0040444.
25. **Wille T**, **Gonder S**, **Thiermann H**, **Seeger T**, **Rauen U**, **Worek F.** Evaluation of functional and structural alterations in muscle tissue after short-term cold storage in a new tissue preservation solution. *Cells Tissues Organs* 194: 501–509, 2011. doi:10.1159/000324148.
26. **Pizanis N**, **Gillner S**, **Kamler M**, **de Groot H**, **Jakob H**, **Rauen U.** Cold-induced injury to lung epithelial cells can be inhibited by iron chelators—implications for lung preservation. *Eur J Cardiothorac Surg* 40: 948–955, 2011. doi:10.1016/j.ejcts.2011.01.052.
27. **Hansen NUB**, **Karsdal MA**, **Brockbank S**, **Cruwys S**, **Rønnow S**, **Leeming DJ.** Tissue turnover of collagen type I, III and elastin is elevated in the PCLS model of IPF and can be restored back to vehicle levels using a phosphodiesterase inhibitor. *Respir Res* 17: 76, 2016. doi:10.1186/s12931-016-0394-8.
28. **Wille T**, **de Groot H**, **Rauen U.** Improvement of the cold storage of blood vessels with a vascular preservation solution. Study in porcine aortic segments. *J Vasc Surg* 47: 422–431, 2008. doi:10.1016/j.jvs.2007.09.048.
29. **Pless G**, **Sauer IM**, **Rauen U.** Improvement of the cold storage of isolated human hepatocytes. *Cell Transplant* 21: 23–37, 2012. doi:10.3727/096368911X580509.
30. **Suzuki T**, **Ota C**, **Fujino N**, **Tando Y**, **Suzuki S**, **Yamada M**, **Kondo T**, **Okada Y**, **Kubo H.** Improving the viability of tissue-resident stem cells using an organ-preservation solution. *FEBS Open Bio* 9: 2093–2104, 2019. doi:10.1002/2211-5463.12748.
31. **Guibert EE**, **Petrenko AY**, **Balaban CL**, **Somov AY**, **Rodriguez JV**, **Fuller BJ.** Organ preservation: current concepts and new strategies for the next decade. *Transfus Med Hemother* 38: 125–142, 2011. doi:10.1159/000327033.
32. **Blankensteijn JD**, **Terpstra OT.** Liver preservation: the past and the future. *Hepatology* 13: 1235–1250, 1991. doi:10.1002/hep.1840130633.
33. **Salahudeen AK**, **Huang H**, **Patel P**, **Jenkins JK.** Mechanism and prevention of cold storage-induced human renal tubular cell injury. *Transplantation* 70: 1424–1431, 2000. doi:10.1097/00007890-200011270-00005.
34. **Laubach VE**, **Sharma AK.** Mechanisms of lung ischemia-reperfusion injury. *Curr Opin Organ Transplant* 21: 246–252, 2016. doi:10.1097/MOT.0000000000000304.
35. **Rauen U**, **Petrat F**, **Li T**, **de Groot H.** Hypothermia injury/cold-induced apoptosis—evidence of an increase in chelatable iron causing oxidative injury in spite of low O_2-/H_2O_2 formation. *FASEB J* 14: 1953–1964, 2000. doi:10.1096/fj.00-0071com.
36. **Sharma BK**, **Bacon BR**, **Britton RS**, **Park CH**, **Magiera CJ**, **O'Neill R**, **Dalton N**, **Smanik P**, **Speroff T.** Prevention of hepatocyte injury and lipid peroxidation by iron chelators and alpha-tocopherol in isolated iron-loaded rat hepatocytes. *Hepatology* 12: 31–39, 1990. doi:10.1002/hep.1840120107.
37. **Octave J-N**, **Schneider Y-J**, **Crichton RR**, **Trouet A.** Iron mobilization from cultured hepatocytes: effect of desferrioxamine B. *Biochem Pharmacol* 32: 3413–3418, 1983. doi:10.1016/0006-2952(83)90370-2.
38. **Bartels-Stringer M**, **Kramers C**, **Wetzels JF**, **Russel FG**, **de Groot H**, **Rauen U.** Hypothermia causes a marked injury to rat proximal tubular cells that is aggravated by all currently used preservation

solutions. *Cryobiology* 47: 82–91, 2003. doi:10.1016/S0011-2240(03)00071-3.
39. **Liou G-Y**, **Storz P.** Reactive oxygen species in cancer. *Free Radic Res* 44: 479–496, 2010. doi:10.3109/10715761003667554.
40. **Krampe B**, **Al-Rubeai M.** Cell death in mammalian cell culture: molecular mechanisms and cell line engineering strategies. *Cytotechnology* 62: 175–188, 2010. doi:10.1007/s10616-010-9274-0.
41. **Rauen U**, **Polzar B**, **Stephan H**, **Mannherz HG**, **de Groot H.** Cold-induced apoptosis in cultured hepatocytes and liver endothelial cells: mediation by reactive oxygen species. *FASEB J* 13: 155–168, 1999. doi:10.1096/fasebj.13.1.155.
42. **Belzer FO**, **Southard JH.** Principles of solid-organ preservation by cold storage. *Transplantation* 45: 673–676, 1988. doi:10.1097/00007890-198804000-00001.
43. **Bienholz A**, **Walter B**, **Pless-Petig G**, **Guberina H**, **Kribben A**, **Witzke O**, **Rauen U.** Characterization of injury in isolated rat proximal tubules during cold incubation and rewarming. *PLoS One* 12: e0180553, 2017. doi:10.1371/journal.pone.0180553.
44. **Switalla S**, **Lauenstein L**, **Prenzler F**, **Knothe S**, **Förster C**, **Fieguth H-G**, **Pfennig O**, **Schaumann F**, **Martin C**, **Guzman CA**, **Ebensen T**, **Müller M**, **Hohlfeld JM**, **Krug N**, **Braun A**, **Sewald K.** Natural innate cytokine response to immunomodulators and adjuvants in human precision-cut lung slices. *Toxicol Appl Pharmacol* 246: 107–115, 2010. doi:10.1016/j.taap.2010.04.010.
45. **Awad EM**, **Khan SY**, **Sokolikova B**, **Brunner PM**, **Olcaydu D**, **Wojta J**, **Breuss JM**, **Uhrin P.** Cold induces reactive oxygen species production and activation of the NF-kappa B response in endothelial cells and inflammation in vivo. *J Thromb Haemost* 11: 1716–1726, 2013. doi:10.1111/jth.12357.
46. **Salehi P**, **Walker J**, **Madsen K**, **Churchill TA.** Control of oxidative stress in small bowel: relevance to organ preservation. *Surgery* 139: 317–323, 2006. doi:10.1016/j.surg.2005.08.003.
47. **Cruthirds DL**, **Novak L**, **Akhi KM**, **Sanders PW**, **Thompson JA**, **MacMillan-Crow LA.** Mitochondrial targets of oxidative stress during renal ischemia/reperfusion. *Arch Biochem Biophys* 412: 27–33, 2003. doi:10.1016/S0003-9861(03)00039-0.
48. **Saba H**, **Munusamy S**, **MacMillan-Crow LA.** Cold preservation mediated renal injury: involvement of mitochondrial oxidative stress. *Ren Fail* 30: 125–133, 2008. doi:10.1080/08860220701813327.
49. **Akram KM**, **Yates LL**, **Mongey R**, **Rothery S**, **Gaboriau DCA**, **Sanderson J**, **Hind M**, **Griffiths M**, **Dean CH.** Live imaging of alveologenesis in precision-cut lung slices reveals dynamic epithelial cell behaviour. *Nat Commun* 10: 1178, 2019. doi:10.1038/s41467-019-09067-3.
50. **Alsafadi HN**, **Uhl FE**, **Pineda RH**, **Bailey KE**, **Rojas M**, **Wagner DE**, **Königshoff M.** Applications and approaches for three-dimensional precision-cut lung slices. Disease modeling and drug discovery. *Am J Respir Cell Mol Biol* 62: 681–691, 2020. doi:10.1165/rcmb.2019-0276TR.
51. **Khan MM**, **Poeckel D**, **Halavatyi A**, **Zukowska-Kasprzyk J**, **Stein F**, **Vappiani J**, **Sevin DC**, **Tischer C**, **Zinn N**, **Eley JD**, **Gudmann NS**, **Muley T**, **Winter H**, **Fisher AJ**, **Nanthakumar CB**, **Bergamini G**, **Pepperkok R.** An integrated multiomic and quantitative label-free microscopy-based approach to study pro-fibrotic signalling in ex vivo human precision-cut lung slices. *Eur Respir J* 58: 2000221, 2021. doi:10.1183/13993003.00221-2020.
52. **Liu G**, **Särén L**, **Douglasson H**, **Zhou X-H**, **Åberg PM**, **Ollerstam A**, **Betts CJ**, **Balogh Sivars K.** Precision cut lung slices: an ex vivo model for assessing the impact of immunomodulatory therapeutics on lung immune responses. *Arch Toxicol* 95: 2871–2877, 2021. doi:10.1007/s00204-021-03096-y.
53. **Singer BD**, **Mock JR**, **D'Alessio FR**, **Aggarwal NR**, **Mandke P**, **Johnston L**, **Damarla M.** Flow-cytometric method for simultaneous analysis of mouse lung epithelial, endothelial, and hematopoietic lineage cells. *Am J Physiol Lung Cell Mol Physiol* 310: L796–L801, 2016. doi:10.1152/ajplung.00334.2015.
54. **Bantikassegn A**, **Song X**, **Politi K.** Isolation of epithelial, endothelial, and immune cells from lungs of transgenic mice with oncogene-induced lung adenocarcinomas. *Am J Respir Cell Mol Biol* 52: 409–417, 2015. doi:10.1165/rcmb.2014-0312MA.
55. **Reichard A**, **Asosingh K.** Best practices for preparing a single cell suspension from solid tissues for flow cytometry. *Cytometry A* 95: 219–226, 2019. doi:10.1002/cyto.a.23690.
56. **Stegmayr J**, **Alsafadi HN**, **Langwiński W**, **Niroomand A**, **Lindstedt S**, **Leigh ND**, **Wagner DE.** Isolation of high-yield and -quality RNA from human precision-cut lung slices for RNA-sequencing and computational integration with larger patient cohorts. *Am J Physiol Lung Cell Mol Physiol* 320: L232–L240, 2021. doi:10.1152/ajplung.00401.2020.
57. **Mukhopadhyay S**, **Hoidal JR**, **Mukherjee TK.** Role of TNFalpha in pulmonary pathophysiology. *Respir Res* 7: 125, 2006. doi:10.1186/1465-9921-7-125.
58. **Temann A**, **Golovina T**, **Neuhaus V**, **Thompson C**, **Chichester JA**, **Braun A**, **Yusibov V.** Evaluation of inflammatory and immune responses in long-term cultured human precision-cut lung slices. *Hum Vaccin Immunother* 13: 351–358, 2017. doi:10.1080/21645515.2017.1264794.
59. **Martin C**, **Uhlig S**, **Ullrich V.** Videomicroscopy of methacholine-induced contraction of individual airways in precision-cut lung slices. *Eur Respir J* 9: 2479–2487, 1996. doi:10.1183/09031936.96.09122479.
60. **Fiegen RJ**, **Rauen U**, **Hartmann M**, **Decking UK**, **de Groot H.** Decrease of ischemic injury to the isolated perfused rat liver by loop diuretics. *Hepatology* 25: 1425–1431, 1997. doi:10.1002/hep.510250620.
61. **Frank A**, **Rauen U**, **de Groot H.** Protection by glycine against hypoxic injury of rat hepatocytes: inhibition of ion fluxes through nonspecific leaks. *J Hepatol* 32: 58–66, 2000. doi:10.1016/S0168-8278(00)80190-7.
62. **Fukuse T**, **Hirata T**, **Ishikawa S**, **Shoji T**, **Yoshimura T**, **Chen Q**, **Matsukura T**, **Hanaoka N**, **Wada H.** Optimal alveolar oxygen concentration for cold storage of the lung. *Transplantation* 72: 300–304, 2001. doi:10.1097/00007890-200107270-00024.
63. **Bretschneider HJ.** Myocardial protection. *Thorac Cardiovasc Surg* 28: 295–302, 1980. doi:10.1055/s-2007-1022099.
64. **Long LH**, **Halliwell B.** Artefacts in cell culture: α-ketoglutarate can scavenge hydrogen peroxide generated by ascorbate and epigallocatechin gallate in cell culture media. *Biochem Biophys Res Commun* 406: 20–24, 2011. doi:10.1016/j.bbrc.2011.01.091.
65. **Rauen U**, **Klempt S**, **de Groot H.** Histidine-induced injury to cultured liver cells, effects of histidine derivatives and of iron chelators. *Cell Mol Life Sci* 64: 192–205, 2007. doi:10.1007/s00018-006-6456-1.
66. **John MB.** Advances in media for cryopreservation and hypothermic storage (Online), 2005. https://www.semanticscholar.org/paper/Advances-in-Media-for-Cryopreservation-and-Storage-Baust/5f17067dfc94612cd762a634a78120e8e995e7ff.
67. **Koop A**, **Piper HM.** Protection of energy status of hypoxic cardiomyocytes by mild acidosis. *J Mol Cell Cardiol* 24: 55–65, 1992. doi:10.1016/0022-2828(92)91159-3.
68. **Upadhya GA**, **Topp SA**, **Hotchkiss RS**, **Anagli J**, **Strasberg SM.** Effect of cold preservation on intracellular calcium concentration and calpain activity in rat sinusoidal endothelial cells. *Hepatology* 37: 313–323, 2003. doi:10.1053/jhep.2003.50069.
69. **Hochachka PW.** Defense strategies against hypoxia and hypothermia. *Science* 231: 234–241, 1986. doi:10.1126/science.2417316.
70. **Gizewski ER**, **Rauen U**, **Kirsch M**, **Reuters I**, **Diederichs H**, **de Groot H.** Rapid decrease in cellular sodium and chloride content during cold incubation of cultured liver endothelial cells and hepatocytes. *Biochem J* 322: 693–699, 1997. doi:10.1042/bj3220693.
71. **Wahlberg JA**, **Southard JH**, **Belzer FO.** Development of a cold storage solution for pancreas preservation. *Cryobiology* 23: 477–482, 1986. doi:10.1016/0011-2240(86)90056-8.

4. Publication II

Archives of Toxicology (2022) 96:321–334
https://doi.org/10.1007/s00204-021-03186-x

ORGAN TOXICITY AND MECHANISMS

Organophosphorus pesticides exhibit compound specific effects in rat precision-cut lung slices (PCLS): mechanisms involved in airway response, cytotoxicity, inflammatory activation and antioxidative defense

Jonas Tigges[1] · Franz Worek[1] · Horst Thiermann[1] · Timo Wille[1,2]

Received: 10 August 2021 / Accepted: 28 October 2021 / Published online: 15 November 2021

Abstract
Organophosphorus compound pesticides (OP) are widely used in pest control and might be misused for terrorist attacks. Although acetylcholinesterase (AChE) inhibition is the predominant toxic mechanism, OP may induce pneumonia and formation of lung edema after poisoning and during clinical treatment as life-threatening complication. To investigate the underlying mechanisms, rat precision-cut lung slices (PCLS) were exposed to the OP parathion, malathion and their biotransformation products paraoxon and malaoxon (100–2000 µmol/L). Airway response, metabolic activity, release of LDH, cytokine expression and oxidative stress response were analyzed. A concentration-dependent inhibition of airway relaxation was observed after exposure with the oxon but not with the thion-OP. In contrast, cytotoxic effects were observed for both forms in higher concentrations. Increased cytokine expression was observed after exposure to parathion and paraoxon (IL-6, GM-CSF, MIP-1α) and IL-6 expression was dependent on NFκB activation. Intracellular GSH levels were significantly reduced by all four tested OP but an increase in GSSG and HO-1 expression was predominantly observed after malaoxon exposure. Pretreatment with the antioxidant *N*-acetylcysteine reduced malaoxon but not paraoxon-induced cytotoxicity. PCLS as a 3D lung model system revealed OP-induced effects depending on the particular OP. The experimental data of this study contribute to a better understanding of OP toxicity on cellular targets and may be a possible explanation for the variety of clinical outcomes induced by different OP.

Keywords Organophosphates · PCLS · Inflammation · Oxidative stress · Bronchoconstriction

Abbreviations

ACh	Acetylcholine
AChE	Acetylcholinesterase
DMEM	Dulbecco's Modified Eagle's Medium
ERK	Extracellular-signal regulated kinases
GM-CSF	Granulocyte–macrophage colony-stimulating factor
GSH	Glutathione
GSSG	Glutathione disulfide
GST	Glutathione-*S*-transferase
HO-1	Heme oxygenase-1
IC50	Inhibitory concentration 50%
IKK	IκB kinase
JNK	C-Jun N-terminal kinase
ROS	Reactive oxygen species
IL-6	Interleukin-6
LDH	Lactate-dehydrogenase
LPS	Lipopolysaccharide
MAPK	Mitogen-activated protein kinase
MFI	Mean fluorescence intensity
MIP-1A	Macrophage inflammatory protein 1A
NAC	*N*-Acetylcysteine
NFκB	Nuclear factor 'kappa-light-chain-enhancer' of activated B-cells
OP	Organophosphorus compound pesticides
PCLS	Precision-cut lung slices
PMSF	Phenylmethylsulfonylfluoride
SEM	Standard error of the mean

✉ Timo Wille
TimoWille@bundeswehr.org

[1] Bundeswehr Institute of Pharmacology and Toxicology, Neuherbergstrasse 11, 80937 Munich, Germany

[2] Present Address: Department CBRN Medical Defence, Bundeswehr Medical Academy, Ingolstädter Str. 240, 80939 Munich, Germany

SOD	Superoxide dismutase
STAT3	Signal transducers and activators of transcription 3
VEGF	Vascular endothelial growth factor

Introduction

Organophosphorus compound pesticides (OP) are a class of highly toxic substances commonly used for crop protection. The widespread use and easy access resulted in high numbers of (self-) poisonings during the past decades (Peter et al. 2014; Eddleston et al. 2005). A conservative estimate suggests more than 100.000 death per year from pesticide self-poisoning worldwide, accounting for 13.7% of global suicides (Mew et al. 2017).

OP like parathion and malathion require biotransformation by cytochrome P450 enzymes to obtain the more toxic oxon-forms (Fukuto 1990; Eyer et al. 2003). The activated OPs exhibit acute toxicity via covalent binding to the active site of the AChE, leading to its inhibition. The subsequent accumulation of acetylcholine (ACh) at the acetylcholine receptor leads to a cholinergic crisis characterized by a toxidrome of muscarinic and nicotinic signs involving miosis, salivation, bronchospasm, bronchorrhea, muscular dysfunction and respiratory paralysis (Holmstedt 1959; Johnson 1987).

Standard treatment involves application of atropine, to antagonize muscarinic effects, in combination with an oxime for reactivation of inhibited AChE (Worek et al. 2020; Hrabetz et al. 2013). Even if therapeutic steps are rapidly induced and the clinical signs of cholinergic crisis mitigate, OP-induced pneumonia poses a life-threatening complication (Kamat et al. 1989; Hrabetz et al. 2013). Apart from the common mechanism of AChE inhibition, some OP are suspected to induce toxic non-AChE dependent effects (Costa 2006). Clinical as well as experimental in vivo data have shown effects of OP exposure on lung tissue indicating direct toxic effects and an interaction with the immune system (Hulse et al. 2014; Nambiar et al. 2007; Hrabetz et al. 2013). Due to the complexity of the pulmonary system, investigation of the underlying mechanisms is challenging. For the purpose of gas exchange, breathing mechanics and host defense, more than 50 different cell types are present in the lung that act together in a well-balanced composition (Travaglini et al. 2020). Due to limitations in the number of different cell types that can be cultured together, cell–cell interactions and matrix effects that may arise in vivo during lung damage cannot be studied in in vitro cell culture experiments (Liu et al. 2019). As an intermediate step between in vitro cell culture investigations and in vivo studies, precision-cut lung slices (PCLS) as an ex vivo tool are used. The viable lung tissue represents the whole complexity of the organ including all resident cell types in their natural spatial composition (Liberati et al. 2010) and has the potential to substantially reduce the number of in vivo experiments with regard to the 3R principle (Russel and Burch 1959). Due to advantages in standardized preparation and tissue culture, PCLS are frequently used as versatile tool for the investigation of cytotoxic effects, inflammatory activation or alterations of the redox system (Henjakovic et al. 2008; Sauer et al. 2014; Behrsing et al. 2013; Lauenstein et al. 2014). Conservation of the natural lung architecture alongside with presence of viable airways, surrounded by a functioning smooth muscle layer, enables the analysis of compound induced effects on airway response and, therefore, the investigation of novel treatment strategies for diseases like asthma or COPD (Herbert et al. 2019; Martin et al. 1996; Wohlsen et al. 2003).

Among the most frequently studied OP are parathion (WHO classification extremely hazardous; class 1A), malathion (WHO classification slightly hazardous; class III) and their respective biotransformation products paraoxon and malaoxon. We, therefore, used these four compounds to study their effects on airway response, cytotoxicity, inflammatory cytokine expression, alterations of the redox system and intracellular signaling cascades in PCLS. These investigations shed light on potential targets for future improvements in the treatment of OP poisoned patients.

Methods

Chemicals

For Tyrode buffer preparation, 2.68 mmol/L KCl (Carl Roth, Karlsruhe, Germany), 1.05 mmol/L $MgCl_2 \cdot 6H_2O$ (Sigma Aldrich, St. Louis, USA), 0.42 mmol/L $NaH_2PO_4 \cdot 2H_2O$ (Merck KGaA, Darmstadt, Germany), 137 mmol/L NaCl (Carl Roth), 1.8 mmol/L $CaCl_2 \cdot 2H_2O$ (Carl Roth), 22 mmol/L $NaHCO_3$ (Carl Roth) and 5.5 mmol/L glucose monohydrate (Merck KGaA) were dissolved in double-distilled water and pH was adjusted to 7.4 by carbogen gassing. PCLS were cultured in Dulbecco's Modified Eagle's Medium/Nutrient mixture F12 (1:1) without phenol red and L-glutamine (DMEM/F-12; Sigma-Aldrich) supplemented with 1% Penicillin/Streptomycin (Sigma-Aldrich) and 0.1% Gentamycin (Thermo Fisher, Waltham, USA). The low melting point agarose was purchased from Sigma-Aldrich. The OP parathion, paraoxon, malathion and malaoxon were purchased from LGC standards (London, United Kingdom) and stock-solutions (0.1 mol/L) were prepared in acetonitrile (Merck KGaA). For bronchoconstriction experiments, a stock solution (0.1 mol/L in DMEM/F-12) of ACh (Sigma Aldrich) was prepared and stored at − 80 °C. The working solution (50 µmol/L in cell culture medium) was freshly

prepared on the day of the experiment. Lysis solution for intracellular protein, cytokine and heme oxygenase 1 (HO-1) detection was prepared using phosphate-buffered saline (Sigma-Aldrich) supplemented with 0.1% Triton-X 100 (Sigma-Aldrich) and cOmplete™ EDTA-free protease inhibitor (Roche, Basel, Switzerland).

Animals

Male Wistar rats were purchased from Charles River Laboratories (Sulzfeld, Germany) and kept in a standard animal housing unit providing an automated 12 h light/dark cycle and air condition, as described in Herbert et al. (2017). Animals were fed with a standard diet and drinking water ad libitum. Upon arrival in the animal housing, rats were kept for at least seven days before using them for PCLS preparation to allow a proper acclimatization (final weight 300–500 g). All experiments were in accordance with the German Animal Welfare Act of 18th May 2006 (BGB1, I S. 1206, 1313) and the European Parliament and Council Directive of 22nd September 2010 (2010/63/EU).

PCLS preparation

For preparation of PCLS, a procedure as described previously (Herbert et al. 2017) with some modifications was applied. Briefly, rats were anesthetized by intraperitoneal injection of 75 mg/kg ketamine (Ketavet 100 mg/mL, zoetis Deutschland GmbH, Berlin, Germany) and 10 mg/kg xylazine (Xylasel 20 mg/mL; Selectavet Dr. Otto Fischer GmbH, Weyarn-Holzolling, Germany) and sacrificed by exsanguination. Low melting point agarose (1.5% in DMEM/F-12) was gently heated until boiling and cooled to 37 °C. Lungs were filled with agarose solution until the lung lobules were entirely enfolded. Afterwards, the lung was removed from the thoracic cavity and cooled on ice for 10 min, followed by additional storage for 20 min in 4 °C pre-cooled DMEM/F-12 to allow agarose solidification. Subsequently, tissue cylinders with a diameter of 8 mm were generated using a biopsy punch. The cylinders were sliced into 250–300 µm thick PCLS using a Krumdieck Tissue Slicer (Alabama Research and Development, Munford, USA) with ice-cold Tyrode buffer (pH 7.4) as slicing medium. Slicing medium was changed after five cores and PCLS were collected in pre-cooled DMEM/F-12 until the slicing procedure was finished for all slices. Afterwards, all PCLS were placed in an incubator (HeraCell 240i; Thermo Fisher Scientific) at 37 °C and 5% CO_2 on a shaker to enable washout of cellular debris and agarose from large airways. The cell culture medium was exchanged every 30 min for 1.5 h and afterwards every 60 min for another 2 h. PCLS were held at 37 °C and 5% CO_2 until experimental use at the next day.

Evaluation of bronchoconstriction

PCLS were removed from the incubator and weighted with steel wires in a 24-well plate to prevent floating and were then transferred to the microplate-holder of an inverted microscope (Axio Observer D1, Carl Zeiss AG, Oberkochen, Germany) with an AxioCam HSm camera (Carl Zeiss AG, Germany). Using the AxioVision software (Version 4.8.2.0, Carl Zeiss AG), airway cross sections were observed for signs of vitality such as beating cilia and spontaneous muscle constrictions. At first, the initial airway area was assessed. Afterwards either the solvent control acetonitrile (1%) or the OP (0.001–100 µmol/L) was added to the slices. After 3 min of incubation time of the OP, ACh (0.5 µmol/L final concentration) was added directly into the culture medium. 2 min after ACh application, a second picture was taken to evaluate time-dependent airway constriction. After 60 min, airway relaxation was calculated using the AxioVision software. Relaxation efficacy of solvent exposed slices was set as 100% and response of all OP-exposed PCLS was related to that value.

Exposure of PCLS with OP compounds

For exposure of PCLS with the OP parathion, paraoxon, malathion or malaoxon, dilutions in DMEM/F-12 were prepared freshly before each experiment, obtaining the final concentrations for exposure between 100 and 2000 µmol/L. Acetonitrile (< 1% for relaxation experiments and < 2% in all other experiments) was used as solvent control and was chosen as it shows low effects on AChE inhibition in human erythrocyte membranes (IC50 of 2.8%) compared to other frequently used solvents such as DMSO (IC50 of 1.1%). In addition, current unpublished work points towards a lower cytotoxicity of acetonitrile in comparison to DMSO, ethanol or methanol in PCLS. Culture medium was replaced by OP-containing medium and PCLS were incubated for 8 or 24 h under standard cell culture conditions (37 °C; 5% CO_2).

Analysis of PCLS viability and cell death

To detect effects of OP on PCLS viability, an Alamar Blue assay (Invitrogen, Carlsbad, USA) was performed. The Alamar Blue assay is based on the reduction of resazurin to the fluorescent dye resorufin by metabolically active cells and, therefore, serves as marker for cellular viability. After OP exposure (100–2000 µmol/L), PCLS were incubated with Alamar Blue reagent for 2 h at 37 °C, and fluorescence intensity was detected using a plate-reading photometer (Tecan Infinite 220 PRO, Tecan Group Ltd., Mennedorf, Switzerland) at excitation wavelength of 560 nm and emission wavelength of 590 nm. Signal intensity was referred to the respective solvent control acetonitrile (< 2%). To detect

effects of *N*-acetylcysteine (NAC) on PCLS viability, lung slices were pre-treated with 5 mmol/L NAC (Sigma-Aldrich) in DMEM/F-12 for 4 h, and afterwards the medium was replaced by the OP-containing exposure medium for 24 h. For determination of cytotoxicity, an LDH (lactate dehydrogenase) assay was performed (Cytotoxicity detection Kit^{PLUS}, Roche), detecting LDH activity in the PCLS supernatant that is released from the cells during cell death. After OP exposure, supernatant was transferred into one well of a 96-well plate. Freshly prepared reaction mix, as described in the manufacturer's instructions, was added to the wells and incubated for 15 min at room temperature. Absorbance was detected at 490 nm and corrected by the reference wavelength of 605 nm. Cytotoxicity was calculated as % of the absorbance induced by the lysis solution (positive control) provided in the assay kit.

Analysis of protein content by BCA

The amount of protein in the PCLS after OP exposure (100–1500 µmol/L) was assessed as marker for tissue destruction and as reference for cytokine and HO-1 expression in the sample. After exposure, three PCLS per substance and concentration were sonicated on ice in an Eppendorf cup with 350 µL of lysis buffer using a Bandelin Sonopuls Homogenizer (3 × 5 s; 30% amplitude) (Bandelin electronic GmbH & Co. KG, Berlin, Germany). Sonicated samples were centrifuged (15,000×*g*, 20 min, 4 °C) and supernatant was transferred into an Eppendorf tube. For protein detection, an Uptima BC Assay kit (Interchim, Montluçon, France) was applied according to the manufacturer's instructions. Absorbance was detected at 562 nm using a plate-reading photometer (Tecan Infinite 220 PRO, Tecan Group Ltd.). The protein concentration was then related to a non-OP exposed, solvent control.

Cytokine expression evaluated by bioplex assay

To evaluate immunomodulatory effects of the OP (100–1800 µmol/L) on PCLS, cytokines released into the PCLS supernatant and intracellular concentrations were detected using a Bio-Plex Pro™ Rat Cytokine 23-Plex Assay, analyzed on a BioPlex 200 system (Bio-Rad Laboratories, Hercules, USA). Lipopolysaccharide (LPS, 100 ng/mL in DMEM/F12) served as positive control. Intracellular protein was extracted as described in "Analysis of protein content by BCA". The PCLS supernatant was removed and supplemented with protease inhibitor cocktail solution. All samples were snap-frozen in liquid nitrogen and stored at − 80 °C until further use in the bioplex system. The bioplex assay was performed according to the manufacturer's protocol with washing steps performed on a HydroFlex microplate washer (Tecan Group Ltd.). Cytokine concentrations of each sample were calculated using the provided assay standards. After normalization to the protein concentration, total amount of cytokines in the PCLS supernatant and cytosol was combined to receive the overall cytokine expression per mg of tissue protein. Cytokine expression is shown as % of the solvent control acetonitrile.

Glutathione detection assay

For the detection of the reduced (GSH) and oxidized (GSSG) form of glutathione in PCLS, a GSH/GSSG-Glo™ Assay (Promega, Madison, USA) was used as described in the manufacturer's instructions with slight modifications. After OP exposure (100–1500 µmol/L) each PCLS was transferred into one well of a white 96-well plate (Thermo Fisher Scientific). 50 µL of lysis reagent (total GSH lysis reagent or oxidized GSH lysis reagent) was added directly to the PCLS and incubated for 5 min at room temperature on a plate shaker (850 rpm) to allow tissue lysis. 50 µL of Luciferin Generation solution was added to each well and incubated for 30 min at room temperature in the dark. Afterwards, 100 µL Luciferin Detection Reagent was added and incubated for 15 min. Luminescence was detected using a plate-reading photometer (Tecan Infinite 220 PRO, Tecan Group Ltd.). GSH and GSSG concentrations are depicted as % of solvent control acetonitrile.

Glutathione-s-transferase (GST) activity assay

To detect effects of OP exposure (100–1500 µmol/L) on the GST activity, a colorimetric GST activity assay Kit (abcam, Cambridge, UK) was used. After OP exposure, three PCLS per substance and concentration were combined and sonicated (3 × 5 s 30% amplitude) in GST Assay Buffer. After centrifugation (10,000×*g*, 15 min, 4 °C), the intracellular fraction was stored at − 80 °C until further use. GST activity was analyzed as indicated in the manufacturer's instructions. Absorbance increase between 2 and 10 min was used to obtain GST activity that was afterwards referred to the solvent control acetonitrile.

Superoxide dismutase (SOD) activity assay

To detect effects of OP exposure on SOD activity in PCLS, a colorimetric Superoxide Dismutase Activity Assay Kit (abcam) was used. In this assay, superoxide is produced by a xanthine oxidase and metabolized into hydrogen peroxide and O_2 by SOD. Superoxide anions react with WST-1 to produce a formazan dye with an absorbance maximum at 450 nm. The higher the SOD activity is, the less superoxide is present in the sample and, therefore, formazan production is decreased. After OP exposure (100–1500 µmol/L), three PCLS per condition

were combined in ice-cold SOD lysis buffer (100 µmol/L Tris/HCl, pH 7.4 containing 0.5% Triton X-100 (Sigma-Aldrich), 5 mmol/L 2-mercaptoethanol (Sigma-Aldrich) and 0.1 mg/mL phenylmethylsulfonylfluoride (PMSF; Roche). Samples were lysed on ice using a Bandelin Sonopuls Homogenizer (3 × 5 s; 30% amplitude). After centrifugation (15,000×*g*, 10 min, 4 °C) sample supernatant was transferred into a fresh tube and snap frozen in liquid nitrogen. Samples were stored at − 80 °C until further use. SOD activity analysis was performed as described in the manufacturer's instructions. Thereof, SOD activity was calculated for each sample and related to the solvent control acetonitrile.

HO-1 and IL-6 detection

After OP exposure, three PCLS per substance and concentration were combined, intracellular protein fraction (HO-1 and IL-6) and supernatant (IL-6) were prepared as described in "Analysis of protein content by BCA" and stored at − 80 °C until further use. For evaluation of nuclear factor 'kappa-light-chain-enhancer' of activated B-cells (NF-κB) activation in OP-induced inflammatory activation, PCLS were exposed to parathion or the solvent control acetonitrile in the presence or absence of 10 µmol/L NF-κB activation Inhibitor VI, benzoxanthiole compound (abcam) for 8 h. DMSO (0.05%) served as solvent control. HO-1 and IL-6 levels were evaluated using commercially available kits (Rat HO-1/HMOX1/HSP32 ELISA Kit; novus biologicals, Littleton, USA and an ELISA Duo Set; R&D Systems, Minneapolis, USA) and were corrected for the protein content of the sample. Results are shown as % of the solvent control acetonitrile.

Signaling pathway activation bioplex

To analyze effects of OP exposure on signaling pathways, the intracellular fraction was analyzed using a bioplex system. Therefore, specific beads for phospho-c-Jun (Ser63), phospho-p38 MAPK (T180/Y182) and pospho-STAT3 (Tyr705) were used. After 8 h of exposure to 1000 µmol/L of the four OP, three PCLS per exposure were combined, washed with cell wash buffer, and lysed in tissue lysis buffer supplemented with 2 mol/L PMSF (Roche) and 1 × lysis buffer QG (Bioplex Cell Signaling Assay Kit). Samples were sonicated (3 × 5 s; 30% amplitude), centrifuged (15,000×*g*, 20 min, 4 °C) and snap frozen in liquid nitrogen. Afterwards, samples were stored at − 80 °C until further use. The Bioplex assay was performed as described in the manufacturer's instructions using 200 µg/mL protein per sample. Afterwards, mean fluorescence intensity (MFI) was analyzed on a bioplex 200 system. MFI of the sample is shown as % of the solvent control acetonitrile.

Data analysis

Data are presented as mean ± standard error of the mean (SEM). Statistical analyses were performed using GraphPad Prism Version 5.04 (GraphPad Software, San Diego, USA). Differences to controls were determined by two-way ANOVA with Bonferroni multiple comparison test. Effects on airway relaxation and NF-κB inhibition were evaluated by one-way ANOVA with Dunnett's multiple comparison test. A p value below 0.05 was considered statistically significant. $*p < 0.05$; $**p < 0.01$; $***p < 0.001$.

Results

Effects of OP exposure on airway relaxation

For the evaluation of OP effects on airway response, PCLS containing airways were exposed to parathion, paraoxon, malathion or malaoxon and airway relaxation was monitored 60 min after ACh stimulus (0.5 µmol/L). OP exposure without ACh did not result in an alteration of the airway area in the highest applied concentrations (control: 102 ± 3%; parathion: 113 ± 3%; paraoxon: 98 ± 4%; malathion: 104 ± 3%; malaoxon: 109 ± 8%). In addition, maximum constriction of the airway after ACh addition was not significantly different between the four tested OP in the highest applied concentrations (airway area after ACh addition: control: 53 ± 9%; parathion: 51 ± 12%; paraoxon: 45 ± 9%; malathion: 46 ± 10%; malaoxon: 50 ± 8%) and is comparable with other PCLS studies (Wigenstam et al. 2021; Herbert et al. 2017). Exposure with parathion or malathion in concentrations between 0.1 and 100 µmol/L had no significant effect on airway relaxation compared to the solvent control [mean relaxation efficiency 100 µmol/L: parathion (118%, Fig. 1A); malathion (90%, Fig. 1C)]. Airway relaxation after exposure to paraoxon (Fig. 1B) was significantly inhibited by concentrations from 0.1 µmol/L (− 26%) to 10 µmol/L (− 43%). Exposure to malaoxon (Fig. 1D) also led to a reduction in airway relaxation efficiency, that was significant after exposure to 1 µmol/L (53%) and 10 µmol/L (− 20%). Negative values indicate a further increased airway constriction compared to 2 min of ACh incubation as reference value for initial airway constriction.

Effects of OP exposure on PCLS viability

To detect effects of OP exposure on the viability of PCLS, intracellular reducing power (Alamar Blue assay), release of LDH and the overall protein content were analyzed

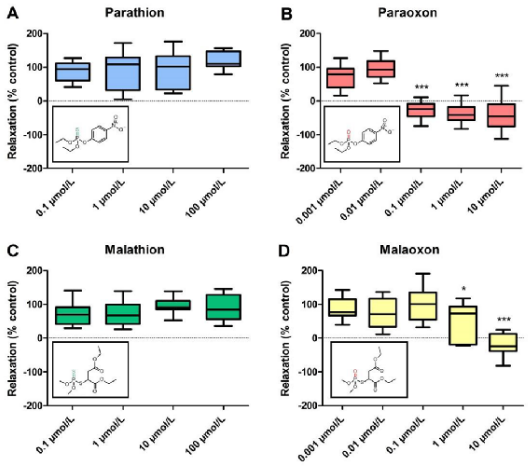

Fig. 1 Inhibitory effect of parathion, paraoxon, malathion and malaoxon on airway relaxation after acetylcholine stimulus. PCLS airways exposed for 3 min to parathion (**A**), paraoxon (**B**), malathion (**C**) or malaoxon (**D**) in different concentrations (0.001–100 µmol/L). Upon acetylcholine stimulus (0.5 µmol/L; 2 min), airway constriction was recorded. Subsequent airway relaxation was evaluated after 60 min. Relaxation of the control was set as 100%. Boxplots show mean with minimum and maximum values. Asterisks indicate significant differences to the control (*$p<0.05$, ***$p<0.001$; $n=10$ airways from at least three different animals)

after 24 h of exposure with different OP concentrations (100–2000 µmol/L). In addition, we used the Alamar Blue assay and protein detection to exclude possible cytotoxic effects that can influence inflammation and oxidative stress after 8 h of OP exposure. OP exposure for 8 h results in a decrease of viability that was significant only in high concentrations for paraoxon (2000 µmol/L), malaoxon (1600 µmol/L) and malathion (2000 µmol/L) and detection of the corresponding protein content as marker for severe tissue damage indicated no significant differences to the solvent control for all four tested compounds (detailed viability data in Fig S1). After 24 h we made contrasting observations. Using an Alamar Blue assay, a decrease in resazurin reduction was observed for paraoxon, malathion and malaoxon (Fig. 2B–D), while no such effect was detectable after parathion exposure (Fig. 2A). Thereby, significant changes to the solvent control were observed at 1200 µmol/L paraoxon (63 ± 5%), 600 µmol/L malaoxon (59 ± 14%) and 1000 µmol/L malathion (63 ± 14%). Based on the viability, EC_{50} concentrations in a very similar range as the significantly different changes were calculated; i.e. ~ 1400 µmol/L (paraoxon), ~ 600 µmol/L (malaoxon) and ~ 1100 µmol/L (malathion). A complete loss of viability was observed only after exposure to ≥ 1400 µmol/L malaoxon.

An increase in LDH was observed in the PCLS supernatant for several concentrations of paraoxon, malathion and malaoxon, whereas parathion induced a significant effect only in the highest applied concentration. Significant

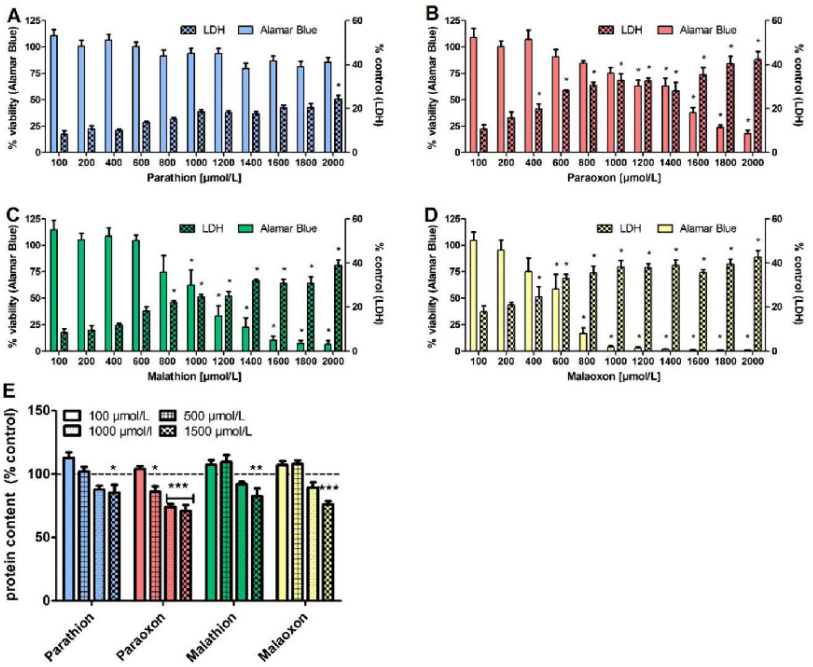

Fig. 2 Effects of parathion, paraoxon, malathion and malaoxon on viability, cell death and protein content. PCLS were exposed for 24 h to different concentrations of parathion (**A**), paraoxon (**B**), malathion (**C**) or malaoxon (**D**) (10–2000 µmol/L). Viability was analyzed by Alamar Blue assay and effects on cellular death were evaluated by measurement of LDH release into PCLS supernatant. For detection of severe tissue destruction, intracellular protein content was detected by BCA assay (**E**). Data are presented as % of control (Alamar Blue assay and protein content) or as % of the positive control Triton-X (LDH). Data are shown as mean ± SEM. Asterisk indicate significant differences to control (*$p<0.05$; **$p<0.01$; ***$p<0.001$; $n=6$ PCLS from three different animals)

differences to the solvent control were observed at concentrations of 2000 µmol/L for parathion (Fig. 2A); 400 µmol/L for paraoxon (Fig. 2B), 800 µmol/L for malathion (Fig. 2C), and 400 µmol/L for malaoxon (Fig. 2D).

Detection of the protein content of the PCLS after OP exposure and subsequent tissue lysis serves as marker for severe tissue injury. Exposure to the four OP led to a decrease of protein content, that was significant for parathion (85 ± 4%), paraoxon (70 ± 5%), malathion (83 ± 6%) and malaoxon (76 ± 3%) at a concentration of 1500 µmol/L (Fig. 2E).

Inflammatory activation in PCLS induced by OP

For the detection of inflammatory activation in PCLS after OP exposure, an incubation period of 8 h was used to evaluate inflammatory activation without the bias of severe cytotoxicity and tissue damage that occurs after 24 h of exposure (Fig. 2). LPS (100 ng/mL) as positive control led to a stong expression of pro-inflammatory cytokines after 8 h of exposure (Fig. S2) and pilot tests to find concentration ranges for inflammatory activation revealed OP concentrations of 100, 600, 1200 and 1800 µmol/L as suitable for cytokine detection.

Induction of IL-6 expression (Fig. 3A) was observed after exposure to parathion (553 ± 53%, $p < 0.001$) and paraoxon (225 ± 35%, $p < 0.05$) at concentrations of 1800 µmol/L and 1200 µmol/L, respectively. In contrast, the expression of vascular endothelial growth factor (VEGF; Fig. 3C) was only increased after parathion exposure (up to 230 ± 35%; 1800 µmol/L, $p < 0.001$), while exposure to the other OP induced no statistically significant differences compared to the control. Expression of granulocyte–macrophage colony-stimulating factor (GM-CSF; Fig. 3D) was moderately upregulated by paraoxon (166 ± 15%; 1200 µmol/L, $p < 0.05$), parathion (217 ± 30%; 1800 µmol/L; $p < 0.001$) and malathion (160 ± 5%; 600 µmol/L, $p < 0.05$) while no changes in GM-CSF expression were observed after exposure to malaoxon. Macrophage inflammatory protein (MIP-1α) expression (Fig. 3B) was significantly increased after exposure to parathion (191 ± 6%; 1800 µmol/L; $p < 0.001$) and paraoxon (160 ± 10%; 1800 µmol/L; $p < 0.001$).

Cytokine expression after NFκB inhibition

To analyze NFκB signaling pathway activation in OP-induced inflammation, parathion exposed PCLS (1800 µmol/L) were co-incubated with an NFκB inhibitor (10 µmol/L) and expression of IL-6 was analyzed. Cytokine expression was significantly increased to 451 ± 39% ($p < 0.01$ vs. solvent control; Fig. 3E) after parathion exposure. Co-incubation with the NFκB activation inhibitor resulted in a significant reduction of IL-6 expression to 231 ± 36% ($p < 0.01$ vs. parathion exposed PCLS without inhibitor).

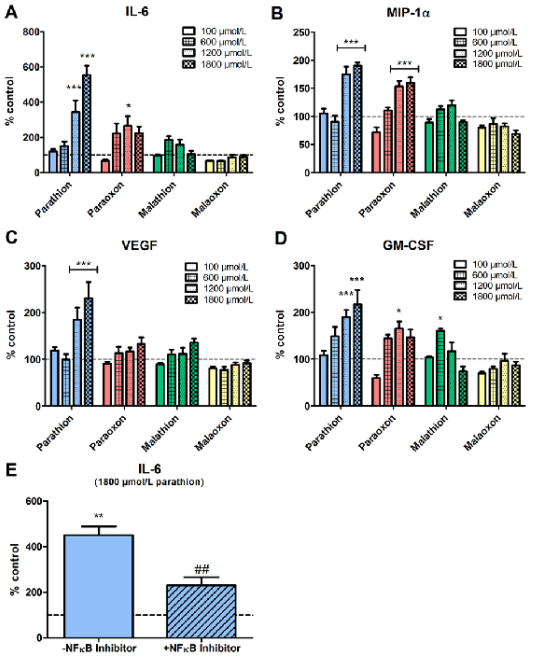

Fig. 3 Expression of cytokines in PCLS after parathion, paraoxon, malathion and malaoxon exposure. PCLS were exposed to increasing concentrations of paraoxon, parathion, malaoxon, malathion (100–1800 µmol/L) for 8 h. Cytokine expression of IL-6 (**A**), MIP-1α (**B**), VEGF (**C**) and GM-CSF (**D**) was detected in the supernatant and cytosolic fraction using a Bioplex-system and was afterwards combined to analyze the overall cytokine production. Observed concentrations are corrected for the protein content and are shown as fold increase of control (indicated by dashed line). For evaluation of NF-κB activation, PCLS were exposed to parathion (1800 µmol/L) with or without addition of an NF-κB Activation Inhibitor (10 µmol/L; **E**). Interleukin-6 was detected in the supernatant and cytosolic fraction by ELISA, and afterwards combined to analyze the overall cytokine production. Data are shown as mean ± SEM. Asterisk indicate significant differences to the control (*$p < 0.05$; **$p < 0.01$; ***$p < 0.001$; $n = 8$ samples from four different animals) Hash characters indicate significant differences to parathion exposure without inhibitor ($^{\#\#}p < 0.01$; $n = 8$ samples from four different animals)

Effects of OP exposure on oxidative stress response

To detect effects of OP exposure on the cellular oxidative stress response, the levels of reduced glutathione (GSH) and oxidized glutathione (GSSG) were detected after 8 h of exposure. A decrease of intracellular GSH was observed after exposure to all four OP, resulting in a reduction to 17 ± 1% (paraoxon); 49 ± 4% (parathion); 30 ± 6% (malaoxon) and 51 ± 16% (malathion) at the

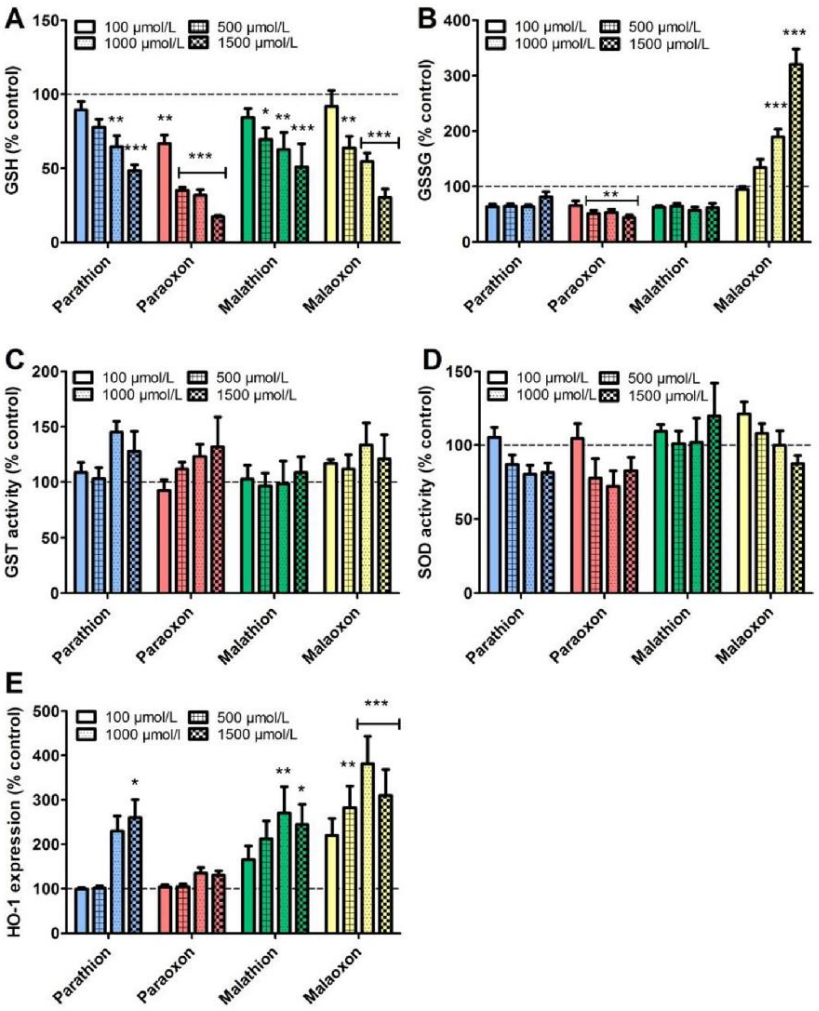

Fig. 4 Effect of parathion, paraoxon, malathion and malaoxon exposure on reduced and oxidized glutathione content, GST- and SOD activity and expression of HO-1. PCLS were exposed for 8 h to different concentrations of paraoxon, parathion, malaoxon, malathion (100–1500 µmol/L). Afterwards the intracellular level of reduced (**A**) and oxidized (**B**) glutathione was detected. Furthermore, intracellular activity of GST (**C**) and SOD (**D**) was evaluated. Expression of intracellular HO-1 was evaluated by ELISA and corrected for the protein concentration. All results are shown as % of control (indicated by dashed line). Data are shown as mean ± SEM. Asterisk indicate significant differences to the control (*<0.05; **$p<0.01$; ***$p<0.001$; $n=6$ PCLS from three different animals (GST and SOD Activity Assay) $n=8$ PCLS from four different animals (GSH, GSSG, HO-1))

highest concentration of 1500 µmol/L (Fig. 4A). Detecting intracellular GSSG levels, a significant reduction after exposure to 1500 µmol/L of paraoxon (44 ± 5%) was observed while effects of parathion (81 ± 9%), and malathion (62 ± 8%) were not significant compared to the solvent control. In contrast, a dose-dependent, significant increase of GSSG after exposure to 1500 µmol/L malaoxon (320 ± 28%; $p<0.001$) was detected (Fig. 4B). To evaluate whether the applied OPs influence the GST activity, which may affect intracellular GSH concentrations, a GST activity assay was performed. After 8 h of exposure, no statistically significant differences to the solvent control were found (Fig. 4C). Exposure to 1500 µmol/L of parathion, paraoxon, malathion and malaoxon resulted in an activity of 127 ± 18%; 132 ± 27%; 108 ± 14% and 120 ± 22%, respectively. As superoxide formation plays a role in the maintenance of the redox system, SOD activity after 8 h of OP exposure was analyzed. SOD activity was not affected in PCLS after 8 h of exposure to the four OP at the highest concentration of 1500 µmol/L (Fig. 4D). For the detection of cellular reactions in response to a possible alteration of the redox system, expression of HO-1 was detected after 8 h of OP exposure (Fig. 4E). While exposure to paraoxon had no effect on HO-1 expression, exposure to 1500 µmol/L parathion resulted in a significantly increased expression (261 ± 40%). A statistically significant induction of HO-1 expression was observed after exposure to 1000 µmol/L of malathion (270 ± 59%;

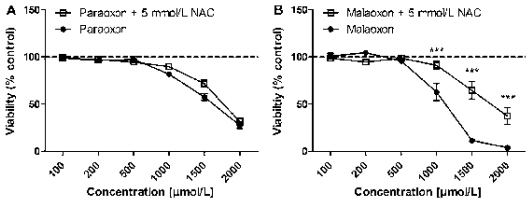

Fig. 5 Effects of *N*-acetylcysteine (NAC) pre-treatment on PCLS viability. PCLS were pre-treated with 5 mmol/L of NAC for 4 h. Afterwards medium was replaced by paraoxon (**A**) or malaoxon (**B**) containing medium for 24 h and viability was analyzed by Alamar Blue assay. Viability is shown as % of control (indicated by dashed line). Data are shown as mean ± SEM. Asterisk indicate significant differences to PCLS without NAC pre-treatment (*$p < 0.05$; $n = 6$ PCLS from three different animals)

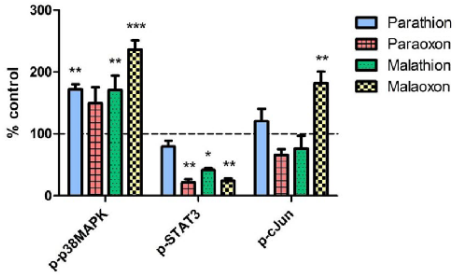

Fig. 6 Phosphorylation of signaling pathways after OP exposure. PCLS were exposed to 1000 µmol/L of parathion, paraoxon, malathion or malaoxon for 8 h. Intracellular levels of the phosphorylated proteins p-p38MAPK, p-STAT3 and p-c-Jun were evaluated using a Bioplex system. Data are calculated as % of control (indicated by dashed line) and are shown as mean ± SEM. Asterisks indicate significant differences to the control (*$p < 0.05$; $n = 4$ samples from four different animals)

$p < 0.01$), while exposure to malaoxon led to a maximal induction to 310 ± 59% at 1500 µmol/L ($p < 0.001$).

Pre-treatment with NAC

While no statistically significant effect of NAC pre-treatment on paraoxon induced cytotoxicity was observed, NAC pre-treatment significantly ($p < 0.05$) reduced the effects of malaoxon on PCLS viability at concentrations of 1000 µmol/L [63 ± 9% (− NAC) vs. 91 ± 4% (+ NAC)]; 1500 µmol/L [11 ± 2% (− NAC) vs. 65 ± 9% (+ NAC)] and 2000 µmol/L [4 ± 1% (− NAC) vs. 37 ± 9% (+ NAC)] (Fig. 5).

Signaling pathway activation after OP exposure

To analyze effects of OP exposure on signaling pathways in PCLS, phosphorylation of p38-MAPK, STAT3 and c-Jun was detected using a bioplex assay. An exposure concentration of 1000 µmol/L was used to detect pathway activation without involvement of direct cytotoxic effects. Phosphorylated p38MAPK was significantly ($p < 0.01$) increased by parathion, malathion and malaoxon, which induced the strongest activation (236 ± 15%). In contrast, phosphorylation of STAT3 was significantly ($p < 0.05$) reduced by paraoxon (22 ± 5%), malathion (42 ± 4%) and malaoxon (24 ± 4%) while no significant reduction was observed after parathion exposure (80 ± 9%). Phosphorylation of c-Jun was significantly induced only by malaoxon (182 ± 19%; $p < 0.01$), while exposure to the other compounds did not induce a significant alteration of phosphorylation status (Fig. 6).

Discussion

Respiratory complications occur in many cases of severe organophosphate poisoning and are a leading cause of death after suicidal or accidental intoxication (Tsao et al. 1990; Hulse et al. 2014). There is increasing evidence that mechanisms other than AChE inhibition may contribute to the high toxicity of OP (Eyer et al. 2010; Xie et al. 2000), e.g. the formation of lung edema, tissue destruction and alterations in the immune response leading to an acute respiratory distress syndrome (Perkins et al. 2011; Lotti 2001). Therefore, toxic effects of parathion, malathion and their respective biotransformation products paraoxon and malaoxon, as representative OP, were investigated in rat PCLS.

Effects of OP exposure on airway reactivity

As inhibition of the AChE is generally seen as primary toxic mechanism of OP, the AChE inhibitory potential of the four investigated compounds in rat PCLS was assessed. PCLS contain viable airways surrounded by a smooth muscle layer, thus constriction of the airways can be provoked by stimulation with neurotransmitters like ACh (Wohlsen et al. 2003). The constriction is spontaneously reversible due to lung resident AChE activity, which results in relaxation of the airways. Airway response upon OP exposure has previously been studied to find novel treatment strategies in OP poisoning (Herbert et al. 2017, 2019; Wigenstam et al. 2021). Addition of the OP without ACh stimulation failed to induce airway constriction, most probably due to limited nervous stimulation in the PCLS. This was also observed in VX-exposed PCLS (Herbert et al. 2017; Wigenstam et al. 2021). We did not observe significant differences in maximum constriction of the airways between the four

applied OP. However, in a PCLS study from Wigenstam et al. (2021), using a slightly different exposure scenario (ACh-OP-ACh instead of OP-ACh), nerve agent exposure in combination with ACh led to an increased bronchoconstriction in PCLS compared to ACh alone. The parent OP parathion and malathion failed to induce an inhibitory effect on airway relaxation, indicating that AChE activity is not impaired (Fig. 1A, C). In contrast, paraoxon and malaoxon significantly decreased airway relaxation in concentrations of 0.1 and 1 µmol/L, respectively (Fig. 1B, D). These results underline the requirement of metabolic activation of thion-OP for substantial AChE inhibition (Eyer et al. 2003; Buratti and Testai 2005). Paraoxon shows a higher inhibitory potential than malaoxon, which is in line with inhibition of rat erythrocyte membrane AChE (second order inhibition rate constant; 2.72×10^6 M^{-1} min^{-1} for paraoxon vs. 4.76×10^5 M^{-1} min^{-1} for malaoxon). In addition, the inhibitory potential is well comparable to human erythrocyte membrane AChE (second order inhibition rate constant; 3.16×10^6 M^{-1} min^{-1} for paraoxon vs. 4.74×10^5 M^{-1} min^{-1} for malaoxon) pointing towards comparable inter-species inhibition data (unpublished data J. Tigges and F. Worek et al. (2020)). The current study nicely shows that AChE-mediated airway response in PCLS is a suitable tool to analyze dose-dependent effects of OP.

Effects of OP exposure on PCLS viability

PCLS are frequently used to analyze cytotoxic effects to the lung without restriction to particular lung cell types (Neuhaus et al. 2018; Sauer et al. 2014). This is of special interest as it has been shown that OP cytotoxicity is dependent on the particular kind of lung cells used (Angelini et al. 2015). After exposure to OP, a decrease in viability, as well as an increase in LDH release was observed. Only parathion did not induce significant cytotoxic effects (Fig. 2A vs 2B-D). Thereby, decrease in viability and increase in LDH showed a good correlation for the investigated structurally different OP parathion, paraoxon, malathion and malaoxon. Although cytotoxicity of both oxon forms is stronger than that of the related thion-OP, malathion exposure led to a significant decrease in viability compared to the solvent control and an increase in LDH release (Fig. 2C). These findings are in line with observations in human neuronal cells (Bharate et al. 2010; Wang et al. 2019) and pulmonary cells (Angelini et al. 2015). As malaoxon has a much higher AChE inhibiting potency than malathion, a mode of action for cell injury which is different from AChE inhibition is highly likely. The cytotoxic potential is underlined by significantly decreased protein concentrations (Fig. 2E), indicating severe tissue injury (Sauer et al. 2014; Behrsing et al. 2013).

Cytotoxicity is induced at much higher concentrations (up to 5000 fold) than those inducing inhibition of airway relaxation. Therefore, these effects may occur mainly when the lung is directly exposed towards OP, for example after inhalation of nebulized pesticides or by aspiration of OP after suicidal ingestion. If the lung is exposed towards OP exclusively via the bloodstream, effects of AChE inhibition may be lethal before local toxic effects can develop. The parent compound malathion induced dose-dependent cytotoxicity while it failed to provoke a decrease in airway relaxation. Furthermore, malaoxon was more cytotoxic than paraoxon, although paraoxon showed stronger AChE inhibitory potential (effects on different toxicological endpoints summarized in Table 1). This further points towards a different mechanism than AChE inhibition, which is extensively discussed in the literature (Costa 2006; Eyer et al. 2010). It has been found that OP have the potential to bind to more than 50 different proteins in the mouse brain, possibly altering protein function, which may explain AChE independent effects. Interestingly, a particular OP binds only to specific proteins, which might be an indicator for different toxicological modes of action and characteristic effects of particular OP (Lockridge et al. 2005).

Effects of OP exposure on inflammatory activation

Epidemiological studies showed an increased rate of infections in the upper respiratory tract of workers chronically exposed to OP compared to a healthy control group (Hermanowicz and Kossman 1984) and animal studies have shown immunomodulatory effects after exposure to parathion or malathion (Liu et al. 2006; Proskocil et al. 2013; Abdo et al. 2021). PCLS are frequently used as model system for the investigation of substance-induced inflammatory activation indicated by an increased expression of inflammatory cytokines (Henjakovic et al. 2008). We, therefore, analyzed the cytokine expression in rat PCLS after OP exposure. Our results indicate that the cytokine expression in PCLS is highly dependent on the OP. While exposure to parathion and paraoxon caused an increase of the cytokines IL-6, GM-CSF, VEGF and MIP-1α, malathion and malaoxon failed to induce such strong alterations in inflammatory response. Increased expression of these cytokines indicates induction of pulmonary inflammation, macrophage activation and acute lung injury (Fernando et al. 2014; Shibata et al. 2001; Voelkel et al. 2006). As the upregulated cytokines are

Table 1 Overview of organophosphate induced effects in PCLS

	Parathion	Paraoxon	Malathion	Malaoxon
Airway relaxation	–	++	–	+
Cytotoxicity	–	+	+	++
Inflammation	++	+	–	–
ROS	+	+	+	++

expressed by activated macrophages, it can be assumed that macrophages play an important role in OP-induced inflammation in PCLS. These suggestions are in line with data obtained from in vitro exposure of macrophage cell lines (Proskocil et al. 2019). Importantly, PCLS contain a mixture of different cells, of which only a portion is involved in immunological response, allowing a more realistic evaluation of inflammatory activation, which is an advantage over single cell-type macrophage cultures. As PCLS were prepared from rat lungs, inter-individual differences need to be considered. In the present study, we observed different basal immunological activation between animals, which necessitates normalization to the individual controls which is a well-known limitation in PCLS (Sauer et al. 2014).

NfκB-signal transduction in OP poisoning

Expression of the above mentioned cytokines is dependent on activation of the NF-κB signal transduction pathway (Kiriakidis et al. 2003; Liu et al. 2017). In brief, activation of cytokine receptors, pattern recognition receptors or T- and B- cell receptors results in stimulation of the IκB kinase (IKK) complex, leading to phosphorylation and subsequent degradation of IκBα. Thereafter, the NF-κB dimers p50/RelA and p50/c-Rel translocate to the nucleus, acting as transcription factor for the induction of target genes at the κB response element (Liu et al. 2017). To evaluate whether inflammatory activation induced by OP is NF-κB dependent, the effects of an IKK-β inhibitor on IL-6 expression after parathion exposure were evaluated (Fig. 3E), as this combination has provoked the strongest response in the Bioplex screening (Fig. 3A). IL-6 expression was significantly decreased after co-incubation of parathion with the IKK-β inhibitor, which demonstrates an activation of the NF-κB signal transduction pathway in response to parathion exposure. It has been found that the NF-κB signal transduction pathway is activated by parathion in differentiated human macrophages and that parent compounds show a stronger activation potential than their metabolites, which is in line with our observations of cytokine expression (Proskocil et al. 2019). The successful inhibition of inflammatory activation confirms PCLS as a potential model system to study the use of candidate therapeutics for treatment of pulmonary inflammation after OP exposure and may be a potential explanation for alterations of the immune system observed in OP-poisoned patients. Anti-inflammatory drugs (COX2 inhibitors) have been already used in an in vivo OP model (rat) (Chapman et al. 2019) and could be evaluated in PCLS.

Effects of OP exposure on antioxidative defense

Elevated levels of reactive oxygen species (ROS) like superoxide or hydrogen peroxide can cause substantial damage to cellular organelles, lipids, proteins and DNA which may result in apoptosis (Sies et al. 2017). Reduced GSH acts as intracellular antioxidant that is used by the glutathione peroxidase for detoxification of ROS. The oxidized GSSG is afterwards reduced to GSH by a glutathione reductase (Rahman et al. 2005). Antioxidative enzymes like SOD have a key role in antioxidant defense by eliminating intracellular superoxide (Afonso et al. 2007). In addition, cells that are under oxidative stress respond with the expression of antioxidative proteins like HO-1, which has tissue protective properties by oxidative cleavage of free heme groups (Ryter and Choi 2005).

Alterations of the antioxidative system were observed in patients after exposure to OP suggesting a role of ROS in OP poisoning (Banerjee et al. 1999; Seth et al. 2001). In PCLS, intracellular GSH levels can be used as marker for the induction of oxidative stress (Sauer et al. 2014). In the present study a significant decrease in intracellular GSH levels for all applied OP in concentrations below those inducing cytotoxic effects was observed (Fig. 4A). Reduced levels of intracellular GSH indicate a cellular reaction towards ROS in response to oxidative stress. Interestingly, the oxidized GSSG was only significantly upregulated after malaoxon exposure, indicating a stronger impairment of oxidative defense of malaoxon than the other OP (Fig. 4B). It has also been shown that loss of intracellular GSH is a mechanism that regulates redox signaling and cell death which may be an explanation for decreased GSH levels without an increase of GSSG (Franco and Cidlowski 2012). As decrease of GSH can be related to an increased biotransformation of OP by the glutathione-*S*-transferase (GST) (Fujioka and Casida 2007), GST activity in PCLS after OP exposure was analyzed. No significant changes in GST activity were observed, indicating that reduced GSH levels are not related to an increase in metabolic activity (Fig. 4C). Impairment of SOD activity seems to be not involved in OP-induced alterations of the antioxidative defense system (Fig. 4D). Expression of HO-1, indicating cellular response to oxidative stress, was significantly upregulated following parathion, malathion and malaoxon exposure, with malaoxon inducing the strongest effects (Fig. 4E). These findings further underline the diversity of OP in induction of antioxidative response and that malaoxon provokes a stronger alteration of the redox system than malathion, parathion or paraoxon. It has been shown that malathion induces oxidative stress in the rat brain that could be due to inhibition of the complex IV of the respiratory chain (Delgado et al. 2006). However, the exact mechanism leading to ROS generation after malaoxon exposure remains elusive.

As medical countermeasure, we analyzed whether preincubation of PCLS with the antioxidative GSH precursor NAC has an impact on OP-induced cytotoxicity. Viability

after malaoxon but not after paraoxon exposure was significantly improved after pre-incubation with NAC (Fig. 5), indicating that malaoxon induced cytotoxicity is at least in part dependent on alterations of the redox system. Future studies could evaluate the therapeutic efficacy of antioxidative drugs such as vitamin E that were already evaluated in vivo (John et al. 2001).

Effects of OP exposure on signaling pathway activation

Mitogen activated protein kinase (MAPK) signaling pathways like the c-Jun N-terminal kinase (JNK), p38MAPK or extracellular signal regulated kinase (ERK) play an important role in a variety of cellular processes like cell differentiation, apoptosis and oxidative stress response (Morrison 2012). In our study we evaluated the intracellular levels of phosphorylated p38MAPK, Signal transducer and activator of transcription 3 (STAT3) and c-Jun as key players in the p38MAPK, ERK and JNK pathways, respectively. An increase in p38MAPK phosphorylation was observed for all investigated OP and was accompanied by a reduction in phosphorylation of STAT3 (Fig. 6). p38MAPK is activated in response to a variety of different noxious stimuli including UV, heat and cytokine stimulation. Phosphorylation results in transcription of target genes involved in cell cycle control and cell death (Morrison 2012). It has been shown that activation of p38MAPK in combination with a decreased activity of the ERK pathway (e.g. STAT3) is important for the induction of apoptosis (Xia et al. 1995) and that MAPK are involved in the toxicity of several OP (Farkhondeh et al. 2020). The JNK signal transduction pathway is involved in several cellular mechanisms including response towards oxidative stress (Ki et al. 2013; Kamata et al. 2005). Significant changes in c-Jun phosphorylation were only observed after malaoxon exposure, which is in line with the oxidative stress inducing potential of this OP (Figs. 4 vs. 6). The observed changes in activation of the investigated pathways underline the cytotoxic and oxidative stress inducing potential and it can be assumed that MAPK activation is involved in the observed toxic effects of OP in rat PCLS.

Conclusions

The OP parathion, malathion and their respective biotransformation products paraoxon and malaoxon induce distinct toxicological effects in PCLS. Effects of these OP on airway relaxation are well comparable with their effects on AChE inhibition. Induction of cytotoxic effects is mediated by much higher concentrations than functional impairment via AChE inhibition. Interestingly, OP showed different potency for inflammatory activation as well as for the disturbance of antioxidative response (summarized in Table 1). These results indicate that OP exert compound-specific toxic effects in rat lung tissue beyond AChE inhibition. PCLS are a valuable tool for the investigation of direct toxic effects (e.g. cytotoxicity or inflammatory activation) as well as for the analysis of tissue architecture and physiological response (airway relaxation), which offers unique possibilities to investigate multiple effects of OP exposure in a single tissue culture system. Future studies using PCLS may address the underlying mechanisms of non-AChE related effects by RNA expression, protein analysis and potential effects on other signaling pathways. In addition, the combined use of various precision cut tissue slices (e.g. lung, liver and kidney) might provide insights into effects of metabolic activation and detoxification.

Supplementary Information The online version contains supplementary material available at https://doi.org/10.1007/s00204-021-03186-x.

Funding Open Access funding enabled and organized by Projekt DEAL. This work was supported from the German Research Foundation (GRK 2338, Targets in Toxicology); project P02 to TW and FW; JT received a Ph.D. stipend in the GRK 2338.

Declarations

Conflict of interest The authors declare that they have no conflict of interest.

References

Abdo W, Elmadawy MA, Abdelhiee EY, Abdel-Kareem MA, Farag A, Aboubakr M, Ghazy E, Fadl SE (2021) Protective effect of thymoquinone against lung intoxication induced by malathion inhalation. Sci Rep 11(1):2498. https://doi.org/10.1038/s41598-021-82083-w

Afonso V, Champy R, Mitrovic D, Collin P, Lomri A (2007) Reactive oxygen species and superoxide dismutases: role in joint diseases. Jt Bone Spine 74(4):324–329. https://doi.org/10.1016/j.jbspin.2007.02.002

Angelini DJ, Moyer RA, Cole S, Willis KL, Oyler J, Dorsey RM, Salem H (2015) The pesticide metabolites paraoxon and malaoxon induce cellular death by different mechanisms in cultured human pulmonary cells. Int J Toxicol 34(5):433–441. https://doi.org/10.1177/1091581815593933

Banerjee BD, Seth V, Bhattacharya A, Pasha ST, Chakraborty AK (1999) Biochemical effects of some pesticides on lipid peroxidation and free-radical scavengers. Toxicol Lett 107(1–3):33–47. https://doi.org/10.1016/S0378-4274(99)00029-6

Behrsing HP, Furniss MJ, Davis M, Tomaszewski JE, Parchment RE (2013) In vitro exposure of precision-cut lung slices to 2-(4-amino-3-methylphenyl)-5-fluorobenzothiazole lysylamide dihydrochloride (NSC 710305, Phortress) increases inflammatory cytokine content and tissue damage. Toxicol Sci 131(2):470–479. https://doi.org/10.1093/toxsci/kfs319

Bharate SB, Prins JM, George KM, Thompson CM (2010) Thionate versus Oxon: comparison of stability, uptake, and cell toxicity of ((14)CH(3)O)(2)-labeled methyl parathion and methyl paraoxon with SH-SY5Y cells. J Agric Food Chem 58(14):8460–8466. https://doi.org/10.1021/jf100976v

Buratti FM, Testai E (2005) Malathion detoxification by human hepatic carboxylesterases and its inhibition by isomalathion and other pesticides. J Biochem Mol Toxicol 19(6):406–414. https://doi.org/10.1002/jbt.20106

Chapman S, Grauer E, Gez R, Egoz I, Lazar S (2019) Time dependent dual effect of anti-inflammatory treatments on sarin-induced brain inflammation: suggested role of prostaglandins. Neurotoxicology 74:19–27. https://doi.org/10.1016/j.neuro.2019.05.006

Costa LG (2006) Current issues in organophosphate toxicology. Clinica Chimica Acta Int J Clin Chem 366(1–2):1–13. https://doi.org/10.1016/j.cca.2005.10.008

Delgado EHB, Streck EL, Quevedo JL, Dal-Pizzol F (2006) Mitochondrial respiratory dysfunction and oxidative stress after chronic malathion exposure. Neurochem Res 31(8):1021–1025. https://doi.org/10.1007/s11064-006-9111-1

Eddleston M, Eyer P, Worek F, Mohamed F, Senarathna L, von Meyer L, Juszczak E, Hittarage A, Azhar S, Dissanayake W, Sheriff MR, Szinicz L, Dawson AH, Buckley NA (2005) Differences between organophosphorus insecticides in human self-poisoning: a prospective cohort study. Lancet 366(9495):1452–1459. https://doi.org/10.1016/S0140-6736(05)67598-8

Eyer F, Meischner V, Kiderlen D, Thiermann H, Worek F, Haberkorn M, Felgenhauer N, Zilker T, Eyer P (2003) Human parathion poisoning. A toxicokinetic analysis. Toxicol Rev 22(3):143–163. https://doi.org/10.2165/00139709-200322030-00003

Eyer P, Worek F, Thiermann H, Eddleston M (2010) Paradox findings may challenge orthodox reasoning in acute organophosphate poisoning. Chem Biol Interact 187(1–3):270–278. https://doi.org/10.1016/j.cbi.2009.10.014

Farkhondeh T, Mehrpour O, Buhrmann C, Pourbagher-Shahri AM, Shakibaei M, Samarghandian S (2020) Organophosphorus compounds and MAPK signaling pathways. Int J Mol Sci. https://doi.org/10.3390/ijms21124258

Fernando MR, Reyes JL, Iannuzzi J, Leung G, McKay DM (2014) The pro-inflammatory cytokine, interleukin-6, enhances the polarization of alternatively activated macrophages. PLoS ONE 9(4):e94188. https://doi.org/10.1371/journal.pone.0094188

Franco R, Cidlowski JA (2012) Glutathione efflux and cell death. Antioxid Redox Signal 17(12):1694–1713. https://doi.org/10.1089/ars.2012.4553

Fujioka K, Casida JE (2007) Glutathione *S*-transferase conjugation of organophosphorus pesticides yields *S*-phospho-, *S*-aryl-, and *S*-alkylglutathione derivatives. Chem Res Toxicol 20(8):1211–1217. https://doi.org/10.1021/tx700133c

Fukuto TR (1990) Mechanism of action of organophosphorus and carbamate insecticides. Environ Health Perspect 87:245–254. https://doi.org/10.1289/ehp.9087245

Henjakovic M, Sewald K, Switalla S, Kaiser D, Müller M, Veres TZ, Martin C, Uhlig S, Krug N, Braun A (2008) Ex vivo testing of immune responses in precision-cut lung slices. Toxicol Appl Pharmacol 231(1):68–76. https://doi.org/10.1016/j.taap.2008.04.003

Herbert J, Thiermann H, Worek F, Wille T (2017) Precision cut lung slices as test system for candidate therapeutics in organophosphate poisoning. Toxicology 389:94–100. https://doi.org/10.1016/j.tox.2017.07.011

Herbert J, Thiermann H, Worek F, Wille T (2019) COPD and asthma therapeutics for supportive treatment in organophosphate poisoning. Clin Toxicol (philadelphia, Pa.) 57(7):644–651. https://doi.org/10.1080/15563650.2018.1540785

Hermanowicz A, Kossman S (1984) Neutrophil function and infectious disease in workers occupationally exposed to phosphoorganic pesticides: role of mononuclear-derived chemotactic factor for neutrophils. Clin Immunol Immunopathol 33(1):13–22. https://doi.org/10.1016/0090-1229(84)90288-5

Holmstedt B (1959) Pharmacology of organophosphorus cholinesterase inhibitors. Pharmacol Rev 11:567–688

Hrabetz H, Thiermann H, Felgenhauer N, Zilker T, Haller B, Nährig J, Saugel B, Eyer F (2013) Organophosphate poisoning in the developed world—a single centre experience from here to the millennium. Chem Biol Interact 206(3):561–568. https://doi.org/10.1016/j.cbi.2013.05.003

Hulse EJ, Davies JOJ, Simpson AJ, Sciuto AM, Eddleston M (2014) Respiratory complications of organophosphorus nerve agent and insecticide poisoning. Implications for respiratory and critical care. Am J Respir Crit Care Med 190(12):1342–1354. https://doi.org/10.1164/rccm.201406-1150CI

John S, Kale M, Rathore N, Bhatnagar D (2001) Protective effect of vitamin E in dimethoate and malathion induced oxidative stress in rat erythrocytes. J Nutr Biochem 12(9):500–504. https://doi.org/10.1016/S0955-2863(01)00160-7

Johnson J (1987) Species-related differences in the inhibition of brain acetylcholinesterase by paraoxon and malaoxon*1. Toxicol Appl Pharmacol 88(2):234–241. https://doi.org/10.1016/0041-008x(87)90009-3

Kamat SR, Heera S, Potdar PV, Shah SV, Bhambure NM, Mahashur AA (1989) Bombay experience in intensive respiratory care over 6 years. J Postgrad Med 35(3):123–134

Kamata H, Honda S, Maeda S, Chang L, Hirata H, Karin M (2005) Reactive oxygen species promote TNFα-induced death and sustained JNK activation by inhibiting MAP kinase phosphatases. Cell 120(5):649–661. https://doi.org/10.1016/j.cell.2004.12.041

Ki Y-W, Park JH, Lee JE, Shin IC, Koh HC (2013) JNK and p38 MAPK regulate oxidative stress and the inflammatory response in chlorpyrifos-induced apoptosis. Toxicol Lett 218(3):235–245. https://doi.org/10.1016/j.toxlet.2013.02.003

Kiriakidis S, Andreakos E, Monaco C, Foxwell B, Feldmann M, Paleolog E (2003) VEGF expression in human macrophages is NF-kappaB-dependent: studies using adenoviruses expressing the endogenous NF-kappaB inhibitor IkappaBalpha and a kinase-defective form of the IkappaB kinase 2. J Cell Sci 116(Pt 4):665–674. https://doi.org/10.1242/jcs.00286

Lauenstein L, Switalla S, Prenzler F, Seehase S, Pfennig O, Förster C, Fieguth H, Braun A, Sewald K (2014) Assessment of immunotoxicity induced by chemicals in human precision-cut lung slices (PCLS). Toxicol in Vitro 28(4):588–599. https://doi.org/10.1016/j.tiv.2013.12.016

Liberati TA, Randle MR, Toth LA (2010) In vitro lung slices: a powerful approach for assessment of lung pathophysiology. Expert Rev Mol Diagn 10(4):501–508. https://doi.org/10.1586/erm.10.21

Liu P, Song X, Yuan W, Wen W, Wu X, Li J, Chen X (2006) Effects of cypermethrin and methyl parathion mixtures on hormone levels and immune functions in Wistar rats. Arch Toxicol 80(7):449–457. https://doi.org/10.1007/s00204-006-0071-7

Liu T, Zhang L, Joo D, Sun S-C (2017) NF-κB signaling in inflammation. Signal Transduct Targeted Ther 2:17023. https://doi.org/10.1038/sigtrans.2017.23

Liu G, Betts C, Cunoosamy DM, Åberg PM, Hornberg JJ, Sivars KB, Cohen TS (2019) Use of precision cut lung slices as a translational model for the study of lung biology. Respir Res 20(1):162. https://doi.org/10.1186/s12931-019-1131-x

Lockridge O, Duysen EG, Voelker T, Thompson CM, Schopfer LM (2005) Life without acetylcholinesterase: the implications of cholinesterase inhibitor toxicity in AChE-knockout mice. Environ Toxicol Pharmacol 19(3):463–469. https://doi.org/10.1016/j.etap.2004.12.008

Lotti M (2001) Clinical toxicology of anticholinesterase agents in humans. In: Krieger RI (ed) Handbook of pesticide toxicology, vol 2, 2nd edn. Academic Press, San Diego, pp 1043–1085

Martin C, Uhlig S, Ullrich V (1996) Videomicroscopy of methacholine-induced contraction of individual airways in precision-cut lung slices. Eur Respir J 9(12):2479–2487. https://doi.org/10.1183/09031936.96.09122479

Mew EJ, Padmanathan P, Konradsen F, Eddleston M, Chang S-S, Phillips MR, Gunnell D (2017) The global burden of fatal self-poisoning with pesticides 2006–15: systematic review. J Affect Disord 219:93–104. https://doi.org/10.1016/j.jad.2017.05.002

Morrison DK (2012) MAP kinase pathways. Cold Spring Harb Perspect Biol. https://doi.org/10.1101/cshperspect.a011254

Nambiar MP, Gordon RK, Rezk PE, Katos AM, Wajda NA, Moran TS, Steele KE, Doctor BP, Sciuto AM (2007) Medical countermeasure against respiratory toxicity and acute lung injury following inhalation exposure to chemical warfare nerve agent VX. Toxicol Appl Pharmacol 219(2–3):142–150. https://doi.org/10.1016/j.taap.2006.11.002

Neuhaus V, Danov O, Konzok S, Obernolte H, Dehmel S, Braubach P, Jonigk D, Fieguth H-G, Zardo P, Warnecke G, Martin C, Braun A, Sewald K (2018) Assessment of the cytotoxic and immunomodulatory effects of substances in human precision-cut lung slices. J vis Exp. https://doi.org/10.3791/57042

Perkins MW, Pierre Z, Rezk P, Song J, Oguntayo S, Morthole V, Sciuto AM, Doctor BP, Nambiar MP (2011) Protective effects of aerosolized scopolamine against soman-induced acute respiratory toxicity in guinea pigs. Int J Toxicol 30(6):639–649. https://doi.org/10.1177/1091581811415874

Peter JV, Sudarsan TI, Moran JL (2014) Clinical features of organophosphate poisoning: a review of different classification systems and approaches. Indian J Crit Care Med 18(11):735–745. https://doi.org/10.4103/0972-5229.144017

Proskocil BJ, Bruun DA, Jacoby DB, van Rooijen N, Lein PJ, Fryer AD (2013) Macrophage TNF-α mediates parathion-induced airway hyperreactivity in guinea pigs. Am J Physiol Lung Cell Mol Physiol 304(8):L519–L529. https://doi.org/10.1152/ajplung.00381.2012

Proskocil BJ, Grodzki ACG, Jacoby DB, Lein PJ, Fryer AD (2019) Organophosphorus pesticides induce cytokine release from differentiated human THP1 cells. Am J Respir Cell Mol Biol 61(5):620–630. https://doi.org/10.1165/rcmb.2018-0257OC

Rahman I, Biswas SK, Jimenez LA, Torres M, Forman HJ (2005) Glutathione, stress responses, and redox signaling in lung inflammation. Antioxid Redox Signal 7(1–2):42–59. https://doi.org/10.1089/ars.2005.7.42

Russel WM, Burch RL (1959) The principles of humane experimental technique. Methuen, London

Ryter SW, Choi AMK (2005) Heme oxygenase-1: redox regulation of a stress protein in lung and cell culture models. Antioxid Redox Signal 7(1–2):80–91. https://doi.org/10.1089/ars.2005.7.80

Sauer UG, Vogel S, Aumann A, Hess A, Kolle SN, Ma-Hock L, Wohlleben W, Dammann M, Strauss V, Treumann S, Gröters S, Wiench K, van Ravenzwaay B, Landsiedel R (2014) Applicability of rat precision-cut lung slices in evaluating nanomaterial cytotoxicity, apoptosis, oxidative stress, and inflammation. Toxicol Appl Pharmacol 276(1):1–20. https://doi.org/10.1016/j.taap.2013.12.017

Seth V, Banerjee BD, Bhattacharya A, Pasha ST, Chakravorty AK (2001) Pesticide induced alterations in acetylcholine esterase and gamma glutamyl transpeptidase activities and glutathione level in lymphocytes of human poisoning cases. Clin Biochem 34(5):427–429. https://doi.org/10.1016/S0009-9120(01)00232-6

Shibata Y, Berclaz P-Y, Chroneos ZC, Yoshida M, Whitsett JA, Trapnell BC (2001) GM-CSF regulates alveolar macrophage differentiation and innate immunity in the lung through PU.1. Immunity 15(4):557–567. https://doi.org/10.1016/S1074-7613(01)00218-7

Sies H, Berndt C, Jones DP (2017) Oxidative stress. Annu Rev Biochem 86:715–748. https://doi.org/10.1146/annurev-biochem-061516-045037

Travaglini KJ, Nabhan AN, Penland L, Sinha R, Gillich A, Sit RV, Chang S, Conley SD, Mori Y, Seita J, Berry GJ, Shrager JB, Metzger RJ, Kuo CS, Neff N, Weissman IL, Quake SR, Krasnow MA (2020) A molecular cell atlas of the human lung from single-cell RNA sequencing. Nature 587(7835):619–625. https://doi.org/10.1038/s41586-020-2922-4

Tsao TC, Juang YC, Lan RS, Shieh WB, Lee CH (1990) Respiratory failure of acute organophosphate and carbamate poisoning. Chest 98(3):631–636. https://doi.org/10.1378/chest.98.3.631

Voelkel NF, Vandivier RW, Tuder RM (2006) Vascular endothelial growth factor in the lung. Am J Physiol Lung Cell Mol Physiol 290(2):L209–L221. https://doi.org/10.1152/ajplung.00185.2005

Wang Y, Kim B, Walker A, Williams S, Meeks A, Lee Y-J, Seo SS (2019) Cytotoxic effects of parathion, paraoxon, and their methylated derivatives on a mouse neuroblastoma cell line NB41A3. Fundam Toxicol Sci 6(2):45–56. https://doi.org/10.2131/fts.6.45

Wigenstam E, Forsberg E, Bucht A, Thors L (2021) Efficacy of atropine and scopolamine on airway contractions following exposure to the nerve agent VX. Toxicol Appl Pharmacol 419:115512. https://doi.org/10.1016/j.taap.2021.115512

Wohlsen A, Martin C, Vollmer E, Branscheid D, Magnussen H, Becker WM, Lepp U, Uhlig S (2003) The early allergic response in small airways of human precision-cut lung slices. Eur Respir J 21(6):1024–1032. https://doi.org/10.1183/09031936.03.00027502

Worek F, Thiermann H, Wille T (2020) Organophosphorus compounds and oximes: a critical review. Arch Toxicol 94(7):2275–2292. https://doi.org/10.1007/s00204-020-02797-0

Xia Z, Dickens M, Raingeaud J, Davis RJ, Greenberg ME (1995) Opposing effects of ERK and JNK-p38 MAP kinases on apoptosis. Science 270(5240):1326–1331. https://doi.org/10.1126/science.270.5240.1326

Xie W, Stribley JA, Chatonnet A, Wilder PJ, Rizzino A, McComb RD, Taylor P, Hinrichs SH, Lockridge O (2000) Postnatal developmental delay and supersensitivity to organophosphate in gene-targeted mice lacking acetylcholinesterase. J Pharmacol Exp Ther 293(3):896–902

4.1 Supplementary information publication II

Supplementary Materials:

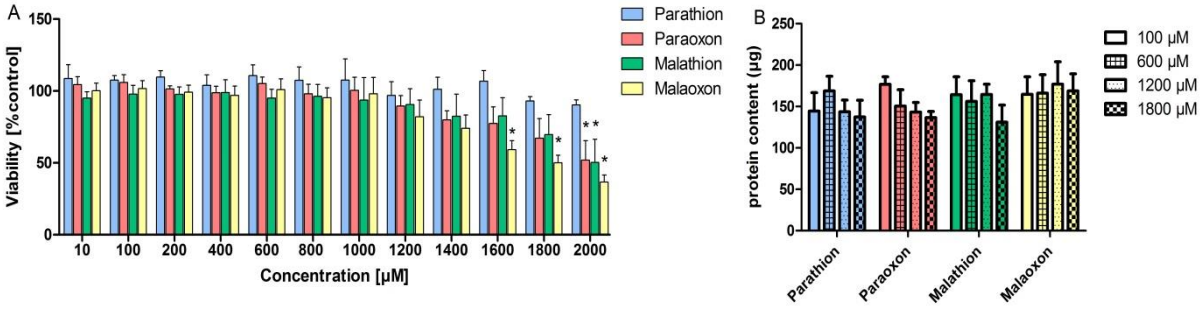

S1: Viability of PCLS after 8 h OP exposure (A) and corresponding protein content (B). To determine optimal concentrations of the OP substances for analysis of cytokine release and induction of oxidative stress, PCLS were treated for 8 h with either paraoxon, parathion, malaoxon, malathion (10 – 2000 µmol/L) or the solvent control acetonitrile. Viability was analyzed by Alamar Blue assay and protein content was measured by BCA assay. Results are shown as % of the solvent control acetonitrile (A) or total protein content (B). Data are shown as mean ± SEM. Asterisk indicate significant differences to the solvent control (*p<0.05; n=3).

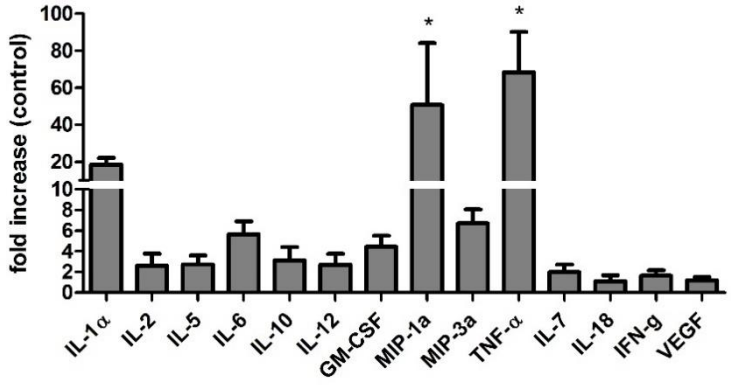

S2: Effects of the positive control LPS on cytokine expression in PCLS. To verify that PCLS are suitable for the investigation of cytokine expression, PCLS were exposed for 8 h with 100 ng/ml LPS and cytokine expression was detected by a multiplex assay. Results are shown as % of the untreated control. Data are shown as mean ± SEM. Asterisk indicate significant differences to the solvent control (*p<0.05; n=3).

5. Publication bibliography

Amend, Niko; Niessen, Karin V.; Seeger, Thomas; Wille, Timo; Worek, Franz; Thiermann, Horst (2020): Diagnostics and treatment of nerve agent poisoning-current status and future developments. In *Annals of the New York Academy of Sciences* 1479 (1), pp. 13–28. DOI: 10.1111/nyas.14336.

Anzueto, A. (1990): Acute inhalation toxicity of soman and sarin in baboons. In *Fundamental and applied toxicology : official journal of the Society of Toxicology* 14 (4), pp. 676–687. DOI: 10.1016/0272-0590(90)90293-s.

Bailey, Kolene E.; Pino, Christopher; Lennon, Mallory L.; Lyons, Anne; Jacot, Jeffrey G.; Lammers, Steven R. et al. (2020): Embedding of Precision-Cut Lung Slices in Engineered Hydrogel Biomaterials Supports Extended Ex Vivo Culture. In *Am J Respir Cell Mol Biol* 62 (1), pp. 14–22. DOI: 10.1165/rcmb.2019-0232MA.

Banerjee, Audreesh; Trivedi, Chinmay M.; Damera, Gautam; Jiang, Meiqi; Jester, William; Hoshi, Toshinori et al. (2012): Trichostatin A Abrogates Airway Constriction, but Not Inflammation, in Murine and Human Asthma Models. In *Am J Respir Cell Mol Biol* 46 (2), pp. 132–138. DOI: 10.1165/rcmb.2010-0276OC.

Buratti, F. M.; Leoni, C.; Testai, E. (2007): The Human Metabolism of Organophosphorothionate Pesticides: Consequences for Toxicological Risk Assessment. In *J. Verbr. Lebensm.* 2 (1), pp. 37–44. DOI: 10.1007/s00003-006-0109-z.

Chambers, Janice; Oppenheimer, Seth F. (2004): Organophosphates, serine esterase inhibition, and modeling of organophosphate toxicity. In *Toxicol Sci* 77 (2), pp. 185–187. DOI: 10.1093/toxsci/kfh060.

Chapman, Shira; Grauer, Ettie; Gez, Rellie; Egoz, Inbal; Lazar, Shlomi (2019): Time dependent dual effect of anti-inflammatory treatments on sarin-induced brain inflammation: Suggested role of prostaglandins. In *Neurotoxicology* 74, pp. 19–27. DOI: 10.1016/j.neuro.2019.05.006.

Costa, Lucio G. (2006): Current issues in organophosphate toxicology. In *Clinica Chimica Acta* 366 (1-2), pp. 1–13. DOI: 10.1016/j.cca.2005.10.008.

Danov, Olga; Lasswitz, Lisa; Obernolte, Helena; Hesse, Christina; Braun, Armin; Wronski, Sabine; Sewald, Katherina (2019): Rupintrivir reduces RV-induced TH-2 cytokine IL-4 in precision-cut lung slices (PCLS) of HDM-sensitized mice ex vivo. In *Respir Res* 20 (1), p. 228. DOI: 10.1186/s12931-019-1175-y.

Eddleston, Michael; Buckley, Nick A.; Eyer, Peter; Dawson, Andrew H. (2008): Management of acute organophosphorus pesticide poisoning. In *The Lancet* 371 (9612), pp. 597–607. DOI: 10.1016/S0140-6736(07)61202-1.

Eyer, Florian; Meischner, Veronika; Kiderlen, Daniela; Thiermann, Horst; Worek, Franz; Haberkorn, Michael et al. (2003): Human parathion poisoning. A toxicokinetic analysis. In *Toxicological reviews* 22 (3), pp. 143–163. DOI: 10.2165/00139709-200322030-00003.

Fisher, R. L.; Hasal, S. J.; Sanuik, J. T.; Hasal, K. S.; Gandolfi, A. J.; Brendel, K. (1996): Cold- and cryopreservation of dog liver and kidney slices. In *Cryobiology* 33 (1), pp. 163–171. DOI: 10.1006/cryo.1996.0016.

Fisher, R. L.; Smith, M. S.; Hasal, S. J.; Hasal, K. S.; Gandolfi, A. J.; Brendel, K. (1994): The use of human lung slices in toxicology. In *Human & Experimental Toxicology* 13 (7), pp. 466–471. DOI: 10.1177/096032719401300703.

Guaiquil, V. H.; Vera, J. C.; Golde, D. W. (2001): Mechanism of vitamin C inhibition of cell death induced by oxidative stress in glutathione-depleted HL-60 cells. In *The Journal of biological chemistry* 276 (44), pp. 40955–40961. DOI: 10.1074/jbc.M106878200.

Guibert, Edgardo E.; Petrenko, Alexander Y.; Balaban, Cecilia L.; Somov, Alexander Y.; Rodriguez, Joaquín V.; Fuller, Barry J. (2011): Organ Preservation: Current Concepts and New Strategies for the Next Decade. In *Transfusion medicine and hemotherapy : offizielles Organ der Deutschen Gesellschaft fur Transfusionsmedizin und Immunhamatologie* 38 (2), pp. 125–142. DOI: 10.1159/000327033.

Gunnell, David; Eddleston, Michael (2003): Suicide by intentional ingestion of pesticides: a continuing tragedy in developing countries. In *Int J Epidemiol* 32 (6), pp. 902–909. DOI: 10.1093/ije/dyg307.

Herbert, Julia; Thiermann, Horst; Worek, Franz; Wille, Timo (2017): Precision cut lung slices as test system for candidate therapeutics in organophosphate poisoning. In *Toxicology* 389, pp. 94–100. DOI: 10.1016/j.tox.2017.07.011.

Herbert, Julia; Thiermann, Horst; Worek, Franz; Wille, Timo (2019): COPD and asthma therapeutics for supportive treatment in organophosphate poisoning. In *Clinical toxicology (Philadelphia, Pa.)* 57 (7), pp. 644–651. DOI: 10.1080/15563650.2018.1540785.

Hermanowicz, Andrzej; Kossman, Stefan (1984): Neutrophil function and infectious disease in workers occupationally exposed to phosphoorganic pesticides: Role of mononuclear-derived chemotactic factor for neutrophils. In *Clinical immunology and immunopathology* 33 (1), pp. 13–22. DOI: 10.1016/0090-1229(84)90288-5.

Hirn, Stephanie; Haberl, Nadine; Loza, Kateryna; Epple, Matthias; Kreyling, Wolfgang G.; Rothen-Rutishauser, Barbara et al. (2014): Proinflammatory and cytotoxic response to nanoparticles in precision-cut lung slices. In *Beilstein J. Nanotechnol.* 5 (1), pp. 2440–2449. DOI: 10.3762/bjnano.5.253.

Hrabetz, Heidi; Thiermann, Horst; Felgenhauer, Norbert; Zilker, Thomas; Haller, Bernhard; Nährig, Jörg et al. (2013): Organophosphate poisoning in the developed world - a single centre experience from here to the millennium. In *Chemico-biological interactions* 206 (3), pp. 561–568. DOI: 10.1016/j.cbi.2013.05.003.

Hulse, Elspeth J.; Davies, James O. J.; Simpson, A. John; Sciuto, Alfred M.; Eddleston, Michael (2014): Respiratory complications of organophosphorus nerve agent and insecticide poisoning. Implications for respiratory and critical care. In *Am J Respir Crit Care Med* 190 (12), pp. 1342–1354. DOI: 10.1164/rccm.201406-1150CI.

Jeyaratnam, J. (1990): Acute pesticide poisoning: a major global health problem. In *World health statistics quarterly. Rapport trimestriel de statistiques sanitaires mondiales* 43 (3), pp. 139–144. Available online at https://pubmed.ncbi.nlm.nih.gov/2238694/.

John, Harald; van der Schans, Marcel J.; Koller, Marianne; Spruit, Helma E. T.; Worek, Franz; Thiermann, Horst; Noort, Daan (2018): Fatal sarin poisoning in Syria 2013: forensic verification within an international laboratory network. In *Forensic Toxicol* 36 (1), pp. 61–71. DOI: 10.1007/s11419-017-0376-7.

Kamat, S. R.; Heera, S.; Potdar, P. V.; Shah, S. V.; Bhambure, N. M.; Mahashur, A. A. (1989): Bombay experience in intensive respiratory care over 6 years. In *Journal of postgraduate medicine* 35 (3), pp. 123–134. Available online at https://pubmed.ncbi.nlm.nih.gov/2699498/.

Lauenstein, L.; Switalla, S.; Prenzler, F.; Seehase, S.; Pfennig, O.; Förster, C. et al. (2014): Assessment of immunotoxicity induced by chemicals in human precision-cut lung slices (PCLS). In *Toxicology in vitro : an international journal published in association with BIBRA* 28 (4), pp. 588–599. DOI: 10.1016/j.tiv.2013.12.016.

Letort, Sophie; Balieu, Sébastien; Erb, William; Gouhier, Géraldine; Estour, François (2016): Interactions of cyclodextrins and their derivatives with toxic organophosphorus compounds. In *Beilstein Journal of Organic Chemistry* 12, pp. 204–228. DOI: 10.3762/bjoc.12.23.

Li, Guang; Cohen, Jonathan A.; Martines, Carolina; Ram-Mohan, Sumati; Brain, Joseph D.; Krishnan, Ramaswamy et al. (2020): Preserving Airway Smooth Muscle Contraction in Precision-Cut Lung Slices. In *Sci Rep* 10 (1), p. 6480. DOI: 10.1038/s41598-020-63225-y.

Lockridge, Oksana; Duysen, Ellen G.; Voelker, Troy; Thompson, Charles M.; Schopfer, Lawrence M. (2005): Life without acetylcholinesterase: the implications of cholinesterase inhibitor toxicity in AChE-knockout mice. In *Environmental toxicology and pharmacology* 19 (3), pp. 463–469. DOI: 10.1016/j.etap.2004.12.008.

Majorova, Dominika; Atkins, Elizabeth; Martineau, Henny; Vokral, Ivan; Oosterhuis, Dorenda; Olinga, Peter et al. (2021): Use of Precision-Cut Tissue Slices as a Translational Model to Study Host-Pathogen Interaction. In *Front. Vet. Sci.* 8, p. 686088. DOI: 10.3389/fvets.2021.686088.

Mew, Emma J.; Padmanathan, Prianka; Konradsen, Flemming; Eddleston, Michael; Chang, Shu-Sen; Phillips, Michael R.; Gunnell, David (2017): The global burden of fatal self-poisoning with pesticides 2006-15: Systematic review. In *Journal of affective disorders* 219, pp. 93–104. DOI: 10.1016/j.jad.2017.05.002.

Misharin, Alexander V.; Morales-Nebreda, Luisa; Mutlu, Gökhan M.; Budinger, G. R. Scott; Perlman, Harris (2013): Flow cytometric analysis of macrophages and dendritic cell subsets in the mouse lung. In *Am J Respir Cell Mol Biol* 49 (4), pp. 503–510. DOI: 10.1165/rcmb.2013-0086MA.

Neuhaus, Vanessa; Danov, Olga; Konzok, Sebastian; Obernolte, Helena; Dehmel, Susann; Braubach, Peter et al. (2018): Assessment of the Cytotoxic and Immunomodulatory Effects of Substances in Human Precision-cut Lung Slices. In *Journal of Visualized Experiments : JoVE* (135). DOI: 10.3791/57042.

Neuhaus, Vanessa; Schaudien, Dirk; Golovina, Tatiana; Temann, Ulla-Angela; Thompson, Carolann; Lippmann, Torsten et al. (2017): Assessment of long-term cultivated human precision-cut lung slices as an ex vivo system for evaluation of chronic cytotoxicity and functionality. In *Journal of Occupational Medicine and Toxicology (London, England)* 12, p. 13. DOI: 10.1186/s12995-017-0158-5.

Okumura, T.; Takasu, N.; Ishimatsu, S.; Miyanoki, S.; Mitsuhashi, A.; Kumada, K. et al. (1996): Report on 640 Victims of the Tokyo Subway Sarin Attack. In *Annals of Emergency Medicine* 28 (2), pp. 129–135. DOI: 10.1016/S0196-0644(96)70052-5.

Oostingh, Gertie Janneke; Wichmann, Gunnar; Schmittner, Maria; Lehmann, Irina; Duschl, Albert (2009): The cytotoxic effects of the organophosphates chlorpyrifos and diazinon differ from

their immunomodulating effects. In *Journal of Immunotoxicology* 6 (2), pp. 136–145. DOI: 10.1080/15476910902977407.

Preuß, Eike B.; Schubert, Stephanie; Werlein, Christopher; Stark, Helge; Braubach, Peter; Höfer, Anne et al. (2021): The Challenge of Long-Term Cultivation of Human Precision-Cut Lung Slices. In *The American Journal of Pathology*. DOI: 10.1016/j.ajpath.2021.10.020.

Proskocil, Becky J.; Grodzki, Ana Cristina G.; Jacoby, David B.; Lein, Pamela J.; Fryer, Allison D. (2019): Organophosphorus Pesticides Induce Cytokine Release from Differentiated Human THP1 Cells. In *Am J Respir Cell Mol Biol* 61 (5), pp. 620–630. DOI: 10.1165/rcmb.2018-0257OC.

Richards, P. G.; Johnson, M. K.; Ray, D. E. (2000): Identification of acylpeptide hydrolase as a sensitive site for reaction with organophosphorus compounds and a potential target for cognitive enhancing drugs. In *Mol Pharmacol* 58 (3), pp. 577–583. DOI: 10.1124/mol.58.3.577.

Rosner, Sonia R.; Ram-Mohan, Sumati; Paez-Cortez, Jesus R.; Lavoie, Tera L.; Dowell, Maria L.; Yuan, Lei et al. (2014): Airway contractility in the precision-cut lung slice after cryopreservation. In *Am J Respir Cell Mol Biol* 50 (5), pp. 876–881. DOI: 10.1165/rcmb.2013-0166MA.

Russell, W. M. S.; Burch, R. L. (1959): The principles of humane experimental technique. The principles of humane experimental technique. London, England: Methuen.

Sakagami, Masahiro (2006): In vivo, in vitro and ex vivo models to assess pulmonary absorption and disposition of inhaled therapeutics for systemic delivery. In *Advanced Drug Delivery Reviews* 58 (9-10), pp. 1030–1060. DOI: 10.1016/j.addr.2006.07.012.

Sauer, Ursula G.; Vogel, Sandra; Aumann, Alexandra; Hess, Annemarie; Kolle, Susanne N.; Ma-Hock, Lan et al. (2014): Applicability of rat precision-cut lung slices in evaluating nanomaterial cytotoxicity, apoptosis, oxidative stress, and inflammation. In *Toxicology and Applied Pharmacology* 276 (1), pp. 1–20. DOI: 10.1016/j.taap.2013.12.017.

Stigler, Lisa; Köhler, Anja; Koller, Marianne; Job, Laura; Escher, Benjamin; Potschka, Heidrun et al. (2021): Post-VX exposure treatment of rats with engineered phosphotriesterases. In *Arch Toxicol*, pp. 1–13. DOI: 10.1007/s00204-021-03199-6.

Tegeder, I.; Niederberger, E.; Israr, E.; Gühring, H.; Brune, K.; Euchenhofer, C. et al. (2001): Inhibition of NF-kappaB and AP-1 activation by R- and S-flurbiprofen. In *FASEB journal : official publication of the Federation of American Societies for Experimental Biology* 15 (1), pp. 2–4. DOI: 10.1096/fj.00-0130fje.

Temann, Angela; Golovina, Tatiana; Neuhaus, Vanessa; Thompson, Carolann; Chichester, Jessica A.; Braun, Armin; Yusibov, Vidadi (2017): Evaluation of inflammatory and immune responses in long-term cultured human precision-cut lung slices. In *Human Vaccines & Immunotherapeutics* 13 (2), pp. 351–358. DOI: 10.1080/21645515.2017.1264794.

Timchalk, Charles (2010): Organophosphorus Insecticide Pharmacokinetics. RI Krieger Academic Press, London, United Kingdom (Pacific Northwest National Lab. (PNNL), Richland, WA (United States), PNNL-SA-64932). Available online at https://www.osti.gov/biblio/1024092.

Travaglini, Kyle J.; Nabhan, Ahmad N.; Penland, Lolita; Sinha, Rahul; Gillich, Astrid; Sit, Rene V. et al. (2020): A molecular cell atlas of the human lung from single-cell RNA sequencing. In *Nature* 587 (7835), pp. 619–625. DOI: 10.1038/s41586-020-2922-4.

van der Hoek, W.; Konradsen, F.; Athukorala, K.; Wanigadewa, T. (1998): Pesticide poisoning: A major health problem in Sri Lanka. In *Social science & medicine (1982)* 46 (4-5), pp. 495–504. DOI: 10.1016/s0277-9536(97)00193-7.

Watson, Christa Y.; Damiani, Flavia; Ram-Mohan, Sumati; Rodrigues, Sylvia; Moura Queiroz, Priscila de; Donaghey, Thomas C. et al. (2016): Screening for Chemical Toxicity Using Cryopreserved Precision Cut Lung Slices. In *Toxicol Sci* 150 (1), pp. 225–233. DOI: 10.1093/toxsci/kfv320.

Wigenstam, E.; Forsberg, E.; Bucht, A.; Thors, L. (2021): Efficacy of atropine and scopolamine on airway contractions following exposure to the nerve agent VX. In *Toxicology and Applied Pharmacology* 419, p. 115512. DOI: 10.1016/j.taap.2021.115512.

Wille, T.; Thiermann, H.; Worek, F. (2020): Organophosphates I. Human Health Effects and Implications for the Environment: an Overview. In J.P.F. D'Mello (Ed.): A Handbook of Environmental Toxicology. Organophosphates I. Human Health Effects and Implications for the Environment: an Overview. With assistance of T. Wille, H. Thiermann, F. Worek: CAB International, pp. 246–260.

Wille, Timo; Neumaier, Katharina; Koller, Marianne; Ehinger, Christina; Aggarwal, Nidhi; Ashani, Yacov et al. (2016): Single treatment of VX poisoned guinea pigs with the phosphotriesterase mutant C23AL: Intraosseous versus intravenous injection. In *Toxicology Letters* 258, pp. 198–206. DOI: 10.1016/j.toxlet.2016.07.004.

Wohlsen, A.; Martin, C.; Vollmer, E.; Branscheid, D.; Magnussen, H.; Becker, W. M. et al. (2003): The early allergic response in small airways of human precision-cut lung slices. In *Eur Respir J* 21 (6), pp. 1024–1032. DOI: 10.1183/09031936.03.00027502.

Worek, Franz; Thiermann, Horst; Szinicz, Ladislaus; Eyer, Peter (2004): Kinetic analysis of interactions between human acetylcholinesterase, structurally different organophosphorus compounds and oximes. In *Biochemical pharmacology* 68 (11), pp. 2237–2248. DOI: 10.1016/j.bcp.2004.07.038.

Worek, Franz; Thiermann, Horst; Wille, Timo (2020): Organophosphorus compounds and oximes: a critical review. In *Arch Toxicol* 94 (7), pp. 2275–2292. DOI: 10.1007/s00204-020-02797-0.

Wright, Benjamin S.; Rezk, Peter E.; Graham, Jacob R.; Steele, Keith E.; Gordon, Richard K.; Sciuto, Alfred M.; Nambiar, Madhusoodana P. (2006): Acute lung injury following inhalation exposure to nerve agent VX in guinea pigs. In *Inhalation toxicology* 18 (6), pp. 437–448. DOI: 10.1080/08958370600563847.

Acknowledgements

Writing this PhD thesis would not have been possible without the support and advice of several people.

First, I would like to thank my supervisor PD Dr. med. Timo Wille for the excellent supervision and the support, professional advice, the encouragement, and the motivation he gave to me. In addition, I would like to thank Prof. Dr. med. Franz Worek for the excellent guidance and the very valuable advice that helped me in many situations.

I thank Dr. Julia Herbert for the introduction into the world of PCLS and the application of the model and Prof. Dr. med. Dirk Steinritz for his helpful scientific advice as member of my thesis advisory committee.

I thank Prof. Dr. med. Horst Thiermann, head of the Bundeswehr Institute of Pharmacology and Toxicology, for giving me the opportunity to conduct my dissertation under these excellent working conditions. Furthermore, I would like to thank Prof. Dr. med. Thomas Gudermann, speaker of the GRK 2338, for the outstanding scientific program provided by the Research Training Group.

Thanks to my colleagues and friends from the GRK2338 and the Bundeswehr Institute of Pharmacology and Toxicology for the good scientific discussions, encouraging advice and support, and the great activities outside of the lab. I am very grateful that colleagues have become friends who have made this time unforgettable.

Finally, I would like to thank my family and my girlfriend Hanne for the motivation and constant support during the last years.